TABLE OF CONTENTS

Page

LIST OF TABLES

LIST OF FIGURES

INTRODUCTION

Asphalt materials (sometimes named as bituminous materials) have been used for road construction and maintenance since the end of the nineteenth century. They are the most common materials that increase the quality of road surfaces and the performance of road structures. The importance of these materials in road construction can be demonstrated by their extraordinary physical and chemical properties (Huang & Di Benedetto, 2015). In order to determine those properties, unified conclusive test methods have to be available, which are as simple as possible, efficient, refined and based on a sound physical background.

The road system is a great asset in Canada. The infrastructure plan investment for Quebec has been released for the period of 10 years starting from 2017 to 2027. It reports that more than 19 percent of the investments are for the road itself. On the other hand, more than 80 percent of pavements in Quebec are flexible pavement in which asphalt is the most expensive layer and plays a key role in its performance. The Canadian climate is characterized by a wide seasonal temperature range, including a series of freeze-thaw (F-T) cycles (El-Hakim & Tighe, 2014). The granular material is subjected to freezing in winter, which may produce ice lenses that result in swelling and differential heave of the pavement structures. The pavement is subjected to partial thaws during the winter and a full thaw in spring. Therefore, the ice becomes water, which causes loss of bearing capacity and can lead to significant damage to the pavement structures. Previous study in two different observation sites and for three years expressed that 90% of annual damage occurs during thaw periods (Bilodeau & Doré, 2017).

Fatigue associated with repetitive traffic loading is considered to be one of the most significant distress modes in flexible pavement. Fatigue cracking is an asphalt concrete pavement distress that results from an accumulation of damage under repeated loading application. In Canada, premature fatigue cracking is recognized as the most important type of distress on major highways (Pascal, Doré, & Prophète, 2004). It appears that the action of traffic alone is not the cause of failure of bituminous asphalts in winter. Instead, it is probably the effect of thermal stress, freeze-thaw cycles, and the moisture infiltration which results in stress that helps to

exceed the tensile strength of the asphalt materials and cause premature cracks in asphalt pavements (Carter & Paradis, 2010). The development of sound correlation relating pavement structural performance to environmental impact is the major area of focus in this research. As yet, there have not been any fatigue criterions to take into account freeze-thaw cycles. This issue is fundamental to the fatigue durability of a road pavement.

CHAPTER 1

BACKGROUND AND LITERATURE REVIEW

1.1 Introduction

The short and long-term effects of the climate change have already started threatening the Canadian infrastructures and the national economy. Despite the beliefs of some politicians, the scientific literature provides undeniable evidence that the climate change will grow and continue at least for several decades even if there is a success of global agreements to reduce greenhouse gasses (Stern, 2006). Changes in temperatures, precipitation patterns, wind conditions and increasing the events of extreme weather conditions during a year are some of the processes of climate change that affects the Canadian low and high volume road systems. Canadian pavement systems are valuable assets of more than 100$ billion (Mills et al., 2009). Previous analysis at 17 sites in southern Canada indicated that the type of distresses is replaced from low temperature cracking patterns to rutting and other damages related to high-temperature fluctuations (Mills et al., 2009). Hence, the development of the relationship between the pavement performance and the environmental impact has been a major area of focus for pavement researchers in Canada.

In cold region areas, harsh temperature fluctuations and daily rapid freeze-thaw cycles affect the performance of pavements. These damages are categorized as a major environmental distress that is implemented in flexible pavements (Kennedy, Roberts, & Lee, 1983; Stroup-Gardiner & Epps, 1987). Previous research in Quebec concluded that the annual wheel truck damage cost could reach 85% during the spring periods (Doré, 2004). These crack observations are usually associated with fatigue damage (Savard, De Blois, Boutonnet, Hornych, & Mauduit, 2005). A previous study reported that more than 90 percent of the fatigue damage to these pavements occurred during partial winter thaw or spring thaw periods (Deblois, Bilodeau, & Dore, 2010). The test observations and findings in the southern Quebec and Canada highlight a tremendous gap between the pavement conditions in the field and desired conditions by the designers. It is clear that the action of traffic alone is not the only cause of

failure of asphalt pavements in these areas. The combination of the effects of water infiltration and temperature fluctuations can also create different stresses to the pavement structures and especially to the asphaltic materials. So, it is essentials for the designers to implement these factors to enhance the life of the asphalt pavements.

1.2 Flexible Pavements

The pavement is the main part of the highway which is the most obvious to the drivers. Asphalt concrete pavements are complex structures composed of several different layers. The first layer of flexible pavements is the visible part that needs to carry most of the load and directly traffics. It is the most expensive layer, and usually consists of asphalt binder and crushed aggregate. It consists of sublayers which are bonded together. The main role of the asphaltic layer is to receive loads from the traffic and passes them to the underlying layers. Below surface course is the granular base course. The granular base course provides the thickness to ensure the quality life of the pavement against traffic and environment. It has a thickness from 100 to 300 millimeters. Traditionally base course has been designed using coarse aggregate which can lead to having less asphalt binder. This can reduce the potential for structural rutting damage and also decrease the cost of the pavement. However, many studies have recently shown that the base course needs to design and care even more than the surface course to increase the durability and improve the fatigue resistance (Maupin & Diefenderfer, 2006; Olard, 2012; Theyse, De Beer, & Rust, 1996). Figure 1.1 indicates a cross-section of a typical asphalt pavement structure.

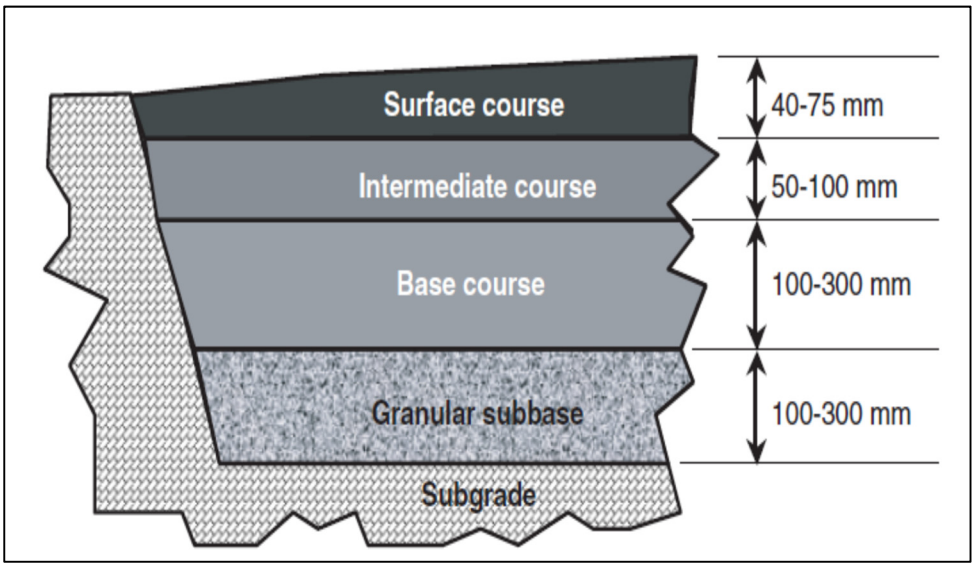

Figure 1.1 Typical cross section of a typical flexible pavement structure
Taken from Jenks et al. (2011)

The thicknesses of flexible pavement layers are calculated based on the traffic volume over a given period of time and environmental conditions. Different methods have been developed to design the flexible pavements. The mechanical-empirical pavement design approach (MEPDG) introduced in NCHRP 1-37A is a method for designing and evaluating pavement structures based on mechanistic-empirical (M-E) analysis which is based on the mechanics of materials that relates an input, such as traffic loads, and environment to an output (pavement response). The stresses, strains, and deflections which are defined as structural responses are measured mechanically in the laboratory or field-performance data based on the environment conditions, loading characteristics, and material properties. These structural responses are considered as inputs in the empirical model to calculate performance predictions such as fatigue and rutting (Huang, 2004). Accuracy of the MEPDG model depends on the quality of the information that we put as inputs and the calibration of empirical models based on the field performance. There are two different types of empirical models that are utilized in the MEPDG. Distresses can be predicted directly, or the distresses are predicted based on calibration against field measured distresses (Carvalho & Schwartz, 2006).

1.3 Asphalt Layers in Flexible Pavements

HMA is a complex material that changes over time depending on the climatic conditions as well as the level of stresses on the pavement structures. The properties of mixes vary according to the formulation: the bitumen content, the characteristics of the aggregates used and the manufacturing procedure. The properties of an HMA are indicated in Figure 1.2. The aggregates have an elastic character, but the behavior of the bitumen is viscoelastic and variable with time.

Figure 1.2 Example of the aggregate, binder, and HMA specimen
Taken from Jenks et al. (2011)

1.4 HMA compositions

Typical asphalt mixture is composed of around 5% asphalt binder and 95% of aggregate by mass. The main components of an asphalt mixture are presented in Figure 1.3. Additives are also added to many HMA mixes to improve the performance or workability. With a good formulation, asphalt mix must have (MTQ, 2005):

• Sufficient amount of binder to guarantee good resistance to fatigue and cracking, and also provide appropriate durability to the mix. The amount of bitumen allow the aggregates to be coated in a sufficiently thick film to minimize the impact of bitumen oxidation during the manufacturing and installation phase;

• Sufficient rigidity to give the mixture good resistance to rutting at high temperatures temperature;

• Good granularity to avoid a smooth surface in the wearing course and therefore the maintenance of user safety. Then you have to have a good granular contact which makes it possible to increase the resistance to permanent deformations of the surface.

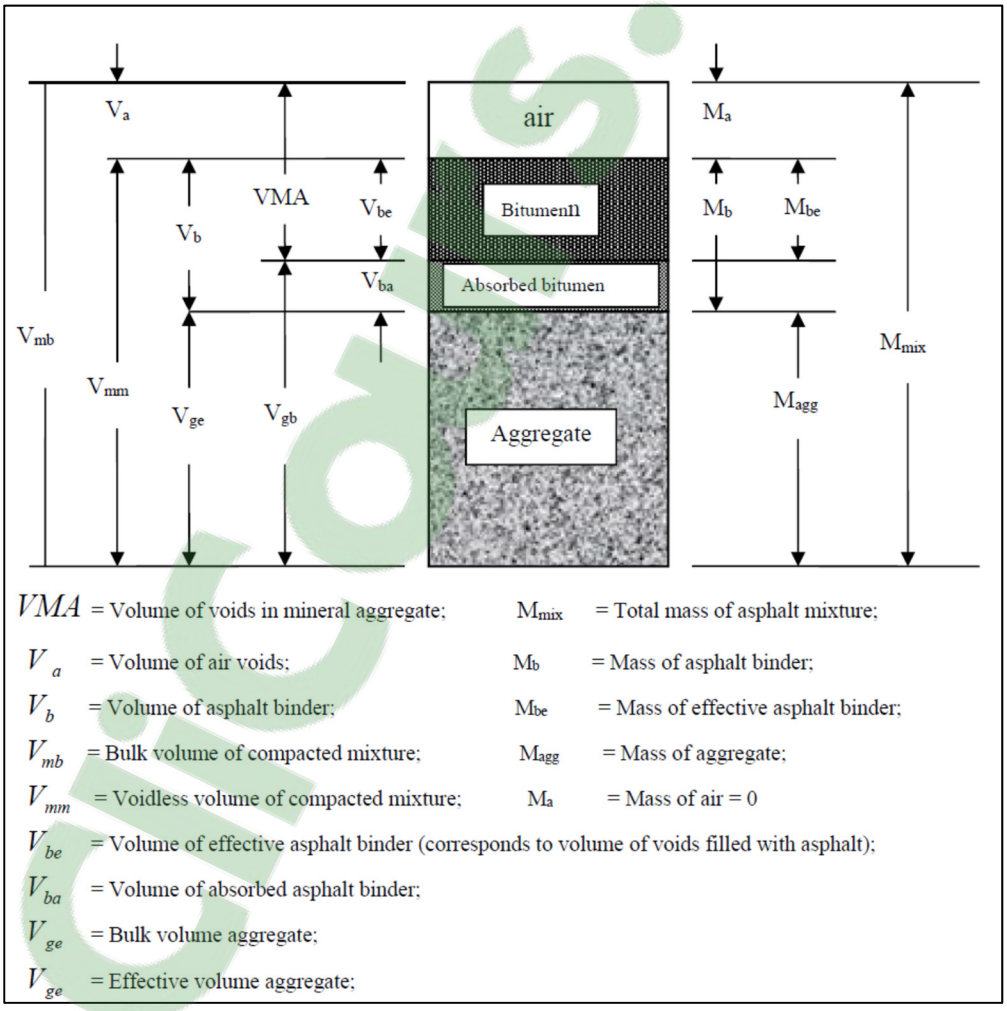

Figure 1.3 Volumetric representation of a compacted mixture
Taken from Jafee & Kajandar (2001)

1.5 Typical Flexible Pavement Stresses

Pavements are designed to sustain stresses. Pavement engineering relies therefore on a good understanding of pavement stresses and on their quantification. Stresses acting on pavements can be classified as load induced or environmentally induced stresses (Doré & Zubeck, 2009).

1.5.1 Load Induced Stresses

Rigid, semi-rigid and flexible pavements distribute the traffic loads in different ways. Flexible pavements distribute the loads through every single layer. During the passing of heavy vehicles, the load transfers from the wheels to pavements and creates tensile or compressive strains at the various directions in the layers of flexible pavements. Figure 1.4 illustrates the layer system and stress distributions through the layers. Major stresses are divided into compressive stress on top of the subgrade and asphalt layers and tensile stress at the bottom of the asphalt layers. These major stresses can produce distresses such as fatigue and rutting over time and after a large number of heavy vehicles.

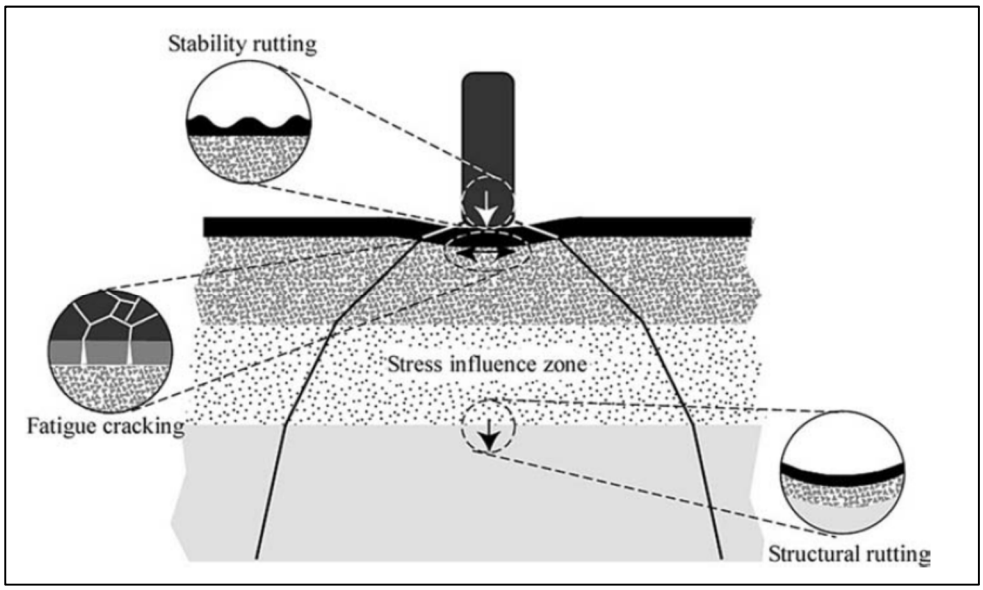

Figure 1.4 Stress distribution in pavement system and stresses at critical interfaces associated with resulting pavement performance problems
Taken from Doré & Zubeck (2009)

Major load-related distresses can be categorized as follows (Huang, 2004):

1) Development of surface rutting (permanent deformation), which is due to the vertical stress or strain on the surface of flexible pavements.
2) Fatigue cracking, which is due to the stresses or strains at the bottom of the asphalt layers (asphalt base course).
3) Structural rutting, which is due to the vertical stresses or strains at the surface of the subgrade soils.

1.5.2 Environmental Stresses

Environmental stresses are due to the direct effects related to the solar energy, temperature, air pressure, wind, precipitation and the level of the humidity. However, the main climatic stresses in the cold region environment are generally due to the effect of temperature and water. Environment stresses have several effects on pavement structures. They can change the stiffness of the asphalt pavements. Loss of durability of asphalt mixes due to the freeze-thaw

cycles creates stripping distress. Stress and deformation in HMA due to the variation of thermal expansion and contraction which can cause crack generation (low-temperature cracking) (Islam & Tarefdar, 2015). The effect of environmental stresses on HMA layer and mixtures are described in details in this part.

1.5.2.1 Thermal Stresses

Thermal stresses are environmental stresses caused by diurnal and shorter-term temperature variations in the bound pavement layer that is restricted from contracting. As the temperature gets colder, a thermal stress starts to develop gradually. Figure 1.5 shows the development of thermal stress under constant cooling rate. The stress does not increase linearly with temperature at warm temperatures (close to 0°C) due to asphalt cement's viscoelastic behavior that allows partial relaxation of stresses. At a certain transition temperature depending mainly on the binder properties, the asphalt concrete starts to behave as a purely elastic material and the thermal stress increases linearly with the temperature (Doré & Zubeck, 2009). Low-temperature cracking occurs when the induced tensile stress exceeds the tensile strength of the asphalt concrete (Islam et al., 2014).

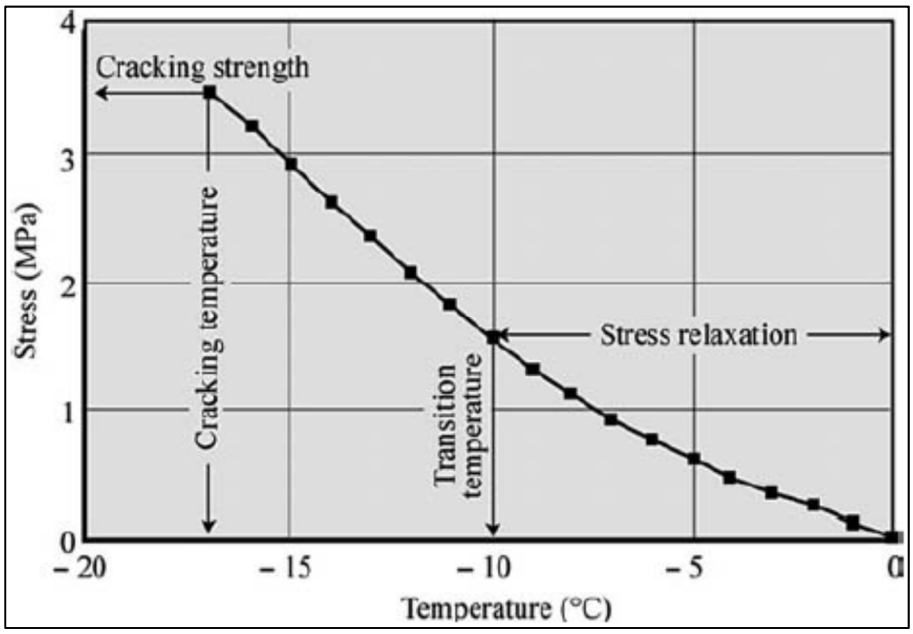

Figure 1.5 Typical stress versus temperature relationship
Taken from Doré & Zubeck (2009)

Low-temperature damage is one of the important distresses in cold region's asphalt pavements. The damage appears as transverse cracks and they gradually widen and provide places for moisture penetration which accelerate pavement failures at the end. There are two conditions that create low-temperature cracking: (a) temperature must be cold enough to produce stresses greater than the strength of the asphalt materials, and (b) the restraint force must be high enough to minimize the slab movement and prevent the thermal stress to be released (Zubeck & Vinson, 1996).

There are two major types of thermal cracking, namely as the low-temperature cracking and thermal fatigue cracking. The fluctuations of temperature may cause thermal fatigue cracking over time (Figure1.6) (Islam et al., 2014).

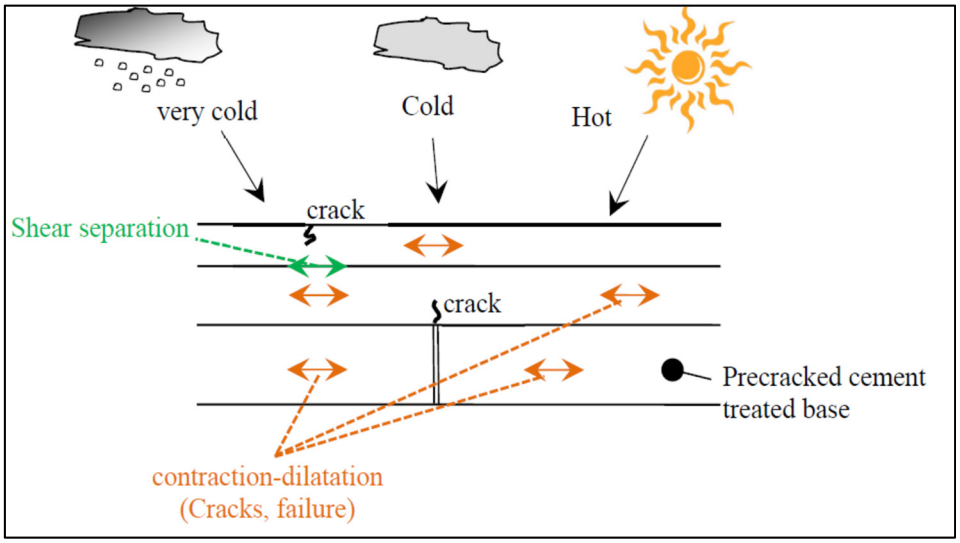

Figure 1.6 Schematic of the temperature induced stresses
Taken from Basueny (2016)

Previous studies reported that the tensile stresses due to temperature fluctuations can even greater than the tensile stresses that are induced by traffic loads (Al-Qadi, Hassan, & Elseifi, 2005; Bayat, Knight, & Soleymani, 2012).

1.5.2.2 Stresses Induced by Frost Heave

Two main mechanisms, identified by Doré (2002), can act on pavements. The first one, referred to as random differential heaving, is mainly associated with variations of soil properties along the highway corridor. The resulting distortions tend to increase pavement roughness during winter and, by forcing pavements to bend upward, can also cause pavement cracking. The second type of differential frost heaving occurs along the transverse axis of the pavement and is the result of the variation of pavement geometry and snow accumulation on pavement sides (Doré, Flamand, & Pascale, 2002). Both mechanisms are likely to force pavements to bend upward (Doré & Zubeck, 2009). Figure 1.7 demonstrates that the snow that accumulates on the pavement sides causes in greater frost penetration at the center of the pavement that creates

excessive tensile stresses on the top of the pavement which can initiate longitudinal cracks (Doré, Konrad, & Roy, 1997).

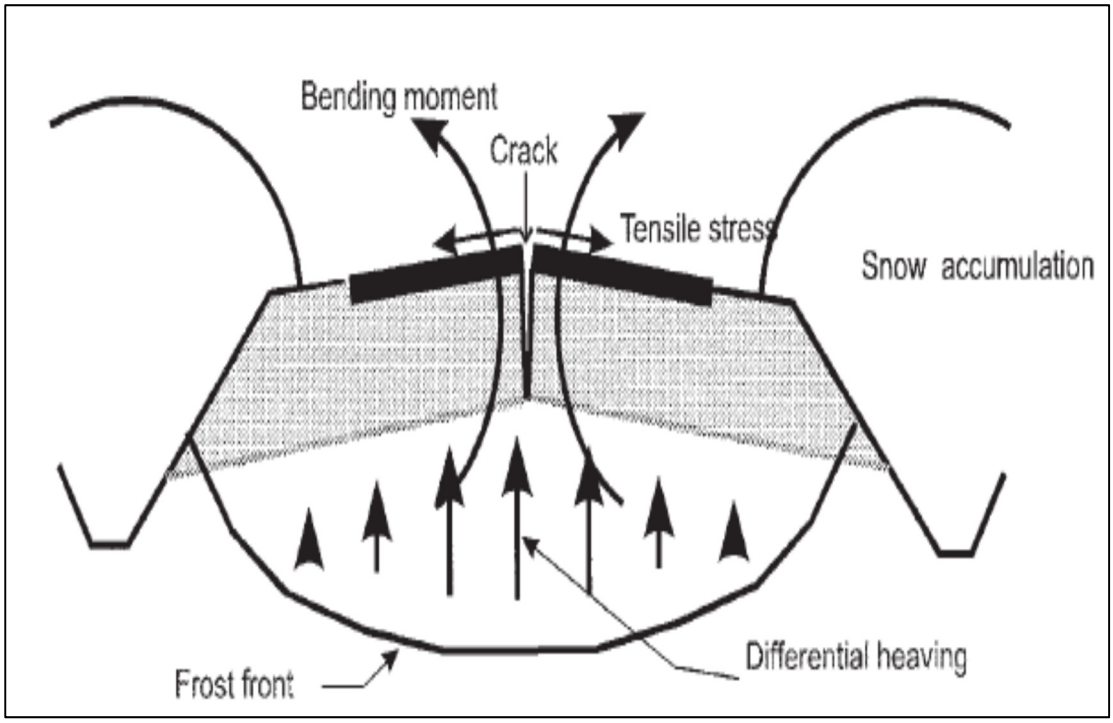

Figure 1.7 Transverse differential heaving
Taken from Doré et al. (1997)

1.5.2.3 Moisture Induced Stresses

Moisture damage is one of the major distress that can greatly influence the pavement life. Moisture content can change the material characteristics of asphalt mixes includes shear strength and stiffness modulus. Moisture can penetrate the surface layer through cracks and joints (Roberson & Siekmeier, 2002). It can also penetrate from underlying saturated base layer through the capillary rise action.

Moisture damage results from the loss of adhesion bond between the bitumen and aggregate interface by the presence of water or loss of the cohesive resistance of asphalt binder (Huang

et al., 2005). These to mechanisms are the last step in a process that commenced with various mechanisms of moisture transport (Caro, Masad, Bhasin, & Little, 2008).

Asphalt mixture moisture conditions in the lab

In cold climate conditions, stresses raise with poor asphalt materials, with traffic loads and water that are key elements in the degradation of flexible pavements in cold regions (Behiry, 2013). Many factors influence the severity of moisture distress in HMA. Some of these factors depend on the material's quality and others depend on the mix design, construction quality, environmental factors, traffic conditions, and additives (Behiry, 2013).

Two famous tests are implemented for the moisture damage in the lab. Freeze-thaw and moisture induced tester (MIST) has been used to analyze the effect of moisture in asphalt mix although they have different effects on the properties of mixes due to their mechanisms to induce moisture distress. Complex modulus and Superpave indirect tensile test (IDT) are also capable to characterize the moisture effect of asphalt mixes indirectly. Previous results reported that both of them are able to precisely analyze the moisture susceptibility of asphalt mixes (Shu et al., 2012).

Moisture Damage Mechanisms

Previous research defined the definition of most common mechanisms of moisture damage in asphalt mixes which are explained as follows (Caro et al., 2008):

Stripping: is the process that causes the separation of binder-aggregate which is due to the adhesion loss in the presence of moisture. Moisture enters the pore structure from the surface of pavement or from the bottom of the asphalt base layer and can detach the aggregate or change the properties of the binder through an emulsification process (Chen & Huang, 2008). Striping is the main degradation mechanism during the freeze-thaw cycles;

Raveling: is defined by the dislodgement of aggregate in asphalt mixes from the surface;

Shelling: a degradation process defined by the removal of aggregate from a seal coat or other surface treatment;

Hydraulic scour: is a degradation process that starts on a saturated asphalt surface by which the pavement material is eroded due to the dynamic action of tires in the presence of water.

Adhesion and Cohesion Theories

Moisture damage is affected by the aggregate texture, aggregate mineralogy, the chemistry of asphalt binder, and the interaction of the aggregate and binder (Solaimanian, Bonaquist, & Tandon, 2006). Moisture damage can degrade asphalt mixes through two main mechanisms: loss of cohesion within the binder and loss of adhesion bond of binder/ aggregate (Terrel & Al-Swailmi, 1992).

As explained earlier, cohesion damage is due to the interaction of moisture and asphalt mastic, which leads to loss of durability and strength of the mix. On the other hand, adhesion failure refers to the degradation mechanisms of aggregate/ binder bond (Copeland, 2007). Adhesive loss usually occurs when mastic film is very thin while cohesive loss happens when the film is very thick (Lytton, 2004). Adhesion loss plays a more important role regarding the moisture distress in an asphalt mix (Caro et al., 2008). The adhesion and cohesion loss are caused by various factors including the water absorption, aggregate-mastic compatibility, heavy traffic loads, aggregate gradation, construction quality, and weather condition (Goh & You, 2012). Another study reported that the surface energy, chemical reaction, mechanical adhesion, and molecular orientation are four theories that can explain the adhesion characteristics in asphalt mixes as in mentioned earlier (Bausano, Kvasnak, & Williams, 2006). Stuart (1990) categorized moisture damage based on three concepts that contribute to the adhesive in different degrees which are: surface energy, mechanical interlock and chemical bonding (Stuart, 1990). Hicks (1991) mentioned that the chemical characteristics of aggregate need to be analyzed after the adhesion failure. Yoon and Tarrer (1988) analyzed the aggregate chemical and physical characteristics. They reported that there is no correlation between moisture

sensitivity of the mix and aggregate properties. They concluded that the aggregate with high PH values is more susceptible to moisture damage and striping than others (McCann, Anderson-Sprecher, & Thomas, 2005).

According to Little and Jones (2003) cohesion loss is a degradation process in asphalt mixes with the presence of water that developed in a mastic and is affected by the rheology of the binder film and the interaction of the mineral filler and asphalt cement (Terrel and Al-Swailmi 1992; Little and Jones 2003). Cheng et al. (2002) reported that the cohesive strength can be damaged in various mixtures by the presence of water in asphalt mixes (Cheng et al. 2003; Jason Bausano, Kvasnak, and Williams 2006).

Void structure in asphalt mixtures

Void structure plays important role in asphalt moisture damage. Moisture expansion during freezing periods and also cracks can increase the air voids and permeability of an asphalt mix which results in a weak pavement (Chen, Lin, & Young, 2004). Some of the transportation agencies control the moisture damage by reducing the percentage of air voids in the mix. For instance, Ministry of Transportation of Ontario (MTO) defines that the surface asphalt course must be reduced as low as possible to control the moisture damage (Mohamed et al. 1993). In spite of that, there is evidence of moisture infiltration and damage in a lower rate (Caro et al., 2008). The characteristics of air voids in asphalt mixes depend mainly on the mix design, aggregate properties, and compaction process. They can be classified into three main categorized as shown in Figure 1.8: semi-effective, effective, permeable (Caro et al., 2008).

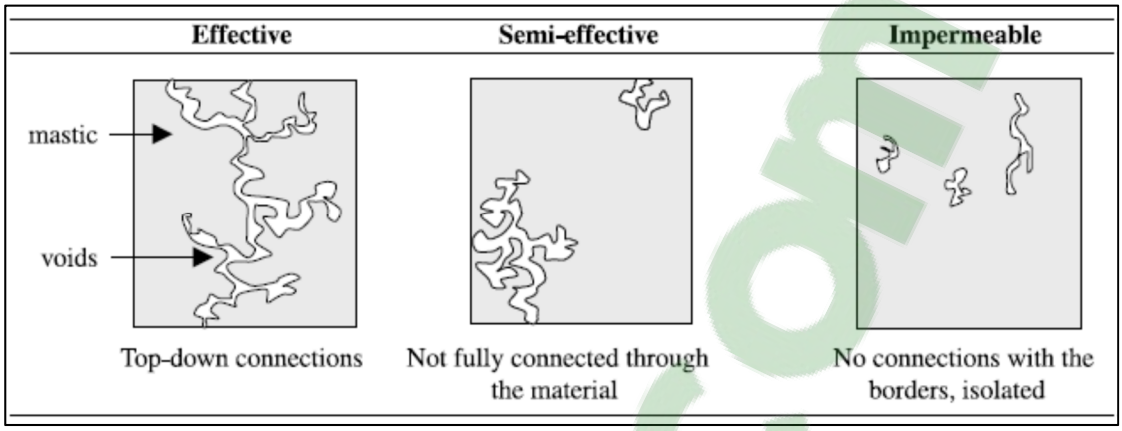

Figure 1.8 Classification of voids in asphalt mixtures
Taken from Chen, Lin, & Young, 2004; Caro et al., 2008)

Voids structures can be determined in different technique such as using 2D image cross-sections of a mix, or 3D which include nuclear magnetic resonance (NMR) imaging transmission electron microscopy visualization and X-ray computed tomography (CT) reconstruction (Barrie, 2000; Kosek, Štěpánek, & Marek, 2005). These technique has been utilized to define the characteristics of the microstructure of mixes (Kosek et al., 2005).

Capillary rise

Capillary rise defines as one of the most important modes of moisture transport in soil mechanic, but there is a little study in on its impact in asphalt mixes. Capillary rise is not expected to occur inside asphalt mix where water is in contact with mastic due to the hydrophobic nature of asphalt binder. However, it takes place in asphalt base mixes because water comes from underlying granular layers especially during thaw period. Percentage of air voids have a direct relation with this phenomena and saturated mix with high air voids has a faster capillary rise (Caro et al., 2008).

Vapor diffusion

The percentage and the rate of the water vapor in a mix depend on three main factors:

Diffusion coefficients, relative humidity and storage capacity and rate (also called the potential of water holding). Diffusion coefficients and the storage capacity depend on material properties while relative humidity is from the environmental conditions (Caro et al., 2008).

1.6 Environmental Conditions in Quebec

The road system is a great asset in Canada and Quebec. The infrastructure plan investment for Quebec has been released for the period of 10 years starting from 2017 to 2027. It reports that more than 19 percent of the investments are for the road itself. On the other hand, more than 80 percent of pavements in Quebec are the flexible type which asphalt is the most expensive layer and plays an important role in its performance.

Flexible pavements in Quebec experience severe seasonal climatic conditions in a year (Doré, & Zubeck, 2009). Freeze-thaw cycles and frost action is a major cause of pavement deterioration in Quebec. The extreme variations in temperatures have significant influences on the performance of pavements (Carter, & Paradis, 2010). Previous research demonstrated that the variations of temperature can create tensile stress at the bottom of the asphalt base layer even more than traffic loads. On the other hand, Québec roads are subjected to seasonal ambient temperature variations of 60°C and daily rapid variations of temperature that may run as high as 30°C. These significant temperature variations in combination with the moisture inside the pores, traffic loads, and loss of bearing capacity due to saturated underlying granular layers during spring period can result in the development of premature deterioration of fatigue cracking.

Analysis of the daily variation of temperatures and its effect on the performance of asphalt pavements in Quebec needs to be examined at a more precise assessment. Fig. 1 shows daily asphalt and air temperatures which were monitored by the Ministry of Transportation of Québec (MTQ) for Trois Rivere, Route 155, a road in the southern part of Québec, from November 1, 2014, to May 1, 2015. It shows that the spring period which is started from

November to May has a high probability of freeze-thaw cycles. A freeze-thaw cycle is considered when the temperature falls below 0ºC or -1ºC and returns above 0ºC or even 1ºC.

1.6.1 Effect of Freeze-thaw Cycles on Asphalt Mixtures

Freeze-thaw cycles can create damage which is related to temperature and moisture susceptibility that is significantly affected the performance and durability of flexible pavements in cold regions (Goh, &You 2012). Freeze-thaw damage on asphalt mix is a major cause of degradation in cold regions. The penetration of water in the pores of asphalt mixes combined with the high variation of temperatures decrease the adhesive bond between the mastic and the aggregate (Ozgan and Serin, 2013; Tang et al., 2013).

The degradation process of an asphalt mix in terms of freeze-thaw cycles are categorized as decreased in strength, performance loss, and adhesion loss between the aggregate and binder. With the increase of freeze-thaw cycles, the splitting strength of mixtures decreased and the volume expanded gradually. The performance stabilized until the next rapid deterioration caused by the loss of interfacial adhesion between the asphalt and aggregate. Feng et al. (2009) indicated the importance of gradation on the performance and durability of asphalt mixes in cold regions. They concluded that the low percentage of voids had the best freeze-thaw performance. They also showed that the freeze-thaw repetitions influence more when the percentage of salt is less than 3%. Mauduit et al., (2010) is observed that the specimens had different swelling at the beginning of the freezing periods. This can be deteriorated asphalt pavements as a result of differential horizontal strains appearing within the structure layers, due to different swelling conditions depending on their moisture content. Another study by Goh and You (2012) conducted the rapid freeze-thaw cycles to assess the potential of the stripping and adhesion loss of asphalt mixes with utilizing an image processing technique. 300 rapid freeze-thaw cycles can represent the daily repetition of freeze-thaw cycles during one year in cold regions area. The image of the surface of the mixes was captured and assessed and the results found that the stripping increases along with a number of freeze-thaw repetitions. Özgan & Serin, 2013 evaluated the freeze-thaw strength of asphalt mixes. The experimental

results from the specimens that were subjected to different freeze-thaw cycles (6, 12, 18, and 24 days) showed the Marshall stability decreased substantially after 6 days of freeze-thaw cycles and gradually gentle for the 12, 18 and 24 days of freeze-thaw cycles. Si, Ma, Wang, Li, & Hu, (2013) analyzed the effect of freeze-thaw cycles by using uniaxial compressive test for an asphalt mix. Results indicated that the resilient modulus and compressive strength decreased with raising in the number of freeze-thaw repetitions. The performance decreased substantially at a first number of freeze-thaw cycles. They also reported that a higher binder-aggregate ratio results in a small reduction in compressive performance under repeated freeze-thaw cycles. El-Hakim & Tighe, 2014 statistically evaluated the mechanistic properties of asphalt mixes subjected to freeze-thaw cycles. The dynamic modulus results indicated a major change in the norm of complex modulus especially at 4 °C and -10 °C. Results also demonstrated the benefit of additional binder content to the mix.

Previous research by Doré & Savard (1998) reported that 90 percent of fatigue damage occurs during spring thaw which is due to the effect of environment and traffic loads. During the thawing period, the melting of snow inducing an important bearing capacity loss. The loss of structural support from underlying layers creates a significant increase in tensile stresses at the bottom of the asphalt layers. In addition, there is another possibility of increased tensile stresses due to temperature variations and water expansion/ contraction which causes an increase in early fatigue cracking. This highlights a significant gap between actual loading conditions in the field and conditions considered during design. Based on these results, it appears that the action of traffic alone is not the cause of failure of bituminous asphalts in winter. Instead, it is probably the effect of thermal stress, thermal cycles, and moisture penetration which results in stress that exceeds the tensile strength of the asphalt materials (Carter & Paradis, 2010).

1.7 Thermomechanical Characteristics of HMA

Under the effect of the mechanical loading and temperatures (external solicitations), asphalt mixes are dominated by complex phenomena. The thermomechanical analysis of asphalt

mixtures is conducted in the laboratory by various tests. The thermomechanical characteristics of an asphalt mix depend on many factors such as the magnitude of applied stress or strain, temperature, and the rate of loading. Figure 1.9 indicates the change of behavior of asphalt cement according to temperature and level of strain amplitude. Asphalt behavior is viscous Newtonian liquid at high temperature and its behavior is like an elastic solid material at low temperatures. At normal temperatures, its behavior is linear or nonlinear viscoelastic (Di Benedetto & Corté, 2004).

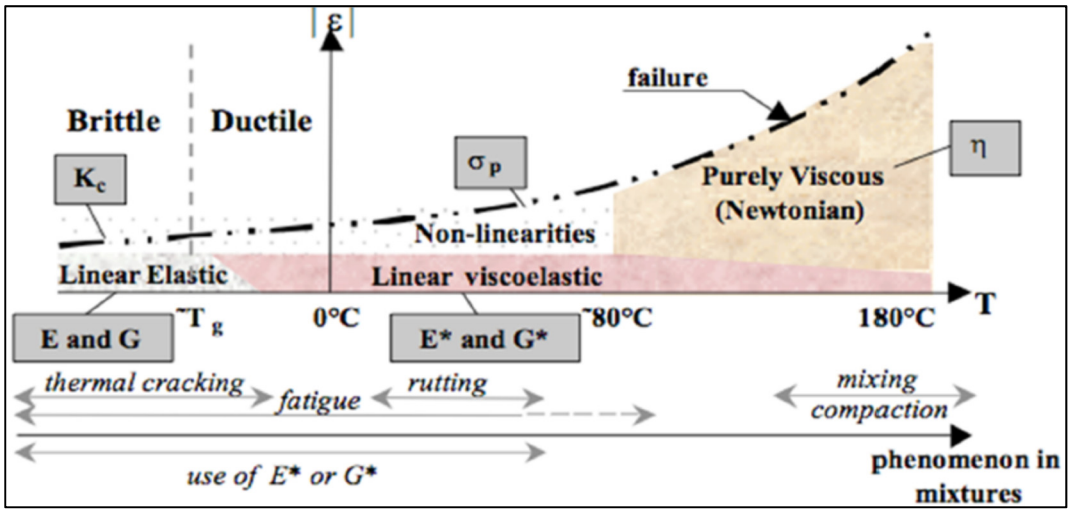

Figure 1.9 Bituminous materials behavior according to the strain level and the temperature
Taken from Olard and Di Benedetto (2003)

It is also possible to categorize the behavior of asphalt mixtures according to the level of strain amplitude and a number of loads repetitions it is shown in Figure 1.10. For a limited number of cycles but high strain amplitude, the asphalt mix has a highly non-linear behavior. With a few hundred of cycles with a low level of strain, the behavior of asphalt materials is linear viscoelastic. In this region, complex modulus test is conducted to analyze the stiffness behavior of an asphalt mix. With tens of thousands of cycles and low level of strain, it is a possibility of fatigue behavior. When stress deviatory cycles are applied from zero, there is the possibility of plastic deformation, which is close to rupture limit.

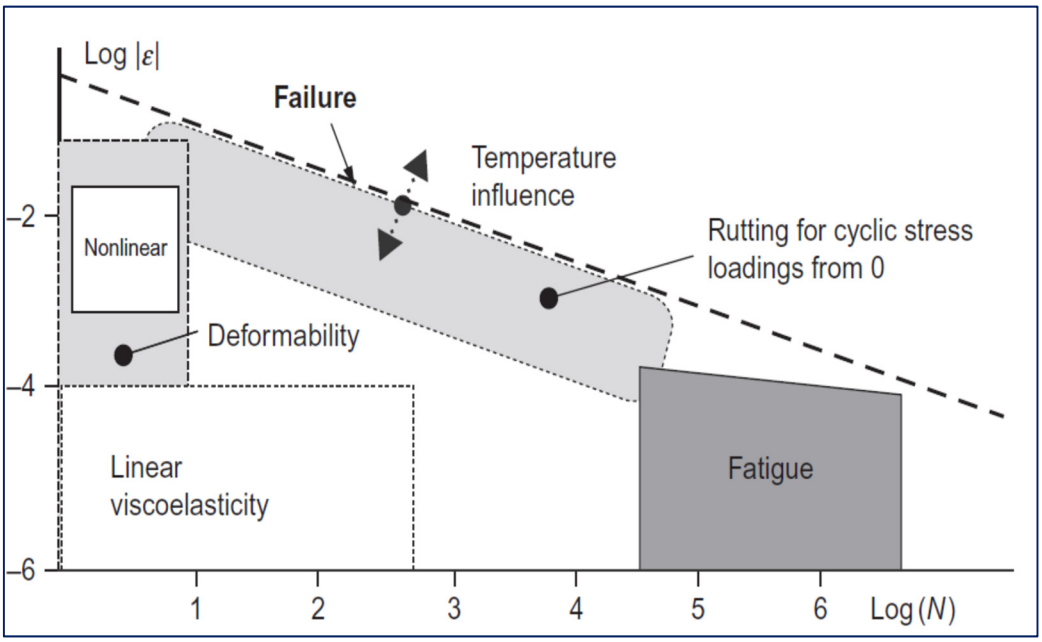

Figure 1.10 Different domains for an asphalt mixture
Taken from Olard and Di Benedetto (2003)

1.7.1 Complex Modulus

Linear viscoelasticity behavior of asphalt mixes is obtained from different types of tests. Complex modulus test by using Tension-compression test on the homogenous cylindrical specimen is utilized in this research to analyze the linear behavior of the asphalt mix. This approach is chosen by the University of Lyon/ENTPE laboratory to study bituminous materials (Di Benedetto et al., 2007a, 2011; Mangiafico et al., 2013; Nguyen et al., 2009, 2013; Pouget et al., 2010; Tapsoba et al., 2014).

The test can be performed under stress or strain control modes. In this research strain control modes have been implemented. The complex modulus can be defined as:

$$\varepsilon(t) = \varepsilon_0 \sin(\omega t) \tag{1.1}$$

where:

$\varepsilon(t)$: The amplitude of sinusoidal strain;

ε_0: Peak (maximum) strain;

ω: Angular velocity; and

t: Time, seconds.

The response of certain stress is also sinusoidal with the same angular frequency (BAAJ) which the formula can be defined as:

$$\sigma(t) = \sigma_0 \sin(\omega t + \emptyset) \tag{1.2}$$

$\emptyset$ is defined as a phase angle which is the lag between stress and strain and can be explained as the viscoelastic characteristic of an asphalt mix (Figure 1.11).

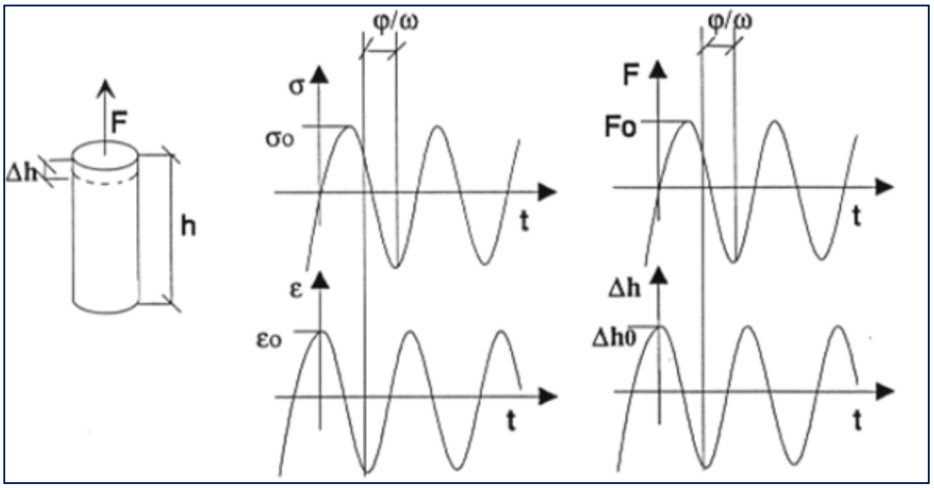

Figure 1.11 Tension-compression sinusoidal load (F) and displacement (Δh) which results in sinusoidal stress and strain at a given point of an asphalt specimen

A vector in cylindrical coordinates can represent applying a sinusoidal stress to the specimen. The applied stress and the resulting recoverable axial strain response of the specimen are measured and used to calculate the modulus. The load amplitude is adjusted based on the material stiffness, temperature, and frequency to keep the strain response within linear viscoelastic range. The phase angle is 0° for purely elastic material, and 90° for a purely viscous

material. The ratio of the amplitude of the sinusoidal stress of pulsation (ω) applied to the material $\sigma = \sigma_0 \, sin(\omega t)$ and the amplitude of the sinusoidal strain $\varepsilon_t = \varepsilon_0 \, sin(\omega t - \varphi)$ that result in a steady state (Eq.1.3) (Di Benedetto et al. 2004).

$$\boldsymbol{E^*} = \frac{\boldsymbol{\sigma}}{\boldsymbol{\varepsilon}} = \frac{\boldsymbol{\sigma_0 e^{i\omega t}}}{\boldsymbol{\varepsilon_0 e^{i(\omega t - \varphi)}}} \tag{1.3}$$

1.7.2 Rheological Models to Analyze the Complex Modulus

Asphalt is a viscoelastic material which can experience both elastic and/or viscosity characteristics at various conditions. Asphalt materials can be modeled based on the interaction of the strain or stress and their temporal dependencies. These models are introduced to measure the prediction of the material's responses at different temperatures and loading conditions. Asphalt behavior has viscous and elastic parts that are modeled as combinations of dashpots and springs (Huang, 2004). There are several mathematical models that are introduced to the characteristics of viscoelastic materials with using dashpots and springs. Some of them are shown in Figure 1.12.

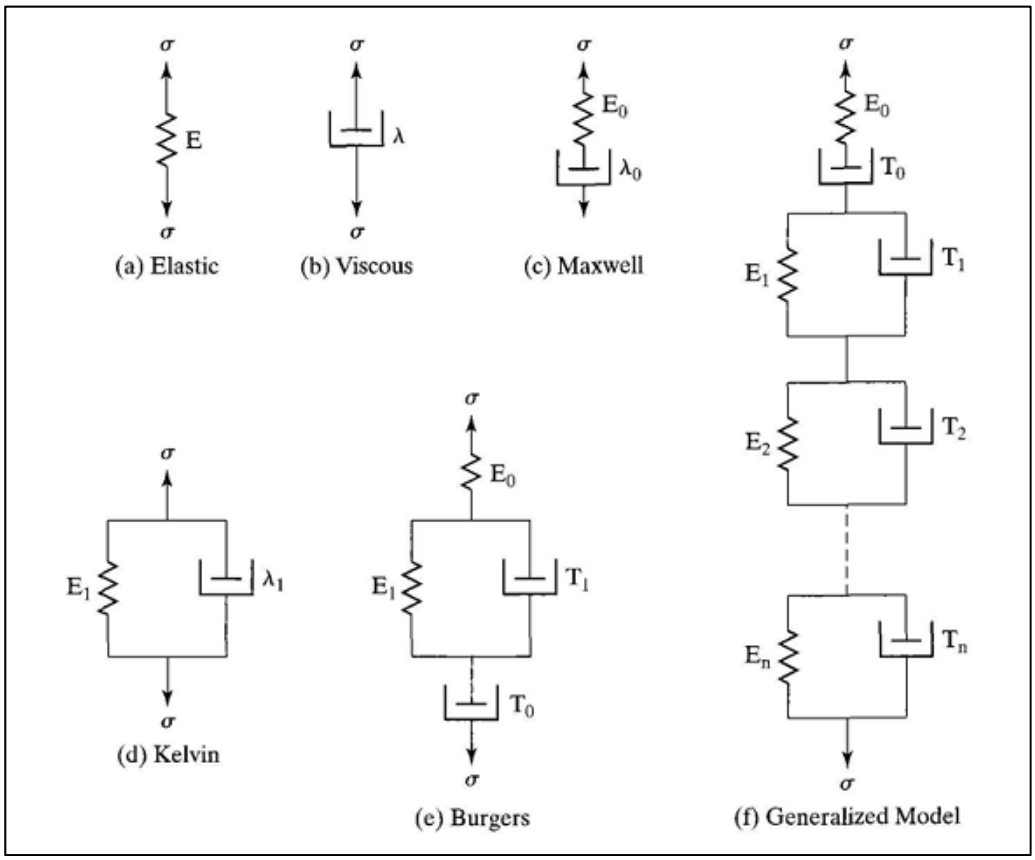

Figure 1.12 Mechanical models for viscoelastic materials
Taken from Arabani & Kamboozia (2014)

The results of complex modulus test of an asphalt mixture can be modeled by using the 2S2P1D (2 ***S***prings, 2 ***P***arabolic elements, 1 ***D***ashpot) model. This model was introduced at the University of Lyon and is a generalization of the Huet-Sayegh model (Olard & Di Benedetto, 2003). The model is based on a simple combination of physical elements (spring, dashpot, and parabolic elements). The model is a combination of physical elements such as spring, parabolic elements, and dashpot). Figure 1.13 indicates the graphical expression of the 2S2P1D model for asphalt mixes.

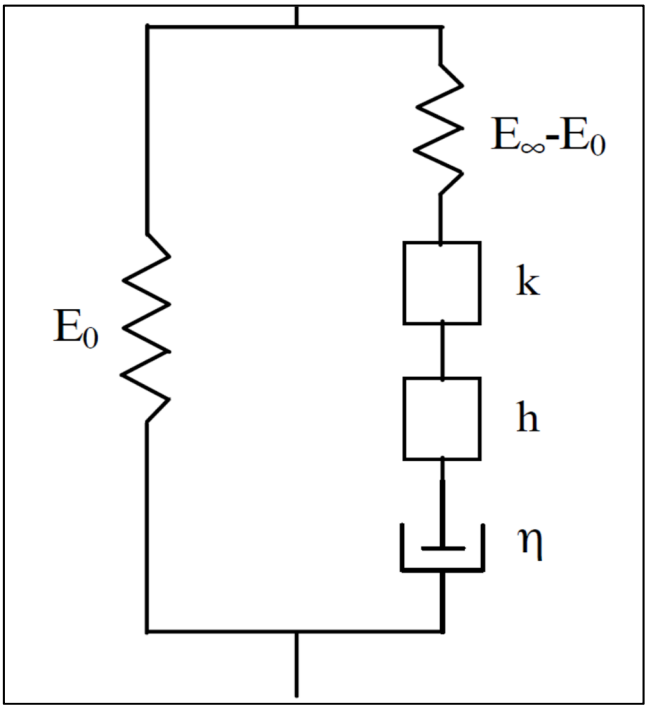

Figure 1.13 Representation of the introduced general model "2S2P1D" for asphalt mixes, h and k are two parabolic creep elements

1.8 Laboratory Performance Tests

Mechanical properties like stiffness modulus and fatigue resistance which are needed to make an analytical based pavement design are very often based on relationships between a parameter that is rather easy to determine by means of laboratory tests and parameters like tensile strength, stiffness and resistance to fatigue.

1.8.1 Fatigue Test

Fatigue failure is one of the main structural distresses in the pavement, which results in stiffness reduction of asphalt mixes with a number of load repetitions. Fatigue cracking starts at the bottom of the asphalt base layer due to the loss of the tensile strength and propagates through

the asphalt layers. Fatigue damage creates after a number of load repetitions. If the short-term loading of traffic is sufficiently high, it can result in stiffness reduction of the asphalt material and by accumulation in the long term, lead to failure.

In this research, the tension-compression method is used which was developed in the "ENTPE" to determine the fatigue damage of bituminous mixes (Di Benedetto et al., 1996). They are loaded in stress or in strain control mode using a sinusoidal cyclic loading. The advantage of this test is the homogeneous state of stress and strain inside the specimen. So the fatigue behavior is obtained directly from the values of stress (σ) and strain (ε).

1.8.1.1 Factors Affect Fatigue Behavior of an Asphalt Mix

The important fatigue studies were conducted in the 1960s and 1970s. Epps & Monismith (1972) prepared a summary of the effects resulting from binder stiffness, asphalt content, aggregate type, aggregate gradation, and air void content. The authors concluded that binder stiffness and air void content have a larger influence on fatigue life than aggregate type and gradation (Prowell, 2010). In general, the most important factors that affect fatigue characteristic of asphalt mixes are (Abojaradeh, 2003):

1) Mix design characteristics, such as the type of bitumen, bitumen content, the percentage of air voids, aggregate gradation;
2) Environmental variables, such as temperature, moisture, and freeze-thaw cycles;
3) Loading frequency, level of the strain amplitude, and whether there is rest period or not;
4) Specimen method of compaction;
5) Test equipment.

1.8.2 Thermal Stress Restrained Specimen Test (TSRST)

The TSRST gives a good idea of how the asphalt performs at low temperatures. Since the mid-1990s, in an effort to identify and prevent this type of contraction cracking, the MTQ has been

testing its pavement mixtures using a restrained specimen testing system known as the TSRST (Thermal Stress Restrained Specimen Test), which was developed as part of the SHRP (Strategic Highway Research Program). The École de Technologie supérieure (ÉTS) uses an MTS system to perform the same test (Carter & Paradis, 2010). First, the specimen is placed and fixed on MTS press system which is a kind of servo-hydraulic press. MTS device restrains the length of the specimen during the test. Then, the specimen is subjected to a constant cooling rate of 10°C/h which results in contraction of the materials and shrinkage of the specimen. The cracks initiate and specimen breaks when the traction stress is larger than the resistance of the asphalt materials.

1.9 Summary

Pavements are engineered structures designed to sustain stresses which provide a safe and comfortable driving surface to the public for a long period of time at the lowest possible costs. Understanding of pavement stresses and their quantifications are the major parts of pavement engineering. Stresses acting are classified as load induced or environmentally induced stresses.

Canada is located in the northern hemisphere where it experiences different climatic conditions throughout a year. The harsh fluctuations of temperature along with daily freeze-thaw cycles decrease the performance of Hot Mix Asphalt (HMA). The thermomechanical analysis of asphalt mix is conducted in the lab by various tests. The viscoelastic characteristics of an asphalt mix depend on many factors such as magnitude of applied stress or strain, temperature, and the rate of lading. Complex modulus test by using Tension-Compression on the homogenous cylindrical specimen is utilized to analyze the linear behavior of asphalt mix at different temperature and loading frequencies. The results can be modeled by using 2S2P1D model. The effect of regional freeze-thaw cycles on fatigue cracking has not been considered in the design methods in cold regions, whose results overestimate the pavement life. In this research, the tension-compression method is used to determine the effect of freeze-thaw cycles on fatigue durability of an asphalt mix.

The main benefit of this research program is to understand that how the asphalt pavement behaves during freeze-thaw cycles. The result of evaluation of asphalt fatigue damage will help to reach the modification to be able to better predict the behavior of asphalt fatigue characteristics in cold regions.

CHAPTER 2

RESEARCH FOCUS AND OBJECTIVES

2.1 Problem Statement

There are different mechanisms that can influence the performance of pavement structures in cold regions:

Frost action during winter: Asphalt is a waterproof material, but water can infiltrate into the asphalt mix from different mechanisms as explained in the literature. Water in big pores will freeze at a higher temperature than in small pores. Unfrozen water being pushed through the asphalt by frozen water as water freezes and expands. On the other hand, temperature decrease generates contraction in the mix. Expansion of water and contraction of the mix produce stresses in the voids of asphalt. If the developed stress exceeds the tensile strength of the asphalt, damage occurs. Expansion of freezing water during the winter causes more damage when it melts in spring.

Cooling process of an asphalt mixture: When an asphalt mix cools, the bitumen contracts more than the aggregate, the bitumen film on the aggregate gradually thins, and micro-cracks form in the pavement at a critical maximum temperature. The pavement becomes more brittle, and the micro-cracks eventually join together, creating cracks caused by thermal contraction.

Thaw action in during spring: One of the most important factors influencing the durability of asphalt mixtures designed for pavement construction is moisture-induced damage. A common manifestation of moisture-induced damage a loss of adhesion at the aggregate–asphalt mastic interface and/or cohesion within the bulk mastic. It has been shown that the mineralogical and chemical composition of aggregates may play a fundamental and more significant role in the generation of moisture damage, than bitumen properties such as penetration grade, acid number, and molecular size distribution.

During early spring; water gathered in the granular underlying layers is rapidly released and cannot be drained effectively because of the underlying frozen layer. Moreover, water at the asphalt mixture is often trapped by the snow and ice accumulated on the pavement sides which tends to seep into the pavement granular material. The bearing capacity of the base layer can be considerably reduced during that period and poorly supported bounded surfacing layers tend to experience excessive fatigue damage (Doré & Zubeck 2009). It does not depend on the quality of asphalt, especially for thick asphalt material.

Study of the mechanism: Contraction and expansion of asphalt materials can affect the pavement fatigue life duration. In the province of Quebec, and on the pavement surface, the number of freeze-thaw cycles averages at between 40 and 51 each year (Lamothe, Perraton, & Di Benedetto, 2014).

The initial hypotheses used in this research program have been implemented based on four mechanisms which explain above. The predicted bottom-up fatigue cracking model in the AASHTOWare mechanical-empirical pavement design software and other similar software is calculated based on stiffness loss due to the repeated traffic loads. Nevertheless, environmental loadings caused by fluctuations of temperature as well as the expansion and contraction of moisture inside the pores are also significant and possibly creates stresses that reduce pavement life especially in the zones where variations of temperature and precipitations are relatively high.

The Canadian climate is affected by different temperature ranges, including a series of freeze-thaw cycles. This environmental impact results in severe damage to the Canadian road network. The conditions of Canada's road infrastructure are deteriorating. More than 38% of pavements are in a poor or very poor conditions (Hesp et al., 2009). The development of sound correlation relating pavement structural performance to environmental impact has been one of the major areas of focus (El-Hakim & Tighe, 2014). Quebec infrastructure plan investment for the period of 2017 to 2027 reports that more than 19% of the investment goes for road network

itself (Lammam &MacIntyre, 2017). This relatively huge money need to manage appropriately in order to increase the quality of road systems. This is while more than 80% of roads in Quebec are flexible. In addition, the freeze-thaw cycles significantly affected the performance of asphalt pavements (Doré & Zubeck, 2009). This type of damage was categorized as water-induced damage and temperature susceptibility of asphalt mixtures and is one of the major distresses that occur in asphalt pavements (Kennedy, Roberts, and Lee 1983; Stroup-Gardiner and Epps 1987; Goh and You 2012). Wheel track damage recorded for three years on two observation sites in the province of Quebec indicates that the annual damage can reach 85% during the winter and spring thaws. On the other hand, the previous study has reported that more than 90 percent of the fatigue damage to these pavements occurred during spring periods (Doré et al., 2002). Especially, the level of damage is higher for secondary roads. This highlights a significant gap between actual loading conditions on the roadway and conditions considered during design. Based on these results, it appears that the action of traffic alone is not the cause of failure of bituminous asphalts in winter. Instead, it is probably the effect of thermal stress, thermal cycles, and moisture penetration which results in stress that exceeds the tensile strength of the asphalt materials.

As it is mentioned earlier, fatigue cracking starts at the bottom of the asphalt base layer which is mostly built with the GB20 mix in Quebec. Its rutting resistant with low binder content that makes it sensitive to fatigue damage. On the other hand, during thaw period, the melting of snow induces bearing capacity loss. The loss of structural support from underlying layers creates a significant increase in tensile stresses at the bottom of the asphalt layers. In addition, there is another possibility of increased tensile stresses due to temperature variations and water expansion/contraction which causes an increase in early fatigue cracking. The effect of temperature variation and moisture at the bottom of the asphalt layer is totally neglected so far. Previous studies investigated the daily thermal strain at the bottom of the asphalt layer. Results indicated that the thermal strain is even higher than the vehicle induced strain (Al-Qadi et al., 2005; Bayat et al., 2012).

2.2 Research Objectives

This research is aimed to focus on the effect of environmental freeze-thaw (FT) condition on the mechanical behavior of the base asphalt mix (GB20). The durability and performance of asphalt base mixtures subjected to repeated daily freeze-thaw cycles have not been studied yet. There have not been any fatigue criterions to take into account daily repeated freeze-thaw cycles. The main objective of this research project is to evaluate the effect of freeze-thaw cycles on the fatigue characteristics and stiffness modulus of the GB20 mix. The specific objectives of this study are indicated in Figure 2.1.

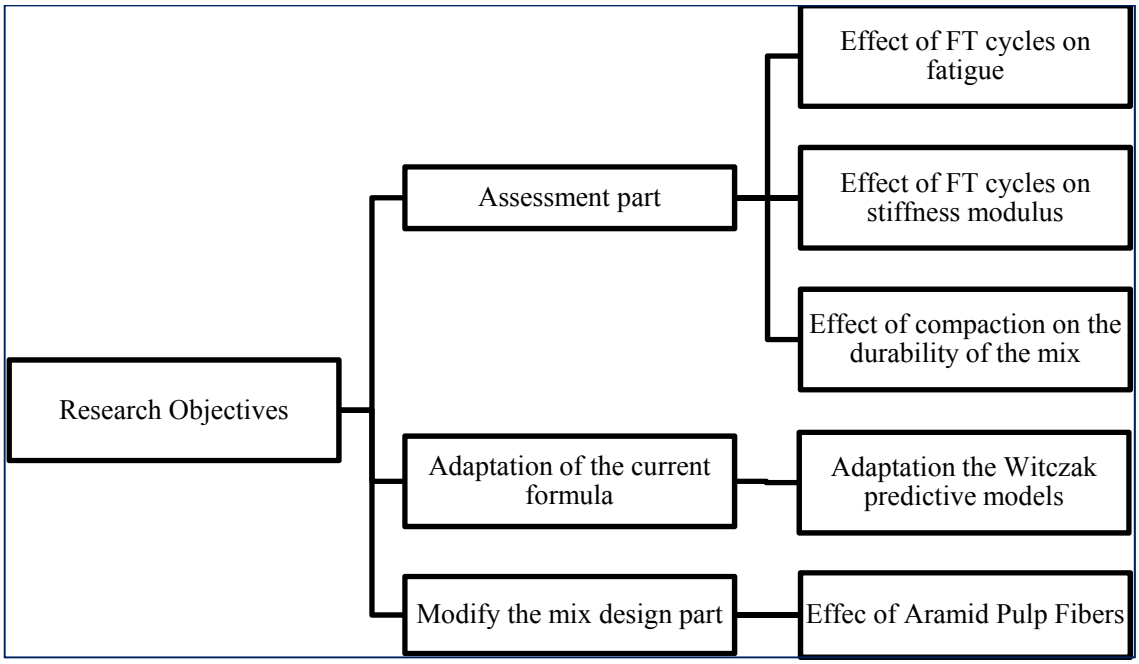

Figure 2.1 Research outline of this study

The main objective of this research project is to analyze the effect of freeze-thaw cycles on the behavior of a base course asphalt mix, GB20.

The specific objectives of this study are:

- To evaluate the effect of freeze-thaw on the rheological behavior of hot mix asphalt;

- To evaluate the effect of freeze-thaw on fatigue behavior of hot mix asphalt;
- To evaluate the effect of compaction and level of air voids on durability of an asphalt mix subjected to freeze-thaw cycles;
- To adapt the current Witczak E* model to increase the durability of the GB20 mix based on the lab results;
- To evaluate the effect of fiber additive on the durability of hot mix asphalt in cold region environment.

2.3 Outline of Thesis

This Ph.D. thesis is manuscript based thesis separated in different sections plus an introduction. In this regard, Chapter 1 covers the literature review on this research with emphasis on the effect of freeze-thaw cycles on flexible pavements. The problem statement, the objectives and the outline of the research are explained in Chapter 2. Chapter 3 explains the effect of compaction and percentage of voids in the performance and durability of the conditioned mix compare with the reference mixture. It is also available and published in the Cold Regions Science and Technology. Chapter 4 demonstrates the importance of freeze-thaw factor in the fatigue and complex modulus prediction formula. It published in the Journal of Materials in Civil Engineering (ASCE). And chapter 5 demonstrates the mix design improvement technique with using Aramid Pulp Fiber in the mix. It published in the Construction and Building Materials.

CHAPTER 3

EFFECT OF LABORATORY COMPACTION ON THE VISCOELASTIC CHARACTERISTICS OF AN ASPHALT MIX BEFORE AND AFTER RAPID FREEZE-THAW CYCLES

Saeed Badeli [a], Alan Carter [b], Guy Doré [c]

[a,b] Department of Construction Engineering, École de Technologie Supérieure,

1100 Notre-Dame Ouest, Montréal, Québec, Canada H3C 1K3
[c] Department of Construction Engineering, Université Laval, Quebec, Canada, G1V 0A6

Article published in Cold Region Science and Technology,
Volume 146, February 2018, PP. 98-109

3.1 Abstract

Environmental conditions, the rate of loading and mixture properties are the most important factors that affect the complex modulus (|E*|) values. The effect of environmental freeze-thaw (FT) cycles on viscoelastic properties of asphalt base materials has not been investigated properly yet. At the bottom of the asphalt base layer in a pavement structure, there is higher tensile strain due to traffic, and it usually has a higher air voids content which is mostly due to a poor compaction during construction. Asphalt mixture with a nominal maximum aggregate size of 20 mm, called ‘‘Grave Bitume’’ (GB20) which is normally used as a base layer in Quebec, was used in this study. The main objective of this study is to compare the complex modulus test results of the dry, partially saturated, and FT conditioned specimens with different compaction levels. Three different air voids (2%, 3.5%, and 7%) are targeted in this project. The saturated specimens are subjected to complex modulus test carried out using the Direct Tension-Compression test. The rheological model 2S2P1D is implemented to simulate the behavior of the mixes according to various temperatures and frequencies. The results indicate that the compaction level significantly affects the behavior of the mix after a large number of rapid FT cycles. The effect of FT cycles on viscoelastic behavior of the mix is added to the Witczak formula in order to improve the prediction of the service life of asphalt GB20 base mix. Comparison between the laboratory determined and predicted data indicate that the

relative bias in the modulus prediction after 300 FT cycles, especially due to the high percentage of voids. This can be eliminated by applying the improved equation to the predicted values.

3.2 Introduction

Asphalt pavements are influenced by two main types of loading: mechanical loading, especially due to heavy trucks, and, climatic effects as a result of moisture, temperature, and freeze-thaw (FT) cycles. Various pavement design theories determine the pavement design while considering traffic load, environmental impact, and pavement life cycle. The development of sound correlations relating the performance of pavement structures to the effect of the environment has gained interest over the years (Carter & Paradis, 2010; Doré & Zubeck, 2009; El-Hakim & Tighe, 2014).

Many researchers have been working on the influence of FT cycles on the degradation of asphalt mixes in the past (El-Hakim & Tighe, 2014; Goh & You, 2012; Lamothe, Perraton, & Di Benedetto, 2015, 2016; Özgan & Serin, 2013; Tang, Sun, Huang, & Wu, 2013; Xu, Guo, & Tan, 2016). In cold regions, FT damage significantly affects the performance and durability of asphalt pavements. Freezing of water in pores of asphalt mixes cause severe degradation and reduction in service life of pavement structures. Water infiltration combined with the variation of temperatures deteriorates the adhesive bond between aggregates and binder (Gubler et al., 2005; Xu et al., 2016) (Gubler, Partl, Canestrari, & Grilli, 2005; Xu et al., 2016). Expansion of water and contraction of the mastic produce pressure in the voids of asphalt which creates stress during harsh winter time. It is basic information that pure water freezes at around 0 °C. A 9% of expansion happens as the water phase turns to ice under normal environmental condition. However, remaining water that is trapped inside the capillary voids does not necessarily freeze at 0°C. Size of the pores plays an important part to define a freezing temperature of trapped water. As pore size decreases, the obliged temperature to freeze the water also lessens (Hale, Freyne, & Russell, 2009).

It is the technical common knowledge that the thermal behavior of bituminous mixes is affected by its moisture content, as well as air voids content (Hassn et al., 2016). Air voids are generally described as the most important parameter to explain mix characteristics and play important role in analysis of asphalt mixes in cold regions. High level of air voids always results in high expectations of moisture flow within mixtures (Xu et al., 2016). As water penetrates through voids and cracks, these effects may bring weak and saturated pavement structures. This is while the behavior of water inside an asphalt mix is highly complicated (Chen & Huang, 2008). Air and water cause volatilization of lighter constituents from asphalt cement and oxidation of asphalt binder, and both processes increases the rate of aging of the mixture, making it stiffer and more brittle (Robert & Suckhong, 1996). The air voids content in an asphalt mixture is a function of the aggregate gradation, the asphalt content, and the degree of compaction. Compaction of asphalt pavements is an important process because it has a significant effect on performance (Asphalt Institute, 1989). Compaction process causes an increase in the aggregate interlock, decrease in the percentage of voids, and decrease in unit weight of a mix. The fatigue results are generally better when the air voids decrease (Di Benedetto, Partl, Francken, & Saint André, 2001). The distribution of air voids is another important factor that impacts the moisture susceptibility of asphalt mixes. It is related to the method of compaction, compaction effort, aggregates characteristics, aggregate gradation, and temperature (Masad et al., 2001). Terrel and Al-Swailmi (1994) evaluated the moisture sensitivity of asphalt mixes having a different percentage of air voids by using the indirect tensile strength test. They found that the conditioned specimens have lower indirect tensile strength, and this reduction depends on the percentage of air voids in the mix (Terrel & Al-Swailmi, 1992). Subsequently, asphalt mixes were classified into different groups namely: impermeable, having pessimum percent of voids, and a high percentage of voids with exhibiting free drainage. At pessimum range, where moisture sensitivity of mix was maximized, was found to have around 8 percent of voids. Masad et al. (2006) assessed moisture damage in different asphalt mixes that were compacted by the same targeted air voids but having different gradations to make diverse air void distributions. They used x-ray computed tomography technique to determine the average void diameter of the mixes. They found a range of pessimum air voids sizes in which moisture damage was maximized (Birgisson, Soranakom, Napier, & Roque, 2004). Feng et al. analyze

the influence of salt and FT cycles on volume, weight, and strength of asphalt mixes. Results showed that damage initiated by the load associated with the ice expansion and deteriorated by the loss of adhesion between the asphalt-aggregate or cohesion loss of asphalt mortar (Feng et al., 2009). They also found that the air voids is one of the main factors influencing on FT strength (Modarres, Ramyar, & Ayar, 2015). Gong et al. (2016) investigated the effect of FT cycle on the low-temperature properties of the asphalt fine aggregate matrix. They found that the tiny air voids in the mix mean less space for volume expansion of freezing water which causes greater expansion pressure in the asphalt with the fine aggregate matrix (Gong et al., 2016).

The extreme temperature variations in Quebec region have significant influences on the performance of asphalt pavements (Carter & Paradis, 2010). Quebec's roads are subjected to seasonal ambient temperature variations of 60°C, and daily rapid variations of temperature that may run as high as 30°C. These significant temperature variations in combination with the moisture inside the pores result in the development of premature deterioration (Lamothe et al., 2015), and it can change the viscoelastic characteristics of the asphalt mixtures (Badeli, Carter, & Doré, 2016). Asphalt layer systems in pavement structures are usually composed of two or three different layers with different thicknesses: wearing course, binder course and base course. Base layer plays a major role in bottom-up fatigue cracking resistance (Badeli, Carter, & Doré, 2018). At the bottom of the asphalt base layer, there is higher tensile strain due to traffic, and it has a higher amount of air voids that is mostly due to a poor compaction during the construction. On the other hand, during thaw periods, water can penetrate through a saturated base by capillary rise. The bearing capacity of underlying layers reduces substantially during the thaw periods due to the melting of ice and insufficient pavement drainage (Doré & Zubeck, 2009). Figure 3.1 shows collected data by the Ministry of Transportation of Quebec (MTQ) that illustrates the daily asphalt temperature (asphalt base course) history for a road in the south part of Quebec (Route 155, Trois Rivière), from the first of November 2014 to the first of May 2015. It can be seen that asphalt temperatures are higher than the air temperatures, although they both follow the same trend.

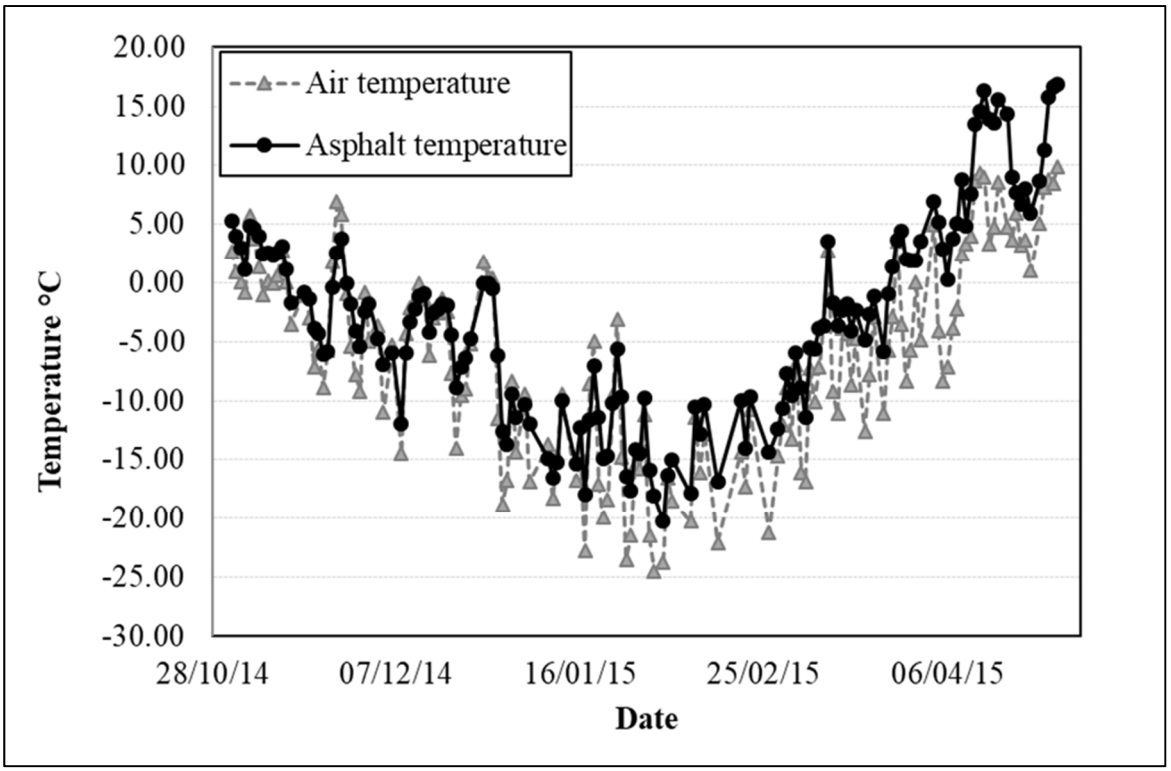

Figure 3.1 Daily temperature history of Route 155 in Trois Rivière in Quebec from November 1st 2014 to May 1st 2015 (Badeli et. al., 2017)

In view of this, the main goal of this paper is to evaluate the impact of compaction level on the viscoelastic characteristics of the asphalt base mix (which is called GB20 in Quebec) before and after rapid FT cycles. Direct Tension-Compression (DTC) complex modulus test is conducted at various temperatures and frequencies on dry, saturated, and FT conditioned specimens having different compaction levels. With an improvement of the Witczak predictive model formula in mechanistic-empirical pavement design guide (MEPDG) which is the research version of the DARwin-ME software by AASHTO, pavement should last longer.

3.3 Experimental Investigation

This section describes specimen preparation, and the procedures of the FT conditioning in detail, including the moisture conditioning, specimen preparation before putting the specimens

in the chamber and temperature programming for rapid FT cycles. Mix design tests were conducted according to the LC method of mix design. LC Method of Mix Design presents the mix design method that was developed by the pavement laboratory (Laboratoire des Chaussées) at the ministry of transportation of Quebec (MTQ).

3.3.1 Materials

Asphalt mixture with a nominal maximum aggregate size of 20 mm, called "Grave Bitume" (GB20) which is normally used as a base course in Quebec, was used in this study. One type of binder was chosen in this study with a Superpave™ Performance Grade of PG 64-28 asphalt binder. The LC method (also known as MTQ's Method of Mix Design) has specifications in accordance with the volume of the effective asphalt binder (V_{be}). To that end, maximum theoretical specific gravity (G_{mm}) was determined in accordance with the LC 26-045 (MTQ, 2005) to find the volume of absorbed bituminous binder (V_{ba}). Once the V_{ba} has been found, the binder content (P_b) was set in order to obtain the desired V_{be}. The various proportions of each aggregate and characteristics of the reference mix are presented in Table 3.1.

Table 3.1 Asphalt mixture composition and volumetric characteristics

Aggregate gradation		
Sieve No.	GB20 mix, Passing (%)	
	Requirements	Used
28 mm	100	100
20 mm	95-100	98
14 mm	67-90	85
10 mm	52-75	70
5 mm	35-50	41
2.5 mm	-	24
1.2 mm	-	16
0.63 mm	-	12
0.315 mm	-	8.0
0.160 mm	-	7.0
0.08 mm	4.0-8.0	5.5
Filler	-	0.4
Volumetric Characteristics of the mix		
G_{mm}[1]	2.552	
V_{ba}[2] (%)	0.952	
V_{be}[3] (%)	10.202	
b[4] (%)	4.504	
[1] maximum theoretical gravity of the mix [2] volume of binder absorbed [3] volume of effective binder [4] binder content		

3.3.2 Specimens Preparation

Shear gyratory compactor (SGC) device was used to verify the ability of compaction of the mix. For this reason, the variation in the air voids (Va) of the specimens under constant pressure (600 kPa) were recorded during SGC test as stated in the LC 26-003 (MTQ, 2005). The rutting resistance was tested with the French laboratory slab compactor (Figure 3.2) according to Quebec Standard LC 26-400 (MTQ, 2005). The rutting depth must be below 10% after 30,000 cycles.

After mix design study and find the desired specifications of reference mix, specimens were prepared with SGC device and divided into three different groups according to the level of

compactions. The measured amount of air voids was calculated. A saturation process in accordance with the Quebec standard introduced the percentage of liquid in the specimen's voids network. Rheological behavior in small strain domain has been conducted to measure the complex modulus before and after the rapid freeze-thaw cycles. Those tests in this paragraph are described in following sections.

Figure 3.2 French laboratory slab compactor (LPC)
Taken from Badeli et. al., 2017

3.3.3 Specimens Classification

Thirty specimens were divided into three groups (A-1, A-2, and A-3) of 10 specimens each according to a different level of gyrations. Table 3.2 shows the classification of the specimens in each group.

Table 3.2 Classification of the specimens in each group

Group	Number of specimens	Target percentage of air voids (%)	Dummy specimens prepared for temperature history analysis in dry condition	Specimens prepared for analysis in dry condition	Specimens prepared for analysis in wet condition	Specimens prepared for analysis after 150 FT cycles	Specimens prepared for analysis after 300 FT cycles
A-1	10	2.00	2	2	2	2	2
A-2	10	3.50	2	2	2	2	2
A-3	10	7.00	2	2	2	2	2

The required mass for SGC test is calculated as Equation (3.1):

$$m = G_{mm} \times \rho \times \frac{\pi \times Ø^2}{4} \times h(min) \quad (3.1)$$

where, m is mass of the mixture expressed in grams; Gmm is maximum theoretical specific gravity of the mixture; ρ is specific density of water; Ø is diameter of the mold cylinder, in millimetres; h(min) is height of the specimen, at 0% air voids, in millimeters (115 mm).

The desired percentages of air voids were determined using the SGC test at different gyration levels, but keeping the same mix design characteristics according to the LC 26-003 method (MTQ, 2005). The theoretical percentage of air voids for each set of the specimens was calculated by Equation (3.2).

$$V_a = 100 \times \frac{h(ng) - h(\min)}{h(ng)} \quad (3.2)$$

where, Va is theoretical air voids in the mix expressed as a percentage; h(ng) is specimen height (mm) at a given number of gyrations; h(min) is the height of the specimen, at 0% air voids in millimeters (115mm).

The compactor settings used in this study were in accordance with Superpave specifications. The SGC was stopped manually when it reached the desired percentage of air voids. Figure 3.3 shows the average theoretical air voids for the 3 groups versus a number of gyrations in different groups.

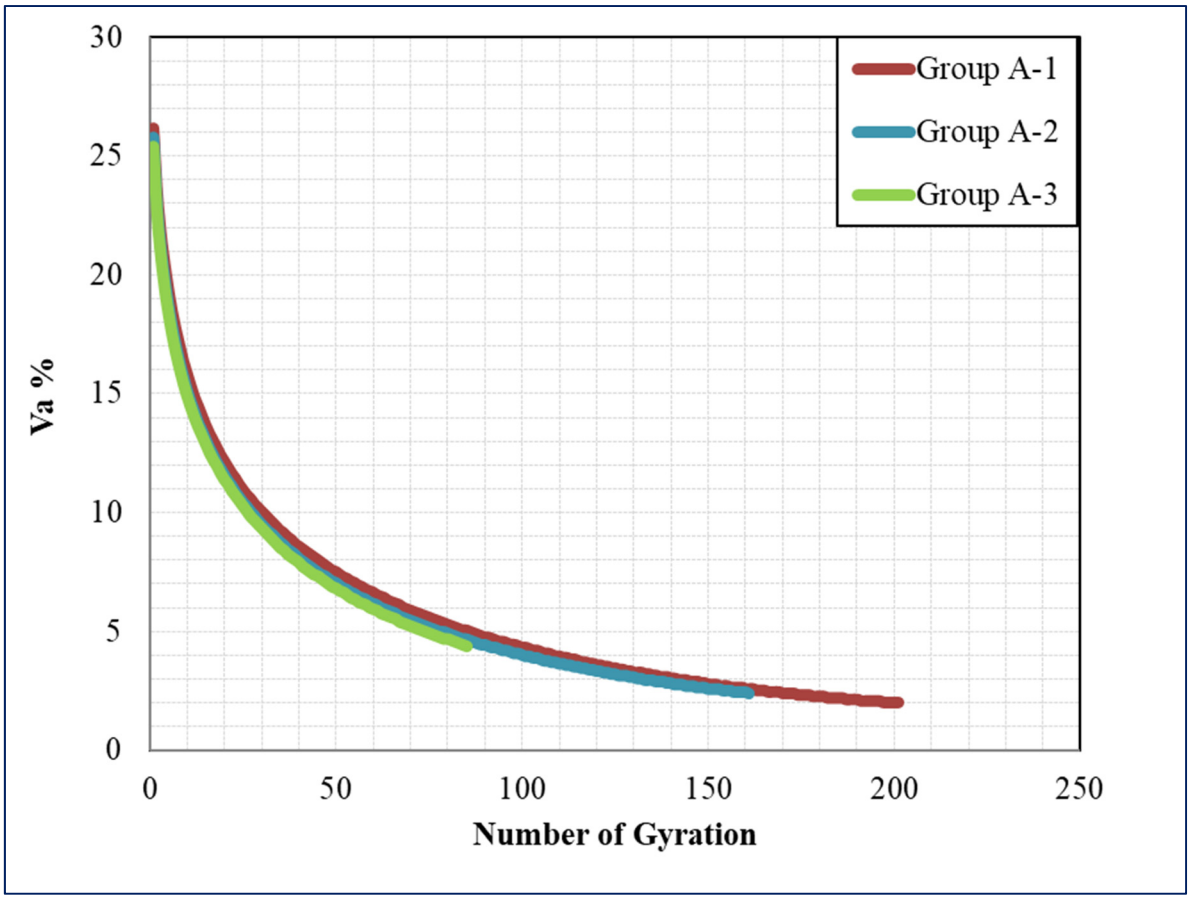

Figure 3.3 Variation in the air voids versus number of gyrations for the all mix groups

After curing time (minimum of two weeks at room temperature), specimens of 75 mm in diameter were cored from the SGC specimens. The cored specimens were trimmed and grinned, then stocked horizontally in sand beds to prevent any bias deformation (Lamothe et al., 2015).

3.3.4 Air Voids Classification

Before putting instrumentation in place, the measured percentage of air voids were calculated according to the Equation (3.3):

$$V_a = (1 - \left(\frac{G_{mb}}{G_{mm}}\right)) \times 100 \quad (3.3)$$

where, V_a is actual percentage of air voids, G_{mb} is the bulk specific gravity of a mix, G_{mm} is the maximum theoretical specific gravity. The bulk specific gravity can be measured by calculating the mass of the specimen in its dry condition when it is submerged in the water tank, and when it was in its saturated surface-dry (SSD) condition (Chehab et al., 2000).

Characteristics of specimens before instrumentation and saturation are given in Table 3.3. In addition to the total air voids of the specimen, percentage of connected air voids is another important parameter for evaluating the pore structures of the mix. Depending on the internal structure of the mixture, there are non-connected air voids which are associated with the method of compaction and the aggregate structures. The durability of asphalt mixes is affected by the total connected air voids (Alvarez et. al., 2009). The moisture cannot enter the mixture through non-connected voids to deteriorate the specimen, and they will have a lower effect on the moisture-related damage to the mix. Yi et al. (2016) worked on the effect of connected inner voids on laboratory moisture test. They reminded that non-connected inner voids have a minor influence on the moisture damage of the mix. Therefore, to characterize the environmental susceptibility of the mixture, a clear understanding about the percentage of connected air voids over the total air voids, is important. The percentages of connected air voids per total air voids have been calculated with Equation (3.4) and are shown in Table 3.3 for all groups.

Table 3.3 Main measured characteristics

Mix group	Number of specimens	Average height (mm)	Average diameter (mm)	Average volume (mm^3)	Average bulk specific gravity of specimens	Max. specific gravity of the mix	Target of air voids (%)	Average measured of air voids (%)	Standard deviation of measured air voids (%)	Average percentage of connected air voids/total voids (%)
A-1	10	157.5	74.01	677,130	2.53	2.57	2.00	1.97	0.12	3.65
A-2	10	146.5	74.01	630,520	2.48	2.57	3.50	3.45	0.12	7.56
A-3	10	142.1	74.01	611,360	2.35	2.57	7.00	6.85	0.18	20.17

$$CV = \frac{WssD - Wdry}{WssD - Wsub} \quad (3.4)$$

where *CV* is connected-voids (%); *WSSD* is saturated surface dry weight (g); *Wdry* is dry weight (g); *Wsub* is saturated surface dry weight submerged in water (g).

As it is indicated, group A-3 had the significantly higher connected voids (20.17%) compare to the A-1 (3.65%) and the A-2 (7.56%).

3.3.5 Moisture Conditioning Procedure

There is no practical and reliable moisture test to simulate the field moisture performance for asphalt mix during the design stage. The reason is that the specimen conditioning method cannot represent the field conditions, resulting in underestimating the effect of moisture for some mixes. Air voids distribution and percentage, as well as the vacuum pressure for achieving moisture saturation, are two main parameters which have a significant impact on the moisture testing results (Yi et al., 2016).

In order to introduce liquid into the specimen's voids network, a saturation process was adapted from the test method specified by LC 26-001 for moisture resistance measurements (MTQ, 2005). Mixtures with more connected voids could easily reach 70% to 80% saturation level without severe vacuum pressure conditioning. The first two specimens at each group were kept the air dry (D) as controlled reference specimen for complex modulus test. The other two specimens from each group were conditioned through vacuum saturation. Two steps were considered. First, the specimen was placed in a container at a minimum of 25 mm above the container bottom whose pressure (P) was kept below or equal to 4 kPa. Then, the desiccator was filled with de-aerated water under vacuum ($P \leq 4$ kPa or 30 mm- Hg), for a conditioning period of 30 minutes. This conditioning mimics field performance for up to four years (Bagampadde et al., 2004). Previous researchers reported that air voids in full-saturated asphalt mix can increase more than 50% after 8 FT cycles (Xu et al., 2016; Ozgan et al., 2013; Freng

et al., 2010). In this study, the degree of saturation was targeted to be less than 70 percent to prevent water damage of the mix. However, mixture with a low percentage of connected air voids (e.g. A-1), is not easy to reach the desired saturation level without being pre-damaged **(**Kringos et al., 2009**).** To this end, a constant low pressure of vacuum is required to reach a certain percentage of saturation in the specimen, without creating severe micro-damage (Yi et al., 2016). The degree of saturation is defined by using the following Equation (3.5):

$$\mathrm{DS} = \frac{100 \times J}{V_a} \tag{3.5}$$

where, DS is a degree of saturation, percent; V_a is Volume of air voids, cubic centimeter, which can be determined from Equation (3.6). *J* is the volume of absorbed water, cubic centimeter, which can be determined from Equation (3.7);

$$V_a = \frac{P_a V}{100} \tag{3.6}$$

where, V is the volume of the specimen, cubic centimeter; P_a is a percentage of air voids calculated from Equation (3.3).

$$J = B' - A \tag{3.7}$$

where, B′ is a mass of the saturated, surface dry specimen after partial saturation, g; and A is a mass of the dry specimen in the air, g.

Table 3.4 gives the data used to calculate the average degree of saturation for each group. At the end of the saturation process, void content calculated again for each specimen to make sure that the saturation process did not create severe micro-damage inside the mix. Then the specimens were wrapped in a latex membrane, and waterproof tapes were placed around the specimens to prevent water loss during the FT cycles.

Table 3.4 Measured Characteristics after Saturation

Mix group	Average measured % of air voids	Average volume of Specimens (mm^3)	Average weight of the specimens (gr)	mass of the saturated, surface dry specimen (gr)	Average degree of saturation of the specimens (%)	Standard deviation of the degree of saturation (%)
A-1	1.97	677,130	1,540	1,542	50.47	3.21
A-2	3.45	630,520	1,548	1,552	63.74	3.10
A-3	6.85	611,360	1,540	1,548	70.32	2.17

3.3.6 Experimental Procedures for Freeze-Thaw Cycles

There is no standard method to evaluate the daily FT cycles of asphalt mixtures. After the saturation process, each set of asphalt specimens were submitted to 150 and 300 freeze-thaw cycles in the programmable chamber (Figure 3.4) as set forth in ASTM C-666.92 (ASTM, 2008), "Standard Test Method for Resistance of Concrete to Rapid Freezing and Thawing". The cooling and heating rate used was 4.5 °C/min. For each FT cycle, two different temperature levels were targeted, which were -18 and 6 °C. At each level, the temperature was kept constant for a period of 1.5 hours. No specimen was oven dried before or after the rapid FT testing since it might affect the viscoelastic characteristics of asphalt mix.

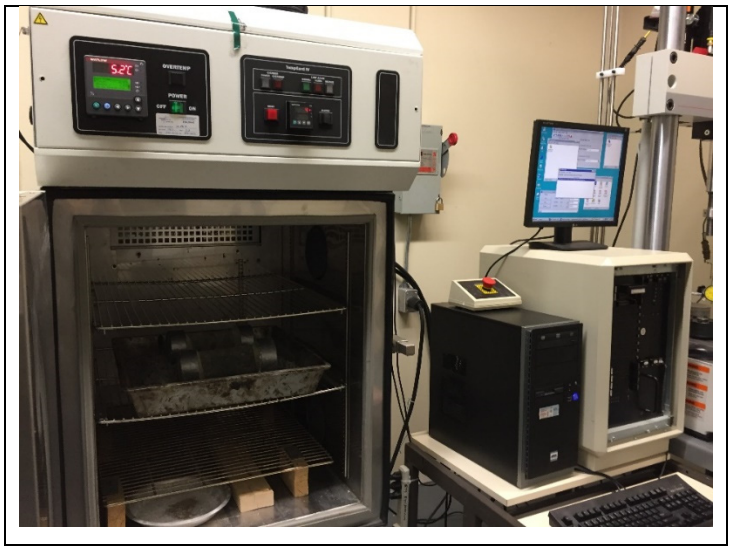

Figure 3.4 Programmable chamber used for FT cycles

In each group, four specimens were saturated and submitted to 150 and 300 FT cycles and another two dried-dummy specimens were equipped with thermocouples in order to analyze the history of temperature during the rapid cooling-heating process. Thermocouples were placed on the surface, beneath and inside the specimens. To place the thermocouple inside, the specimen was drilled and the hole was filled with bitumen prior to the introduction of the thermocouple (Figure 3.5).

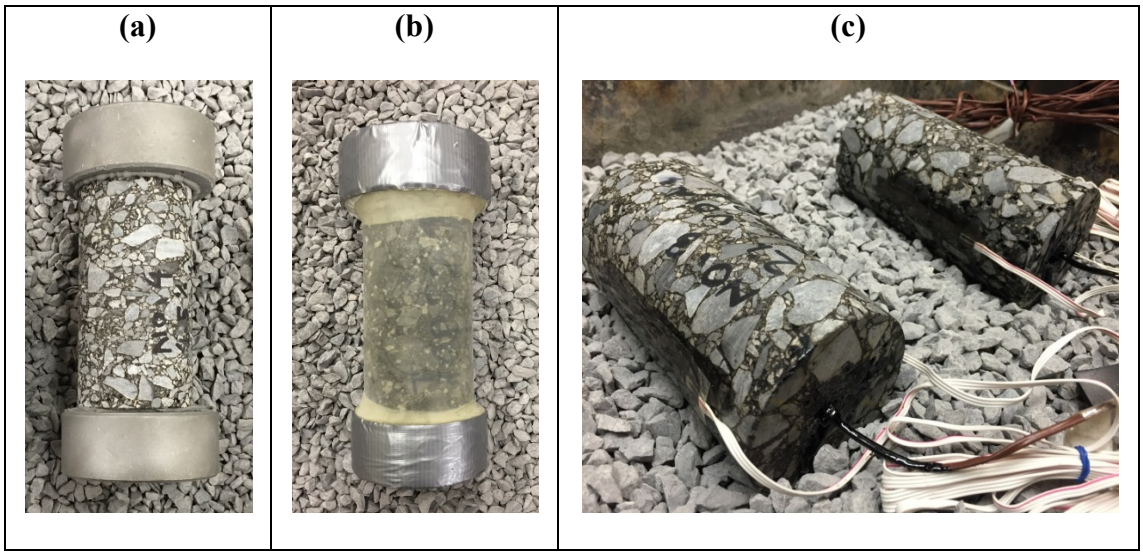

Figure 3.5 Specimens prepared for freeze-thaw cycles and thermo-mechanical test: (a) Reference specimen; (b) specimen covered by Latex membrane to avoid water evaporation during handling and FT cycles; (c) Instrumentation of dummy specimens (temperature sensors inside and around the specimens)

3.3.7 Linear viscoelastic Investigation

In order to analyze the structural behavior of asphalt mix and its evolution with time in the laboratory, thermomechanical properties in small strain domain amplitude of the specimens were investigated with regard to complex modulus (|E*|) test. Comparison the |E*| and fatigue durability test results in the previous study indicated that the analysis of the complex modulus test can predict the durability of asphalt mix under the repeated FT cycles in the lab (Badeli et al., 2017).

|E*| is observed for very small strain amplitude and corresponds to the linear viscoelastic behavior of mixtures. The complex modulus is the expression of the stiffness of a viscoelastic material under cyclic loading and is calculated by Equation (3.8):

$$|E^*| = \frac{\sigma_0}{\varepsilon_0} \tag{8}$$

Where σ_0 is the maximum stress amplitude and ε_0 is the peak recoverable strain amplitude. The Phase angle (φ) is described as a phase lag of the strain behind the stress under the sinusoidal cyclic solicitation. The phase angle is 0° for a purely elastic material, and 90° for a purely viscous material. The ratio of the amplitude of the sinusoidal stress of pulsation ω applied to the material $\sigma = \sigma_0 \sin(\omega t)$ and the amplitude of the sinusoidal strain $\varepsilon_t = \varepsilon_0 \sin(\omega t - \varphi)$that result in a steady state (Equation (3.9)) (Di Benedetto et al., 2001).

$$|E^*| = \frac{\sigma}{\varepsilon} = \frac{\sigma_0 e^{i\omega t}}{\varepsilon_0 e^{i(\omega t - \varphi)}} \tag{3.9}$$

In this project, |E*| tests were performed before, after saturation, and after analyzing rapid freeze-thaw cycles by using the Direct Tension-Compression test on cylindrical specimens. An environmental chamber (MTS) was used for thermal conditioning during the |E*| tests (Figure 3.6). The temperature was controlled by three temperature probes which were placed on the surface of the specimens. The strain was detected with three extensometers placed on the specimens at an angle of 120° from one another. The target applied strain was fixed at 50 μ-strain to ensure that the measurement was maintained within the linear viscoelastic domain as explained in Figure 3.7 (Di Benedetto et al., 2004). Researchers showed that the time-temperature superposition principle can be conducted with good approximation to asphalt mixtures in the small strain domain (Nguyen et al., 2012).

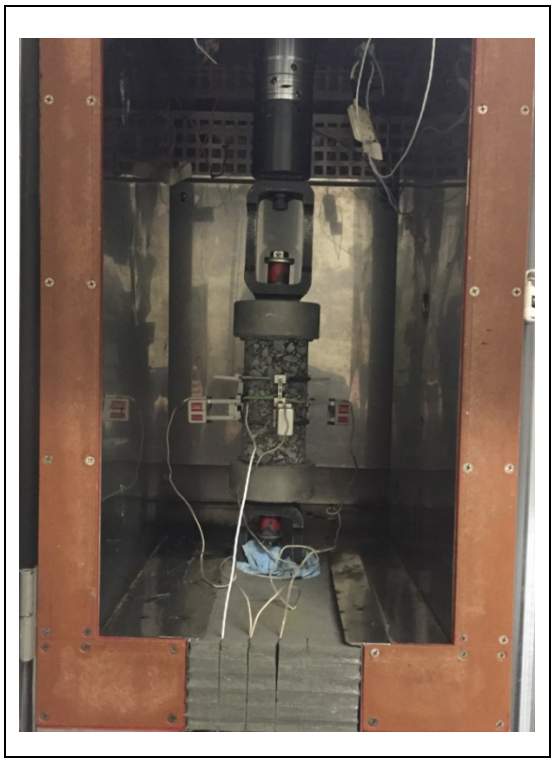

Figure 3.6 MTS measurement system for complex modulus test

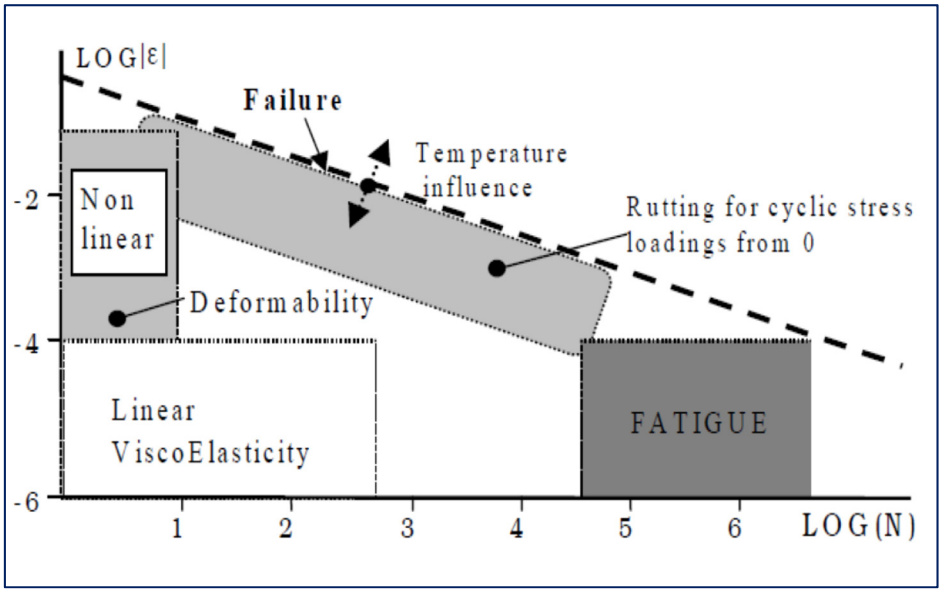

Figure 3.7 Different domains of behavior observed on asphalt mixture
Taken from Olard et al. (2003)

MTS press was used over a range of various temperatures (−35°C, −25°C, −15°C, −5°C, +5°C, +15°C, +25°C and +35°C) and frequencies (10, 3, 1, 0.3, 0.1, and 0.03 Hz). A stabilization time period (6 hours) was considered when the temperature was changed. During this period, the load applied to the specimen is null. This rest period ensures a homogeneous temperature inside and outside the specimen (Tapsoba et al., 2014). A rest period which is about 5 min is also applied between two successive cyclic loading periods to avoid self-heating effect. For each mix, a total of two cored specimens were tested. As per Di Benedetto and De la Roche (1998), complex modulus test results can be presented using isothermal curves, isochronal curves, Cole-Cole plane and Black space diagram.

3.4 Results and Discussions

3.4.1 Physical analysis of the Specimens

After completing 150, and then 300 FT cycles, percent water loss is calculated. No specimens were oven dried before or after the FT cycles since it might affect the viscoelastic characteristics of asphalt mixes. Table 3.5 gives the information about the characteristic of the specimens after 150 and 300 FT cycles. Mix A-1 had the highest level of water loss during the evolution of FT cycles. It experienced 24% and 36% water loss after 150 and 300 FT cycles respectively. The water loss for the mix A-2 was 12% after 150 FT cycles and 22% after 300 FT cycles. Moreover, the average water loss for the mix A-3 is 17% after 150 FT cycles and 31% after 300 FT cycles. A large percentage of water loss for the A-1 is probably due to the low percentage of connected-voids in the specimens.

Table 3.5 Characteristic of the specimens used for freeze-thaw cycles

Mix group	Average measured % of air voids (%)	Average degree of saturation of the specimens (%)	Average percentage of voids after saturation (%)	Average degree of saturation of the specimens after 150 FT cycles (%)	Average degree of saturation of the specimens after 300 FT cycles (%)	Average volume of water in the specimens before FT cycles (mm^3)	Volume of absorbed water after 150 FT cycles (mm^3)	Volume of absorbed water after 300 FT cycles (mm^3)
A-1	1.97	50	2.30	38	32	5,900	4,850	3,830
A-2	3.45	63	3.80	55	49	12,800	11,200	10,330
A-3	6.85	70	7.30	58	48	30,700	24,900	18,550

3.4.2 Temperature History during a Cooling-Heating Cycle

Figure 3.8 indicates variations of temperature in the chamber and at different depths of the specimens applying from the 1st to the 8th freeze-thaw cycles. As it is shown in Figure 3.8, there is a difference between the temperature sensor placed in the core of the specimen and the temperature sensor placed on the surface of the specimen especially for a mix with a low percentage of air voids. ΔT is almost equal for both specimens during the first 2 cycles, but it was reduced gradually for the specimen with a high percentage of voids as time passes. This behavior was expected and is due to the rapid rate of the heating and cooling cycles. This non-homogeneity of the temperature during rapid heating-cooling cycles may increase the potential for thermal cyclic damage since there is a different level of contraction and expansion in the mix for a high percentage of air voids. The average of the temperature at different stages of the mixtures during 300 FT cycles is shown in Figure 3.9. Average of the temperature placed in the core of the specimen with 2% of air voids was higher than the specimen with 7% air voids during 300 FT cycles.

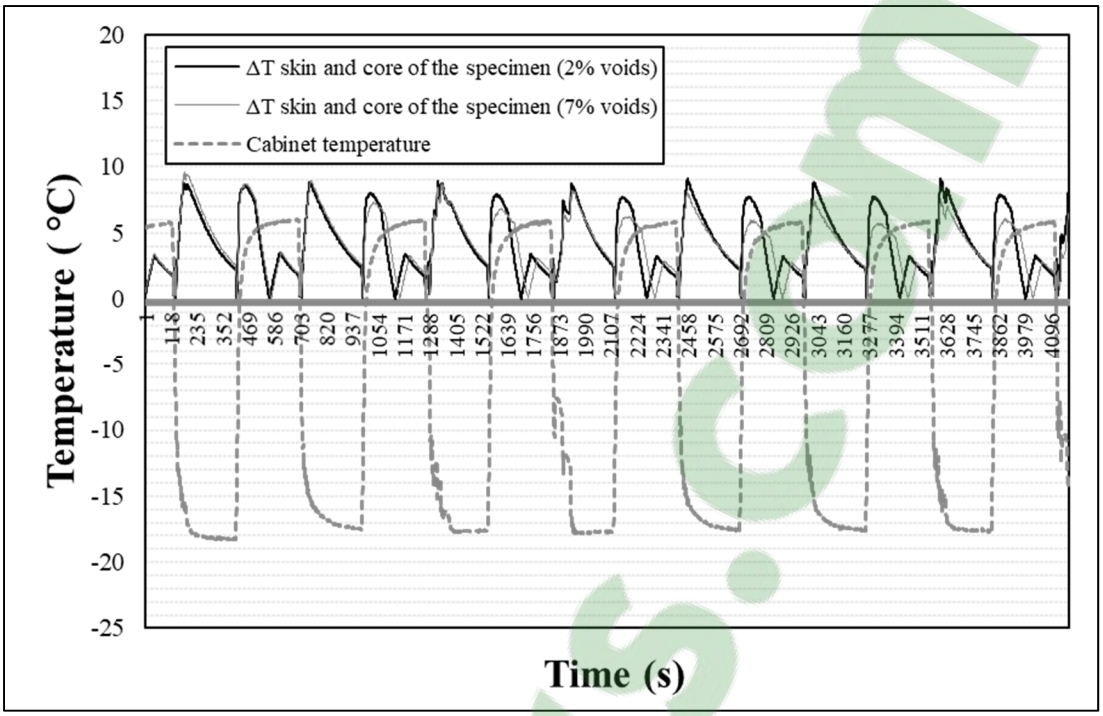

Figure 3.8 Temperature regime for low (2%) and high (7%) percentage of voids from the first to the 8th freeze-thaw cycles

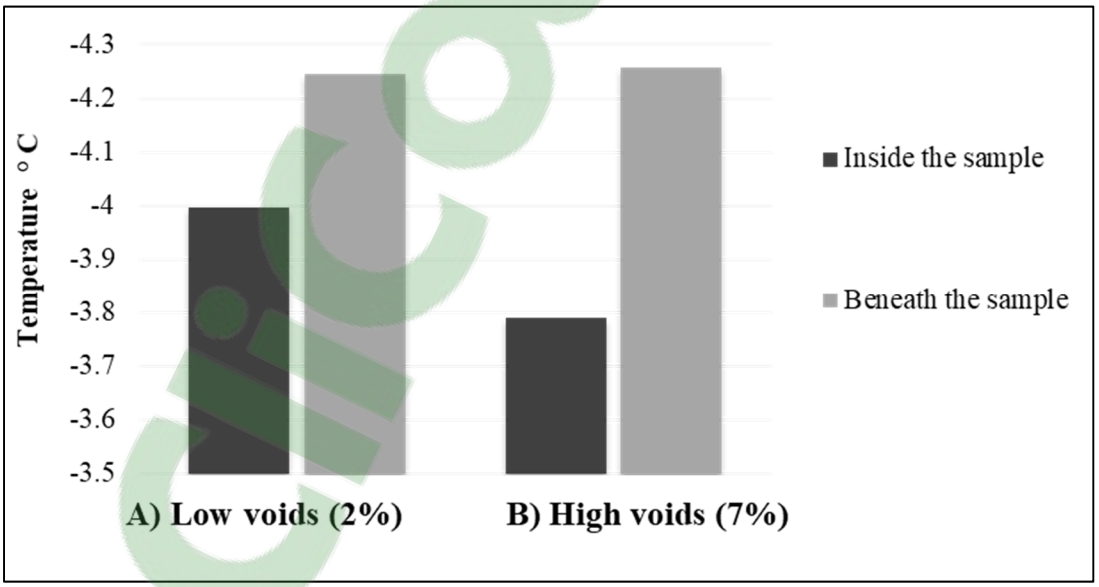

Figure 3.9 Average surface and inside temperature for the specimens studied during cooling-heating cycles

Analysis of the temperature in the previous study conducted by Hassn et al. (2016) indicated that the asphalt mix with a high percentage of air voids has lower thermal conductivity than the mix with a lower percentage of air voids. On the other hand, amount of energy in water inside the pores can be absorbed during thawing and released during freezing. This amount of energy that can be released or absorbed during phase change is called the latent heat of fusion. Latent heat of fusion for freezing or thawing water is constant at 334 kJ/kg. For pavement materials, the latent heat of fusion, Ls, can be obtained from Equation (3.10) (Doré and Zubeck, 2007).

$$L_s = \frac{\omega}{100}\frac{\rho_d}{\rho_w}L \tag{3.10}$$

where ω is the gravimetric water content of soil or pavement material, ρd and ρw are the densities of dry specimen and water, respectively, and L is the latent heat of fusion is constant at 334 kJ/kg or 334 MJ/m3 for freezing or thawing water.

Based on the Eq. (13), the specimen with high percentage (7%) of voids has a much higher latent heat of fusion (Ls= 19.22 kJ/kg) than the specimen with low percentage (2%) of voids (Ls= 1.368 kJ/kg). These can show the importance of the compaction effort which results to have different density. The amount of energy concentrated in the asphalt mixtures with different air voids content, but with the same material specifications and mix design, during FT cycles depends only upon the density of the asphalt mixes.

3.4.3 Complex Modulus Results

The complex modulus results in this study were analyzed by using the 2S2P1D model. Previous studies showed the ability of the 2S2P1D model to simulate the asphalt behavior over a range of temperature and frequency in wet and dry conditions (Di Benedetto et al., 2004; Perraton et al., 2016; Lamothe et al., 2016; Lamothe et al., 2017; Tremblay et al., 2017). It was also found that this model is appropriate to evaluate the viscoelastic behavior by considering the FT cycles (Lamothe et al., 2017). The 2S2P1D (two Springs, two Parabolic elements, and one Dashpot) modeling are presented in Figure 3.10.

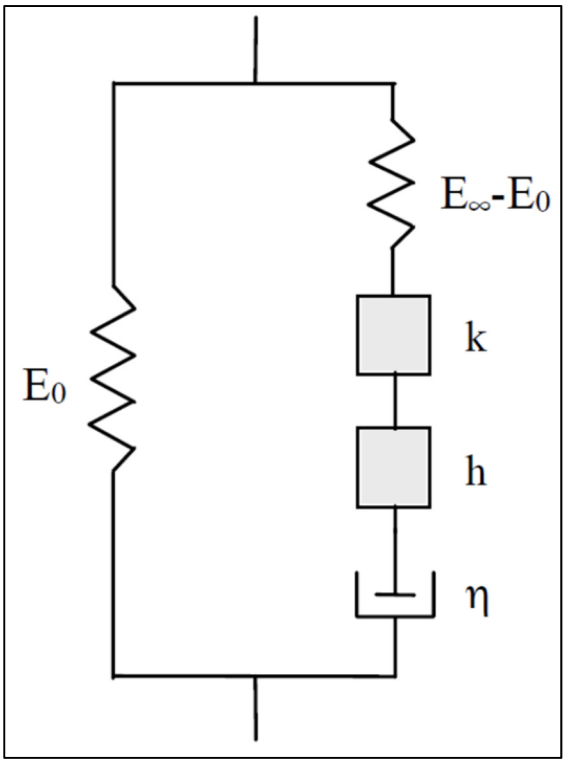

Figure 3.10 Representation of the introduced general model "2S2P1D" for asphalt mixtures Taken from Di Benedetto et al. (2004)

This model has been developed in the laboratory of DGCB (Département de Génie Civil et Bâtiment) at the ENTPE (École Nationale de Travaux Publics de l'État, (Lyon, France)) on the linear viscoelastic characteristics of bituminous materials (Olard et al., 2003; Di Benedetto et al., 2004). Equation (3.11) was used in order to analyze the results of complex modulus with the 2S2P1D rheological model which was expressed by Olard et al. (2003).

$$E^*_{2S2P1D} = E_{00} + \frac{E_0 - E_{00}}{1 + \delta(i\omega\tau_E)^{-k} + (i\omega\tau_E)^{-h} + (i\omega\beta\tau_E)^{-1}} \quad (3.11)$$

where i is complex number defined by $i^2 = -1$, E_0 is the glassy modulus when ($\omega \rightarrow 0$), E_{00} is the static modulus when ($\omega \rightarrow \infty$), ω is the pulsation (equal to $2\pi f_r$), f_r is frequency, δ (delta) is constant, β is dimension constant linked with η, which is the newtonian viscosity (η =

$(E_0 - E_{00})\beta\tau_E$), and h, k are the parameters (constants) parabolic elements of the model (0 < k < h < 1).

τ_E is characteristic time, which depends only with temperature and which accounts for the classical equivalence principle between frequency and temperature. The changing of τ_E by temperature can be explained by means of a shift factor if the time-temperature superposition principle holds (Eq. (12)):

$$\tau_E(\mathrm{T}) = \ a_T(T) \times \tau_{0E} \tag{3.12}$$

where $a_T(T)$ is shift factor at temperature T and $\tau_{0E} = \tau(T_{\mathrm{ref}})$ at reference temperature T_{ref}.

Therefore seven criterion in the 2S2P1D formula (E_{00}, E_0, δ, k, h, β, and $\boldsymbol{\tau_{0E}}$) are needed to analyze the linear viscoelastic characteristics of the tested specimens at a given temperature and frequency. The progressions of τ_E were determined by the William-Landel-Ferry (WLF) model (Ferry, 1980). τ_{0E} was quantified at the selected reference temperature T_{ref}. When the temperature effect is determined, the number of criterion becomes nine, including the two WLF criteria (Equation (3.13)) (C1 and C2 determined at the reference temperature).

$$log(a_T) \ = \ \frac{-C_1\,(T - T_{ref})}{C_2 \ + \ (T - T_{ref})} \tag{3.13}$$

The 2S2P1D modeling parameters are stated in Table 3.6. The k, h, δ, and τ_E (s) parameters explain the binder rheology of the mixes (Di Benedetto et al. 2004) which are almost same for the specimens in each group. A-1 has the highest glassy modulus compares to the other groups, which is due to it has a higher density. After saturation, an increase of 1000 MPa, 1000 MPa, and 2500 MPa happens for the glassy modulus of the mix A-1, A-2, and A-3 respectively. Table 3.6 also indicates that the evolution of FT cycles does not have considerable influence on the glassy modulus (E_0, which describes as maximum modulus for high frequency and/or low temperature) and static modulus (E_{00}, which describes as maximum modulus for low frequency and/or high temperature) for A-1, and A-2. Whereas, E_0 decreases substantially after

300 FT cycles for group A-3. The reduction of E_0 by increasing the number of FT cycles was anticipated in the recent study (Lamothe et. al., 2017).

Table 3.6 Parameters of the introduced 2S2P1D model for the corresponding groups

Group	Condition	V_a%	E_{00} (MPa)	E_0 (MPa)	k	h	δ	τ_E (s)
A-1	Dry	2.0	50	44,000	0.17	0.52	2.20	0.006
	0 FT	2.0	75	45,000	0.17	0.54	2.20	0.006
	150 FT	2.0	50	44,000	0.17	0.54	2.20	0.006
	300 FT	2.0	50	44,000	0.17	0.54	2.20	0.006
A-2	Dry	3.5	30	42,000	0.18	0.55	2.20	0.006
	0 FT	3.5	32	43,000	0.18	0.55	2.20	0.006
	150 FT	3.5	22	41,600	0.18	0.55	2.20	0.006
	300 FT	3.5	22	41,200	0.18	0.55	2.20	0.006
A-3	Dry	7.0	35	40,000	0.18	0.52	2.20	0.006
	0 FT	7.0	35	42,500	0.18	0.52	2.20	0.006
	150 FT	7.0	15	41,500	0.18	0.55	2.20	0.006
	300 FT	7.0	12	33,000	0.17	0.55	2.20	0.006

3.4.4 Effect of Freeze-Thaw and Water

In order to objectively compare the results of complex modulus analyzed by the 2S2P1D model for different mixes, a condition effect coefficient, C^*_{CEC} was calculated. The calculation of the conditioning effect coefficient (C^*_{CEC}) was developed by Di Benedetto (2007), and is defined as the ratio between the complex modulus of a specific mix which was made with a specific condition, in our case the conditioned mix at the equivalent frequency, and the complex modulus of a reference mix, at the same frequency as written in Equation (3.14). C^*_{CEC} has been used recently and has indicated to be very efficient to compare complex modulus experimental test results (Perraton et al., 2016; Tremblay et al., 2017).

$$C^*_{CEC} = \frac{E^*_{FTC}}{E^*_{REF}} \tag{3.14}$$

where C* $_{CEC}$ is the conditioning effect of the coefficient, E^*_{FTC} is the value of complex modulus for the conditioned specimens, and E^*_{REF} is the value of complex modulus for the reference specimens. E^*_{FTC} and E^*_{REF} are complex modulus results obtained based on the master curve. An example of the master curve is shown in Figure 3.11. The top part of the master curve corresponds to the maximum stiffness value (at high frequency and/or low temperature) and the bottom part corresponds to the minimum stiffness value (at low frequency and/or high temperature).

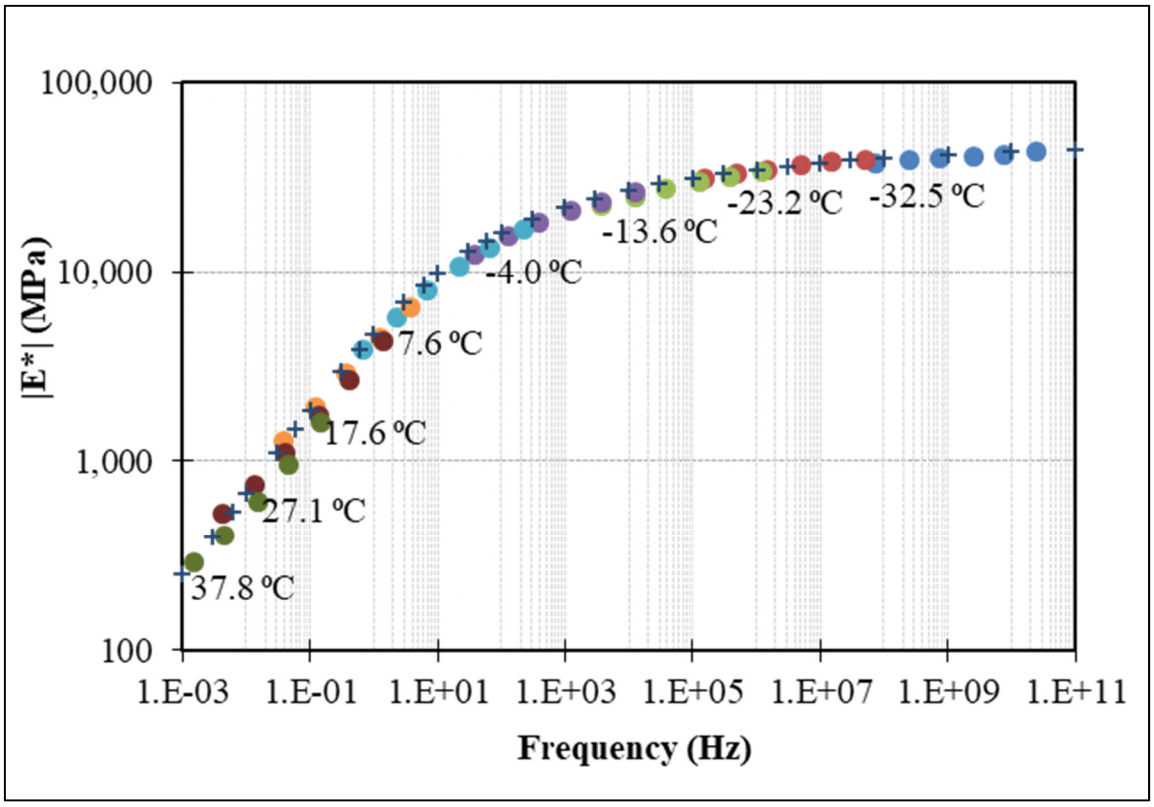

Figure 3.11 Example of the master curve of the norm of complex modulus for a reference specimen in the group A-1

It should be noted that C* CEC of one means that there is no difference before and after the conditioning. The norm of the complex conditioning effect coefficient C* CEC is plotted for the mixes with different level of voids are shown in Figure 3.12.

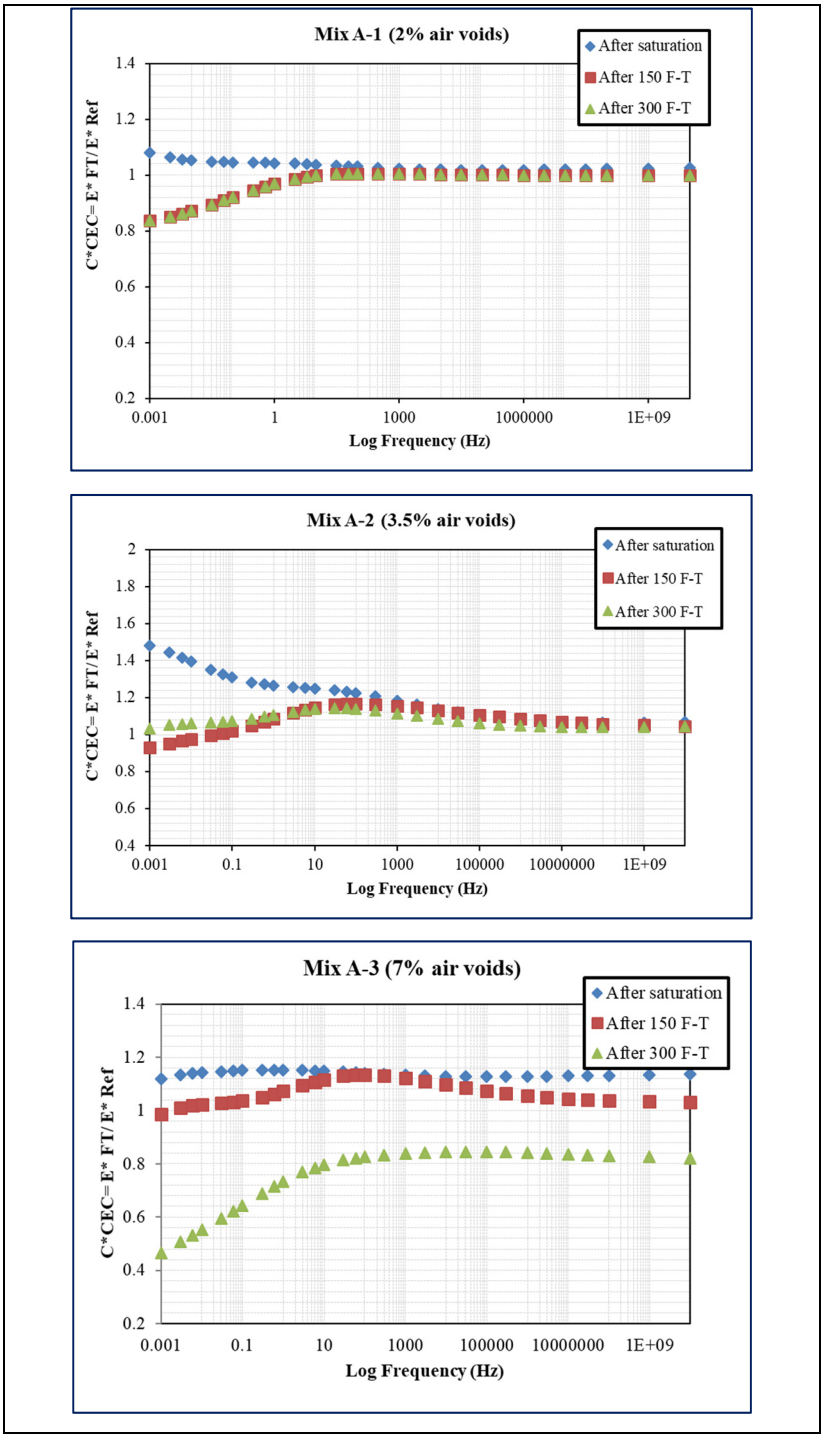

Figure 3.12 Comparison of the effect of 150 rapid FT cycles and 300 rapid FT cycles on the stiffness behavior of all the mixes

Figure 3.12 presents that increased in complex modulus occurred after saturation and at the frequencies above the freezing point of water (based on equivalent temperatures in Figure 3.11). This bias behavior was probably caused by pore water pressure within the specimens. A similar increase in resilient modulus due to the saturation process was seen in past studies (Lottman, 1982; Coplantz, and Newcomb, 1988). Coplantz and Newcomb (1988) mentioned this behavior may be due to the difficulty of the temperature of the vacuum saturation bath.

All mixes show the decrease in modulus at high temperatures/low frequencies after FT cycles compare to the reference. C*CEC reduces gradually as frequency increases. This continues until a frequency of around 100 Hz which is the equivalent of the freezing point (0°C) according to the master curve (Figure 11). All groups experience a small bump for the 150 FT curve, on Figure 3.12, at frequencies near the freezing point, which reduces gradually as frequency increases. This is probably due to the water expansion. El-Hakim and Tighe (2014) were considered water expansion as the main premature damage occurred during FT cycles (El-Hakim and Tighe, 2014).

C*CEC remains constant at frequencies higher than around 105, which is around -14°C. This temperature can be considered as glass transition temperature of the mix, where the mix starts to have the glassy behavior as temperature decreases and the behavior becomes completely elastic. As temperature reduces further, the ice in the pores does not significantly change the viscoelastic behavior of the conditioned mix. Because of that, the C*CEC value is close to one for all curves except for the mix A-3.

There is a significant decrease of complex modulus after 300 freeze-thaw cycles for the A-3 mix (7% of voids). The C*CEC remains constant at around 0.8 below the freezing point, or after 100 Hz. This is while increased in stiffness of saturated specimens was seen in this research and also in the previous studies (Lamothe et al., 2017; Lachance-Tremblay et al., 2017). The reduction in stiffness for saturated mix after the 300 FT cycles can be considered as the premature damage in the specimens.

3.4.5 Cole-Cole Plane and Black Curves

The results of complex modulus test can be presented in Cole-Cole plane. The storage modulus (E1) is plotted on the real axis (x-axis), and the loss modulus (E2) is plotted on the imaginary axis (y-axis). Three tendencies can be noticed: tendency at lower temperatures, intermediate temperatures and at high temperatures. Cole-Cole plane shows that at low temperatures, real modulus increases and the loss modulus decreases. This representation allows assessment of the quality of the test but mainly at intermediate and low temperatures (Pellinen, 2002). Figure 3.13 show the complex modulus results in the Cole-Cole plane.

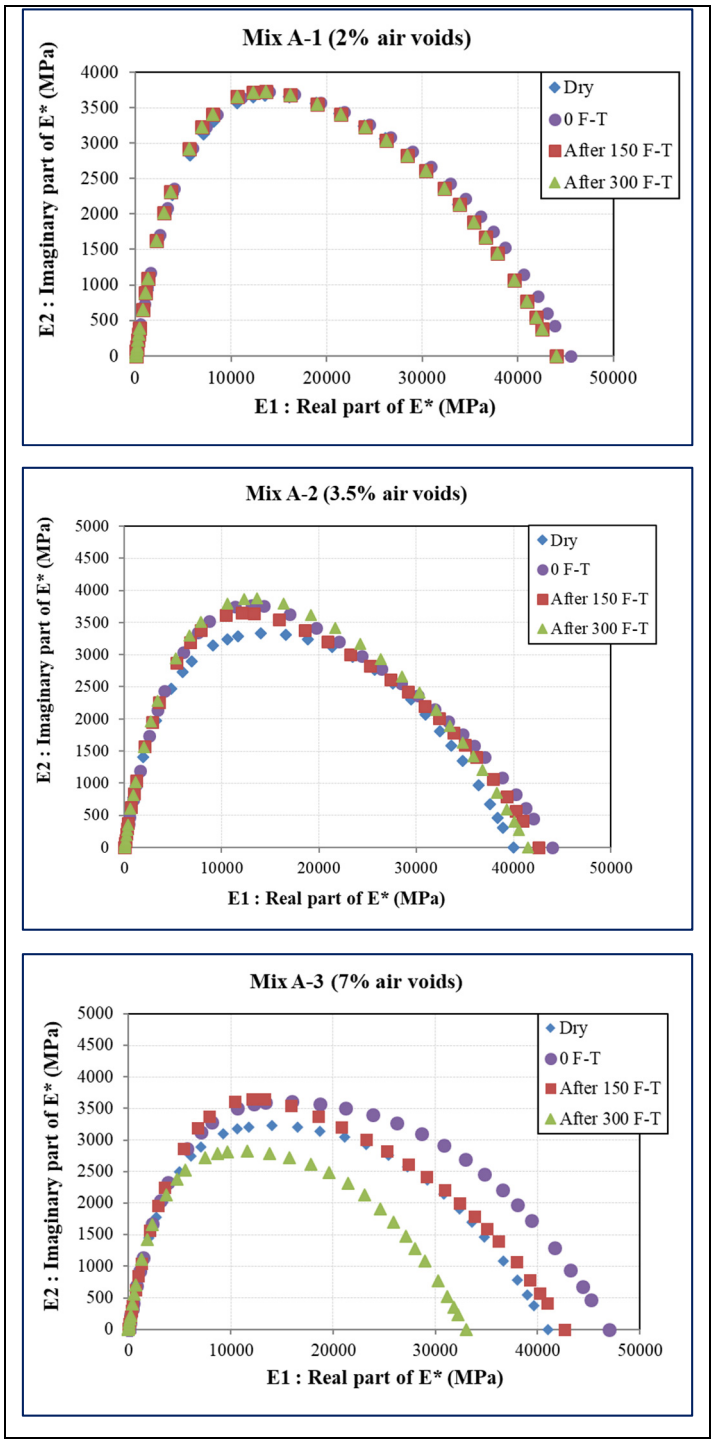

Figure 3.13 Representation of Complex modulus test results in Cole-Cole diagram for all mixes

A-3 shows significant differences between the reference and 300 FT cycles. The curve shrinks and data are moving along the left side of the curve after 300 FT cycles, while, the diagram does not show significant differences between the reference and after 150 FT cycles. After saturation and before FT cycles, the storage modulus increased at low temperatures. This increase is clearer for the mix A-3. This increase in storage modulus is due to the effect of ice formation inside the pores. The storage modulus at low temperatures decreases as a number of FT cycles increase which was seen in the past study (Lamothe et al., 2017; Lachance-Tremblay et al., 2017). The stiffness reduction of partially saturated specimens after a large number of FT cycles could result from the microcracks that were started during FT cycles.

The cole-cole plane allows assessment of the quality of the test but mainly at intermediate and low temperatures. To assess the quality of data at high temperatures the Black space provides a better way of inspecting data (Pellinen, 2001). Figure 3.14 present complex modulus results in black space diagram. It can be seen that the phase lag angle reduces after reaching a maximum value. This behavior is due to the viscosity of the mix at high temperature (around +38 °C) and depends mostly on the type of the bitumen (Basueny et al., 2014). The maximum value of the phase angle after 300 FT cycles increase for the mix A-3.

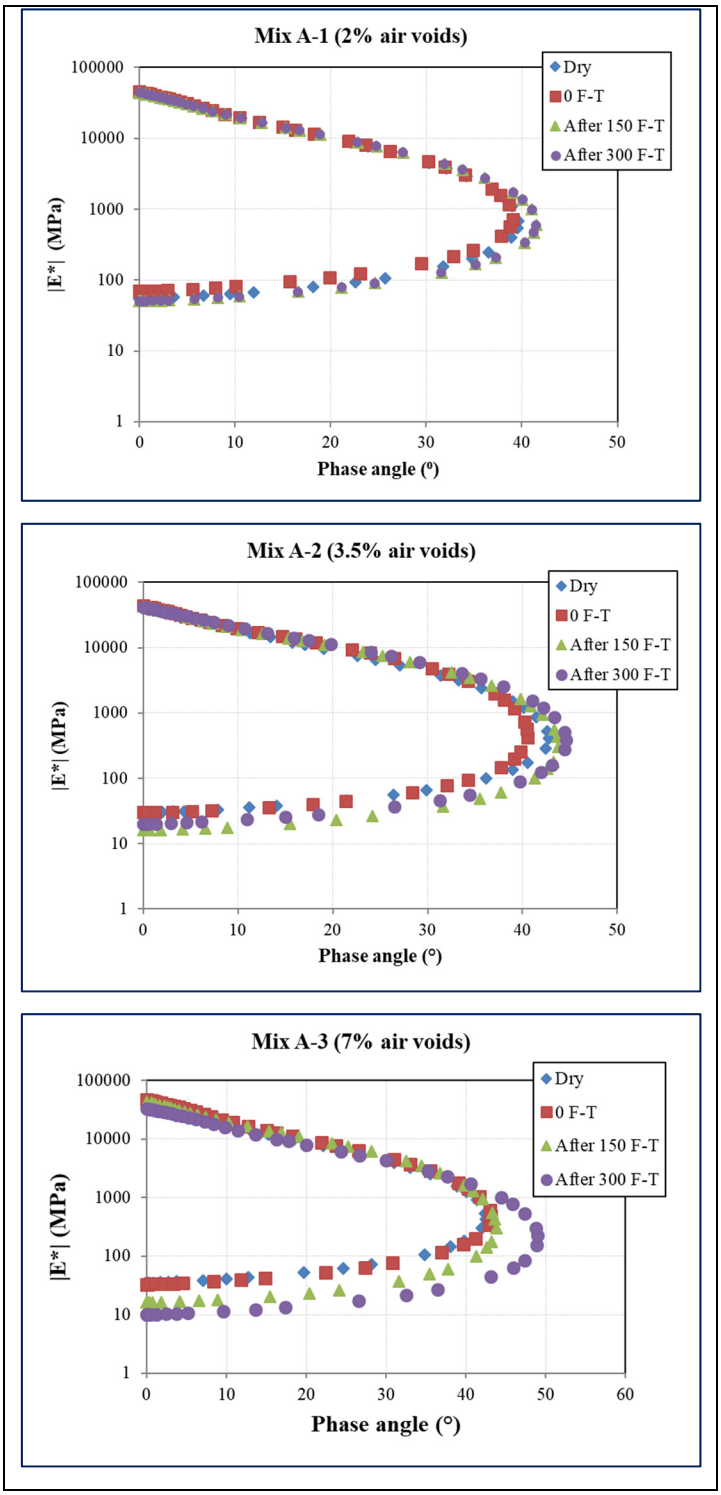

Figure 3.14 Representation of Complex modulus test results in Black Curve diagram for all mixes

In general, since the characteristics of mixes were similar for all groups, the increase in viscosity (at very high temperatures) and decrease in stiffness (at very low temperatures) after 300 FT cycles for the group A-3 is probably due to the stripping problem. Stripping of the mix after a large number of FT cycles is due to the loss of adhesion at the cement-aggregate interfaces and in part by the failure of the cohesion within the binder (Williams and Miknis, 1998; Copeland et al., 2006; Caro et al., 2008). The results clearly indicated that the level of compaction affects the durability of the mixes. The composition of voids can be changed by water easier due to a large number of connected-air voids and high volume of water. The damage from the accumulation of ice expansion load can be named as FT fatigue damage and it will deteriorate the asphalt-aggregate bond and allows water to be displaced with the mastic and increase the stripping of aggregates (Si et al., 2014). Previous lab test indicated that the rapid 300 FT damage considerably decreases the fatigue life of the mix (Badeli et al., 2017).

3.5 Precision of Testing

A repeatability strategy was conducted, demonstrating the quality of the test. Since the complex modulus test is the non-destructive, it is possible to check the same specimen again. In this paper, two specimens were chosen for each complex modulus test to increase the precision of the test. The result for each frequency and temperature is the average of the two repetitions. A ratio of the norm of the complex modulus at each temperature and frequency is calculated for two specimens, and if the results have 10% difference, the tests are considered good and the average of |E*| is used. Otherwise, a third specimen is tested (did not happen in this study).

3.5.1 Adjustment of the Witczak Model for GB20 mix with using PG 64-28 Binder

|E*| values are usually obtained from conducting the laboratory testing on asphalt mixes. However, complex modulus test requires a long waiting time and a series of expensive testing equipment and materials. The E* predictive models have been developed as an alternative

method of obtaining the complex modulus values. The E* values can be determined from the basic properties of asphalt mix and materials without conducting complex modulus test. However, there are many different parameters that influence the complex modulus of mixes, such as environmental parameters which are not addressed in the E* predictive models (Yu, 2012). The previous section proves that the effect of a large number of FT cycles is responsible for lower stiffness value which can affect the life of the mixture. Improvement of the predictive model is essential to prevent the premature failure of the mixes. The current MEPDG uses the two different Witczak models for complex modulus (E*) estimation. Both models predict complex modulus of an asphalt mixture at any frequency and temperature as a function of a binder stiffness parameter, mix aggregate gradation and mix volumetric properties. The major difference between these two models is the definition of binder stiffness in the formula. The NCHRP 1-37A model suggests the binder stiffness with regard to the viscosity, whereas the NCHRP 1-40D suggests it in the matter of the G* and δ (phase angle) (El-Badawy et al., 2011; Witczak et al., 2007; Sholar et al., 2005). The NCHRP 1-37A model was used in this study to be able to compare the Moduli |E*| which were experimentally determined from the laboratory with values obtained by the model. The model is shown in Eq. (15) (Bari and Witczak, 2006):

$$\begin{aligned}\text{Log}|E^*_{Witczak}| = {} & -1.249937 + 0.029232.P_{200} - 0.001767(P_{200})^2 - 0.002841.P_4 - 0.05809 \\ & - 0.802208\frac{V_{be}}{V_{be}+V_a} \\ & + \frac{3.871977 - 0.0021.P_4 + 0.003958.P_{38} - 0.000017{P_{38}}^2 + 0.005470.P_{34}}{1+e^{(-0.603313-0.313351\log f-0.393532\log\eta)}}\end{aligned} \tag{15}$$

where, $E^*_{Witczak}$ is asphalt mix dynamic predictive modulus (10^5 psi), η is viscosity of binder (10^6 poise), f is the Loading frequency (Hz), V_a is air voids in the mix (percentage by volume), V_{be} is Effective binder content (% by volume), P_{200} is percentage of passing number 200 sieve, P_4 is Cumulative percentage of retained on number 4 sieve, P_{38} is cumulative percentage of retained on 3/8 inch sieve, P_{34} is cumulative percentage of retained on 3/4 inch sieve.

Moduli |E*| which were experimentally determined from the lab test can be compared with values obtained by Witczak predictive model ($E^*_{Witczak}$). A total three groups of 24 specimens

with different percentage of air voids were used to compare with values obtained by the predictive model. For each specimen, the dynamic moduli obtained from eight different temperatures, and seven frequencies have been used for the comparison. The results are shown in Figure 3.15.

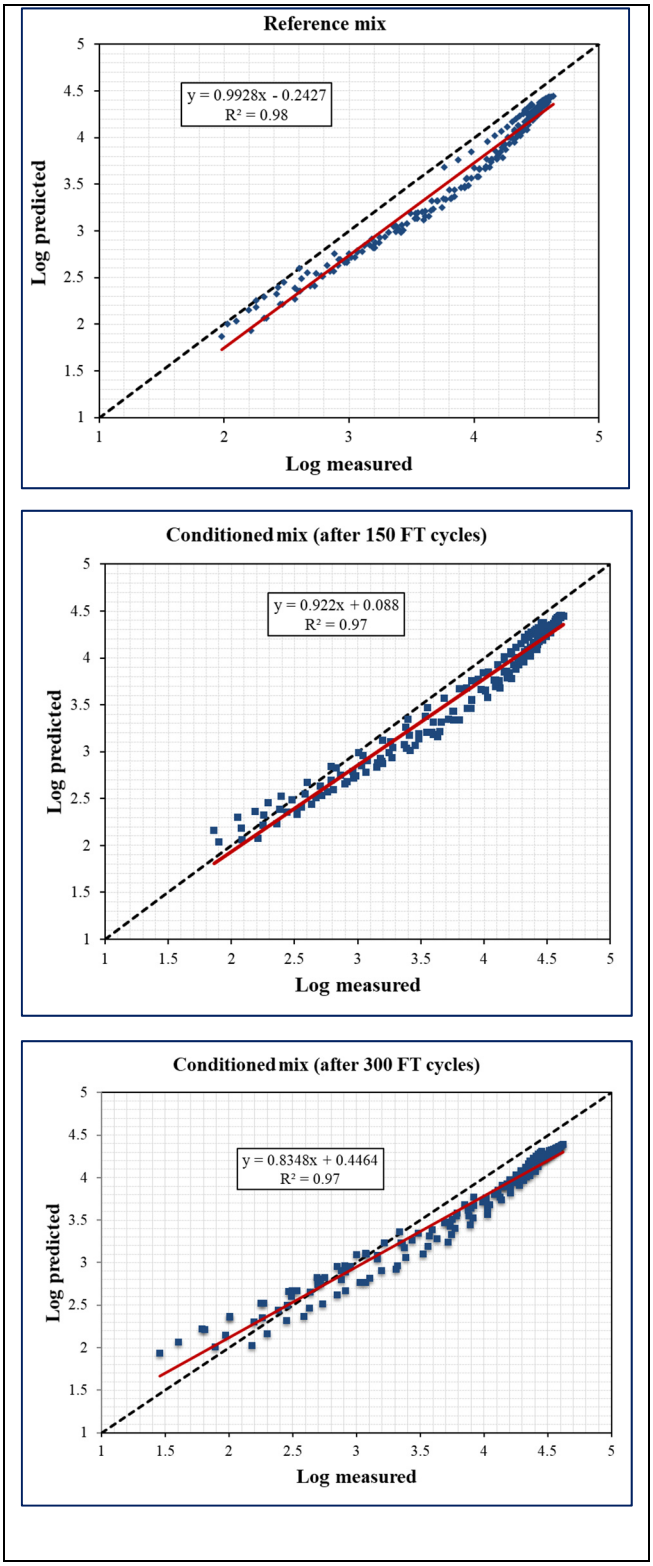

Figure 3.15 Comparison between
the laboratory-measured and predicted E*

A comparison between the laboratory determined and predicted data has indicated underestimated prediction of the complex modulus after 300 FT cycles by the un-calibrated NCHRP 1-37A model, indicating that the NCHRP 1-37A model is not precise enough on mixture after a large number of rapid FT cycles. The Witczak predictive model shows a poor goodness of prediction with the same value of R^2 before the condition of rapid FT cycles. This can prove that a correction factor proposed for an existing model is required based on the effect of environmental FT cycles. Under this circumstance, calibrated models are essential rather than directly applying the NCHRP 1-37A model to predict the dynamic modulus after a large number of rapid FT cycles. In this study, the customized models not only for a specific mixture but also for the mixes with different air void content have been developed (Figure 3.16). The relative bias in the dynamic moduli prediction, especially at high temperatures, low frequencies, and a high percentage of voids by using the Witczak model, can be eliminated by applying Equation 3.16 on the predicted values from this model.

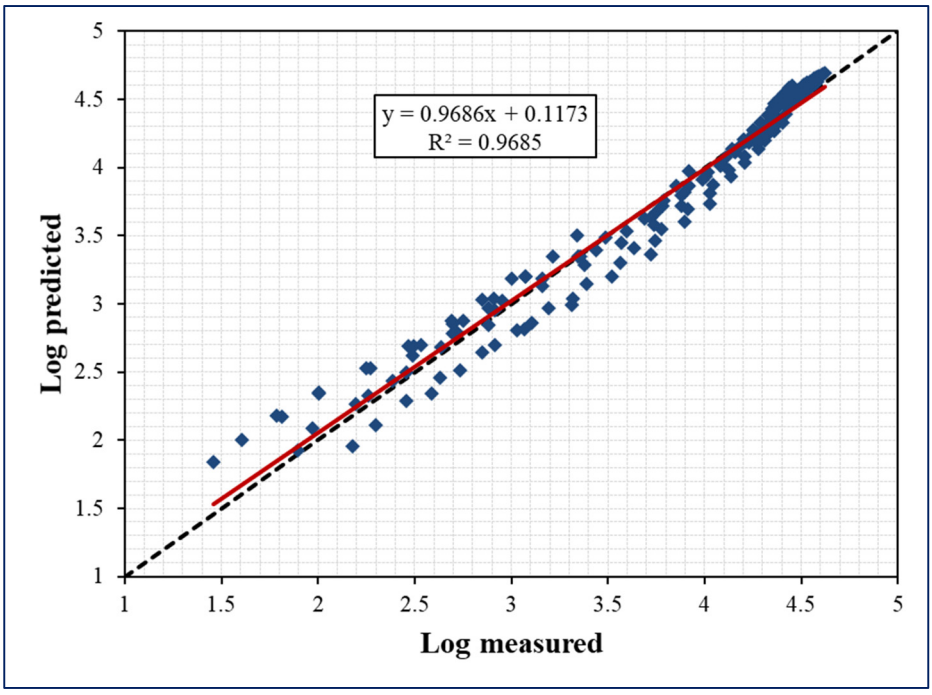

Figure 3.16 Performance of the corrected model after calibration for the conditioned mix after 300 FT cycles

$$E^*_{Corrected} = 1.1603\ E^*_{Witczak} - 0.4007 \quad (3.16)$$

where, $E^*_{Corrected}$ is dynamic modulus corrected for bias, in MPa; and $E^*_{Witczak}$ is dynamic modulus predicted from the NCHRP 1-37A model in MPa.

3.6 Conclusion

This paper presents results on the behavior of the GB20 mixtures with different compaction levels in the linear viscoelastic domain before and after the 150 and 300 FT cycles. The cooling and heating rate used was 4.5 °C/min. For each temperature cycle, two different temperature levels were targeted, which were -18 and +6 °C. In each group, two dummy specimens were equipped with thermocouples in order to analyze the temperature history during the rapid cooling-heating process. All specimens were subjected to complex modulus test carried out using the direct tension-compression test. The rheological model 2S2P1D was used to simulate the behavior of the mixes according to various temperatures and frequencies. Based on the analysis and results, the following observations were found:

1) A large percentage of water loss for the A-1 was seen after the 300 FT cycles. This is probably due to the low percentage of connected-voids in the specimens which means that only surface pores were filled with deaerated water.
2) Specimen with high percentage of voids has a much higher latent heat of fusion (L_s= 19.22 kJ/kg) than the specimen with low percentage of voids (L_s= 1.368 kJ/kg). These can show the importance of the compaction effort which results to have different density. The amount of energy concentrated in the asphalt mixtures with different air voids content, but with the same material specifications and mix design, during FT cycles depends only upon the density of the asphalt mixes.
3) A-1 has the highest glassy modulus. Results also indicate that the evolution of FT cycles does not have considerable influence on the glassy modulus and static modulus for A-1,

and A-2. Whereas, E0 decreases substantially after 300 FT cycles for the mix with low compaction level (A-3).

4) Results indicate that increased in complex modulus occurred after saturation and at the frequencies above the freezing point of water. This bias behavior was probably caused by pore water pressure within the specimens or due to the difficulty of the temperature of the vacuum saturation bath.
5) A-3 shows significant different behavior between the reference and 300 FT cycles in Cole-Cole graph. The curve shrinks and data are moving along the left side of the curve after 300 FT cycles, while, the diagram does not show significant differences between the reference and after 150 FT cycles.
6) Analysis of Cole-Cole graph shows that after saturation and before FT cycles, the storage modulus increased at low temperatures. This increase is clearer for the mix A-3. This increase in storage modulus is probably due to the effect of ice formation inside the pores. The storage modulus at low temperatures decreases as a number of FT cycles increase.
7) The maximum value of the phase angle after 300 FT cycles increase for the mix A-3. The increase in viscosity (at very high temperatures) and a decrease in stiffness (at very low temperatures) after 300 FT cycles for the group A-3 is probably due to the stripping problem.
8) Comparison between the laboratory determined and predicted data indicated that the relative bias in the modulus prediction after 300 FT cycles, especially due to the high percentage of voids. This can be eliminated by applying the improved equation to the predicted values.

Further analysis is required based on the effect of compaction on mixes having different binders incorporating the full FT cycles in the lab. In the meantime, the field data with different compaction levels can be obtained from the site condition to find an actual predicted formula.

3.7 Acknowledgments

The research work presented in this paper is part of the National Sciences and Engineering Research Council of Canada (NSERC) Industrial Research Chair on the Interaction of Heavy Loads–Climate–Pavement of Laval University (i3C).

3.8 References

Asphalt Institute, 1982. Research and Development of the Asphalt Institute's Thickness Design Manual (MS-I) Ninth Edition, Research Report No. 82-2.

ASTM-C666, 2008. Standard Test Method for Resistance of Concrete to Rapid Freezing and Thawing. American Society for Testing and Materials, Washington, DC.

Bagampadde, U., Isacsson, U., Kiggundu, B.M., 2004. Classical and contemporary aspects of stripping in bituminous mixes. Road materials and pavement design, 5(1), pp.7-43.

Bari, J., 2005. Development of a new revised version of the Witczak E* predictive models for hot mix asphalt mixtures (Doctoral dissertation, Arizona State University).

Basueny, A., Perraton, D., Carter, A., 2014. Laboratory study of the effect of RAP conditioning on the mechanical properties of hot mix asphalt containing RAP. Materials and structures, 47(9), pp.1425-1450.

Badeli, S., Carter, A., Doré, G., 2016. The importance of asphalt mixture air voids on the damage evolution during freeze-thaw cycles. Canadian Technical Asphalt Association.

Badeli, S., Carter, A., Doré, G., 2017. Complex modulus and fatigue analysis of an asphalt mix after daily rapid freeze-thaw cycles. Journal of materials in civil engineering. DOI: 10.1061/(ASCE)MT.1943-5533.0002236.

Birgisson, B., Soranakom, C., Napier, J.A.L., Roque, R., 2004. Microstructure and fracture in asphalt mixtures using a boundary element approach. Journal of materials in civil engineering, 16(2), pp.116-121.

Carter, A., Paradis, M., Laboratory Characterization of the Evolution of the Thermal Cracking Resistance with the Freeze-thaw Cycles.

Caro, S., Masad, E., Bhasin, A., Little, D.N., 2008. Moisture susceptibility of asphalt mixtures, Part 1: mechanisms. International Journal of Pavement Engineering, 9(2), pp.81-98.

Chehab, G., O'Quinn, E., Kim, Y., 2000. Specimen geometry study for direct tension test based on mechanical tests and air void variation in asphalt concrete specimens compacted by superpave gyratory compactor. Transportation Research Record: Journal of the Transportation Research Board, (1723), pp.125-132.

Chen, J.S., Lin, K.Y., Young, S.Y., 2004. Effects of crack width and permeability on moisture-induced damage of pavements. Journal of Materials in Civil Engineering, 16(3), pp.276-282.

Coplantz, J.S., Newcomb, D.E., 1988. Water sensitivity test methods for asphalt concrete mixtures: A laboratory comparison (No. 1171).

Copeland, A., Kringos, N., 2006. Determination of bond strength as a function of moisture content at the aggregate-mastic interface. In 10th International Conference on Asphalt Pavements. Quebec, Canada. August 12-17, 2006 (pp. 709-718).

Di Benedetto, H., De La Roche, C., 1998. State of the art on stiffness modulus and fatigue of bituminous mixtures. Rilem Report, pp.137-180.

Di Benedetto, H., Partl, M.N., Francken, L., Saint André, C.D.L.R., 2001. Stiffness testing for bituminous mixtures. Materials and Structures, 34(2), pp.66-70.

Di Benedetto, H., Olard, F., Sauzéat, C., Delaporte, B., 2004. Linear viscoelastic behaviour of bituminous materials: From binders to mixes. Road Materials and Pavement Design, 5(sup1), pp.163-202.

Benedetto, H.D., Delaporte, B. and Sauzéat, C., 2007. Three-dimensional linear behavior of bituminous materials: experiments and modeling. International Journal of Geomechanics, 7(2), pp.149-157.

Doré, G., Zubeck, H.K., 2009. Cold regions pavement engineering.

El-Hakim, M., Tighe, S., 2014. Impact of freeze-thaw cycles on mechanical properties of asphalt mixes. Transportation Research Record: Journal of the Transportation Research Board, (2444), pp.20-27.

El-Basyouny, M.M., Witczak, M., El-Badawy, S., 2005. Verification for the calibrated permanent deformation models for the 2002 design guide (with discussion). Journal of the Association of Asphalt Paving Technologists, 74.

Feng, D., Yi, J., Wang, D., Chen, L., 2010. Impact of salt and freeze–thaw cycles on performance of asphalt mixtures in coastal frozen region of China. Cold Regions Science and Technology, 62(1), pp.34-41.

Goh, S.W., You, Z., 2012. Evaluation of hot-mix asphalt distress under rapid freeze-thaw cycles using image processing technique. In CICTP 2012: Multimodal Transportation Systems—Convenient, Safe, Cost-Effective, Efficient (pp. 3305-3315).

Gong, X., Romero, P., Dong, Z., Sudbury, D.S., 2016. The effect of freeze–thaw cycle on the low-temperature properties of asphalt fine aggregate matrix utilizing bending beam rheometer. Cold Regions Science and Technology, 125, pp.101-107.

Gubler, R., Partl, M.N., Canestrari, F., Grilli, A., 2005. Influence of water and temperature on mechanical properties of selected asphalt pavements. Materials and Structures, 38(5), pp.523-532.

Hale, W.M., Freyne, S.F., Russell, B.W., 2009. Examining the frost resistance of high performance concrete. Construction and Building Materials, 23(2), pp.878-888.

Hassn, A., Aboufoul, M., Wu, Y., Dawson, A., Garcia, A., 2016. Effect of air voids content on thermal properties of asphalt mixtures. Construction and Building Materials, 115, pp.327-335.

Hofko, B., 2015. Combining performance based lab tests and finite element modeling to predict life-time of bituminous bound pavements. Construction and Building Materials, 89, pp.60-66.

Hofko, B., Blab, R., Alisov, A., 2016. Influence of compaction direction on performance characteristics of roller-compacted HMA specimens. International Journal of Pavement Engineering, 17(1), pp.39-49.

Kringos, N., Azari, H., Scarpas, A., 2009. Identification of parameters related to moisture conditioning that cause variability in modified Lottman test. Transportation Research Record: Journal of the Transportation Research Board, (2127), pp.1-11.

Lachance-Tremblay, É., Perraton, D., Vaillancourt, M., Di Benedetto, H., 2017. Degradation of asphalt mixtures with glass aggregates subjected to freeze-thaw cycles. Cold Regions Science and Technology.

Lamothe, S., Perraton, D., Di Benedetto, H., 2015. Contraction and expansion of partially saturated hot mix asphalt samples exposed to freeze–thaw cycles. Road Materials and Pavement Design, 16(2), pp.277-299.

Lamothe, S., Perraton, D., Di Benedetto, H., 2016. Deterioration of HMA partially saturated with water or brine subjected to freeze-thaw cycles. In 8th RILEM International Symposium on Testing and Characterization of Sustainable and Innovative Bituminous Materials (pp. 705-717). Springer Netherlands.

Lamothe, S., Perraton, D., Benedetto, H.D., 2017. Degradation of hot mix asphalt samples subjected to freeze-thaw cycles and partially saturated with water or brine. Road Materials and Pavement Design, 18(4), pp.849-864

Lottman, R.P., 1982. NCHRP Report 246: Predicting Moisture-Induced Damage to Asphalt Concrete-Field Evaluation Phase. TRB, National Research Council, Washington, D.C.

Masad, E., Somadevan, N., Bahia, H.U., Kose, S., 2001. Modeling and experimental measurements of strain distribution in asphalt mixes. Journal of Transportation Engineering, 127(6), pp.477-485.

Modarres, A., Ramyar, H., Ayar, P., 2015. Effect of cement kiln dust on the low-temperature durability and fatigue life of hot mix asphalt. Cold Regions Science and Technology, 110, pp.59-66.

MTQ : Ministère des Transports du Québec, 2005. Enrobés : Formulation selon la méthode LC. Gouvernement du Québec, 111 p.

Nguyen, H.M., Pouget, S., Di Benedetto, H., Sauzéat, C., 2009. Time-temperature superposition principle for bituminous mixtures. European Journal of Environmental and Civil Engineering, 13(9), pp.1095-1107.

Ngu Nguyen, Q.T., Di Benedetto, H., Sauzéat, C., Tapsoba, N., 2012. Time temperature superposition principle validation for bituminous mixes in the linear and nonlinear domains. Journal of Materials in Civil Engineering, 25(9), pp.1181-1188.

Olard, F., Di Benedetto, H., Eckmann, B., Triquigneaux, J.P., 2003. Linear viscoelastic properties of bituminous binders and mixtures at low and intermediate temperatures. Road materials and pavement design, 4(1), pp.77-107.

Özgan, E., Serin, S., 2013. Investigation of certain engineering characteristics of asphalt concrete exposed to freeze–thaw cycles. Cold Regions Science and Technology, 85, pp.131-136.

Perraton, D., Di Benedetto, H., Sauzéat, C., Hofko, B., Graziani, A., Nguyen, Q.T., Pouget, S., Poulikakos, L.D., Tapsoba, N., Grenfell, J., 2016. 3Dim experimental investigation of linear viscoelastic properties of bituminous mixtures. Materials and Structures, 49(11), pp.4813-4829.

Pellinen, T.K., 2002. Investigation of the use of dynamic modulus as an indicator of hot-mix asphalt peformance.

Robert, L.Y., Suckhong, L., 1996. Short-term and Long-term aging behavior of rubber modified asphalt paving mixture. Transportation Research Record, 1530, pp.11-17.

Sholar, G., Roque, R., Birgisson, B., 2005. Evaluation of a predicted dynamic modulus for Florida mixtures. Transportation Research Record 1929, Transportation Research Board, Washington, D.C., 200–207.

Si, W., Ma, B., Li, N., Ren, J.P., Wang, H.N., 2014. Reliability-based assessment of deteriorating performance to asphalt pavement under freeze–thaw cycles in cold regions. Construction and Building Materials, 68, pp.572-579.

Tang, N., Sun, C.J., Huang, S.X., Wu, S.P., 2013. Damage and corrosion of conductive asphalt concrete subjected to freeze–thaw cycles and salt. Materials Research Innovations, 17(sup1), pp.240-245.

Terrel, R.L., Al-Swailmi, S., 1994. Water sensitivity of asphalt-aggregate mixes: test selection. SHRP Report A-403. Strategic Highway Research Program. National Research Council, Washington, DC.

Yi, J., Shen, S., Wang, D., Feng, D., Huang, Y., 2016. Effect of Testing Conditions on Laboratory Moisture Test for Asphalt Mixtures. Journal of Testing and Evaluation, 44(2), pp.856-867.

Yu, J., 2012. Modification of dynamic modulus predictive models for asphalt mixtures containing recycled asphalt shingles. Iowa State University.

Williams, T.M., Miknis, F.P., 1998. Use of environmental SEM to study asphalt-water interactions. Journal of Materials in Civil Engineering, 10(2), pp.121-124.

Witczak, M., El-Basyouny, M., El-Badawy, S., 2007. Incorporation of the New (2005) E* Predictive Model in the MEPDG. NCHRP 1-40D Final Report.

Xu, H., Guo, W. and Tan, Y., 2016. Permeability of asphalt mixtures exposed to freeze–thaw cycles. Cold Regions Science and Technology, 123, pp.99-106.

CHAPTER 4

COMPLEX MODULUS AND FATIGUE ANALYSIS OF AN ASPHALT MIX AFTER DAILY RAPID FREEZE-THAW CYCLES

Saeed Badeli [a], Alan Carter [b], Guy Doré [c]

[a,b] Department of Construction Engineering, École de Technologie Supérieure,
1100 Notre-Dame Ouest, Montréal, Québec, Canada H3C 1K3
[c] Department of Construction Engineering, Université Laval, Quebec, Canada, G1V 0A6

Article published in the Journal of Materials in Civil Engineering,
Volume 30, Issue 4, April 2018
manuscript number: MTENG-5843R2, DOI: 10.1061/(ASCE)MT.1943-5533.0002236

4.1 Abstract

Quebec roads are subjected to seasonal ambient temperature variations and daily rapid variations of temperature. These significant temperature variations in combination with the moisture inside the pores result in the development of premature deterioration in asphalt pavement. At present, the impact of regional freeze-thaw cycles on fatigue cracking has not been considered in the Mechanistic-Empirical pavement design method or other design methods in cold regions, which results overestimate the pavement life. Hence, the main objective of this study was to conduct the thermo-mechanical tests on an asphalt mixture before and after rapid freeze-thaw cycles. Considering the differences regarding the 2S2P1D model parameters, it was found that the influence of freeze-thaws condition on the stiffness behavior of the mix is higher with increasing the number of cycles from 150 to 300. Regarding fatigue test results, the reference mixture was more resistant to fatigue cracking than the conditioned mix after 300 freeze-thaw cycles.

4.2 Introduction

Pavement structures in Canada experience severe seasonal climatic conditions in a year (Doré & Zubeck, 2009). The extreme fluctuations of temperature in Quebec region have significant influences on the performance of asphalt mixtures (Carter & Paradis, 2010). Quebec roads are subjected to seasonal ambient temperature variations of 60oC, and daily rapid variations of temperature that may run as high as 30oC (Paradis & Langlois, 2006). These significant temperature variations in combination with the moisture inside the pores result in the development of premature deterioration of asphalt mixtures.

4.2.1 Background

Many researchers have been conducting different studies to analyze the mechanism of freeze-thaw damage in pavement structures in the past (Janoo and Berg 1990, Simonsen and Isacsson 1999, Williams and Miknis 1998, Doré and Imbs 2002). The mechanism of freeze-thaw cycles in asphalt mixtures is described as water infiltration inside the asphalt voids combined with the variation of positive and negative ambient temperatures. Damage of asphalt mix during the freeze-thaw cycles is started by changing the volume of the mix caused by the expansion of water under low temperature when it turns to ice and deteriorated by the loss of adhesion between the asphalt and aggregate or cohesion of asphalt mortar (Goh & You, 2012). The ice expansion load will change the voids composition. If the comprehensive stress from ice expansion is smaller than the tensile strength of the material, micro-damage will accumulate (Si, Ma, Li, Ren, & Wang, 2014). But after a large number of freeze-thaw cycles, stress will eventually exceed the tensile strength of the material and macro damage will appear (Feng, Yi, Wang, & Wang, 2009). The damage from the accumulation of ice expansion load will deteriorate the asphalt-aggregate bond and allows water to be displaced with the mastic and increase the stripping of aggregates (Si et al., 2014). The stripping due to the loss of adhesion at the asphalt cement-aggregate interfaces and/or in part by the failure of the cohesion within the binder (Williams and Miknis 1998, Copeland et al. 2006, Caro et al. 2008). Goh and You (2012) used an image processing technique to study the stripping of aggregates on the surface

of asphalt mix after rapid freeze-thaw cycles. They concluded that stripping and cracks increased with each freeze-thaw cycle.

Another important factor in studying the mechanism of freeze-thaw cycles is contraction and expansion of the asphalt material due to the daily and yearly repetitions of temperature fluctuations. Temperature affects asphalt pavements in two different ways: 1. Thermal expansion and contraction of asphaltic materials due to the seasonal variations of temperature. 2. The structural responses due to the day-night temperature variations (Jackson and Vinson 1996, Jackson and Vinson 1996, Islam and Tarefder 2014). Biao et al. (2010) analyzed the effect of temperature and aggregate gradation on the flexural tensile strength of asphalt mixes. They showed that coarse aggregate gradation improves the flexural tensile strength of asphalt mixes at low temperatures. The results indicate that temperature evidently influences the flexural tensile characteristics of mixes. Another result of the past studies by Tarefder and Islam (2014) showed that more than 98% of total fatigue damage in asphalt mixes is developed by thermal damage due to the effect of yearly and daily temperature fluctuations.

In addition to the mechanism of freeze-thaw cycles, many researchers have been working on the performance characteristics of asphalt mixes after freeze-thaw cycles in the past (Zeng and Shields 1999, Bausano and Williams 2009, Özgan and Serin 2013, Lamothe et al. 2014, Tang et al. 2014). The effect of salt on the performance of asphalt mixtures was studied by Feng et al. (2009, 2010). They concluded that freeze-thaw condition has a significant effect when the percentage of salt is less than 3%. Lamothe et al. (2015) indicated that in the temperature range of −18°C to +10°C, the partially saturated specimens with water were subjected to more significant deformations (contractions and expansions) in comparison with specimens saturated with brine. Compaction effort and compaction method can influence the air void distribution in the mix that influences the moisture damage which is one of the critical damages occurred during freeze-thaw cycles (Arambula, Masad, & Martin, 2007; Masad & Somadevan, 2002; Tashman, Masad, D'Angelo, Bukowski, & Harman, 2002). Badeli et al. (2016) investigated the damage evolution created during rapid freeze-thaw cycles of partially saturated specimens with different level of compactions. The results revealed that the level of

compaction affects the complex modulus value, and rapid freeze-thaw cycles decrease the value of the complex modulus.

The harsh climate and extreme temperature variations in Québec region (Canada) have a significant effect on the performance of asphalt pavements. The province of Quebec receives an average rainfall of about 1200 mm per year with 159 wet days (http://www.climat-quebec.qc.ca/). The Figure 4.1 is collected data by the Ministry of Transportation of Quebec (MTQ) which illustrates the daily asphalt temperature history for Trois Rivere, Route 155 road in the south part of Quebec from the first of November 2014 to the first of May 2015. It can be seen that asphalt temperatures are higher than the air temperatures, although they both behaved same. Daily freeze-thaw cycles can be defined as a number of days in a year when the minimum asphalt temperature goes below 0 degrees Celsius and maximum asphalt temperature is greater than 0 degrees Celsius. The daily number of freeze-thaw cycles in some areas in the USA and Canada is also available in the LTPP database (LTPP 2016) (Figure 4.2). Although LTPP data for freeze-thaw cycles is based on air temperature, with considering the MTQ results, it can be stated that there is a possibility to have even more than 60 numbers of daily freeze-thaw cycles in asphalt pavements in the south part of Quebec each year. These daily temperature fluctuations in combination with the expansion and contraction of moisture inside the voids of asphalt pavement create different types of stress. These stresses can raise the potential to create premature deterioration and can influence the total fatigue damage to asphalt pavements.

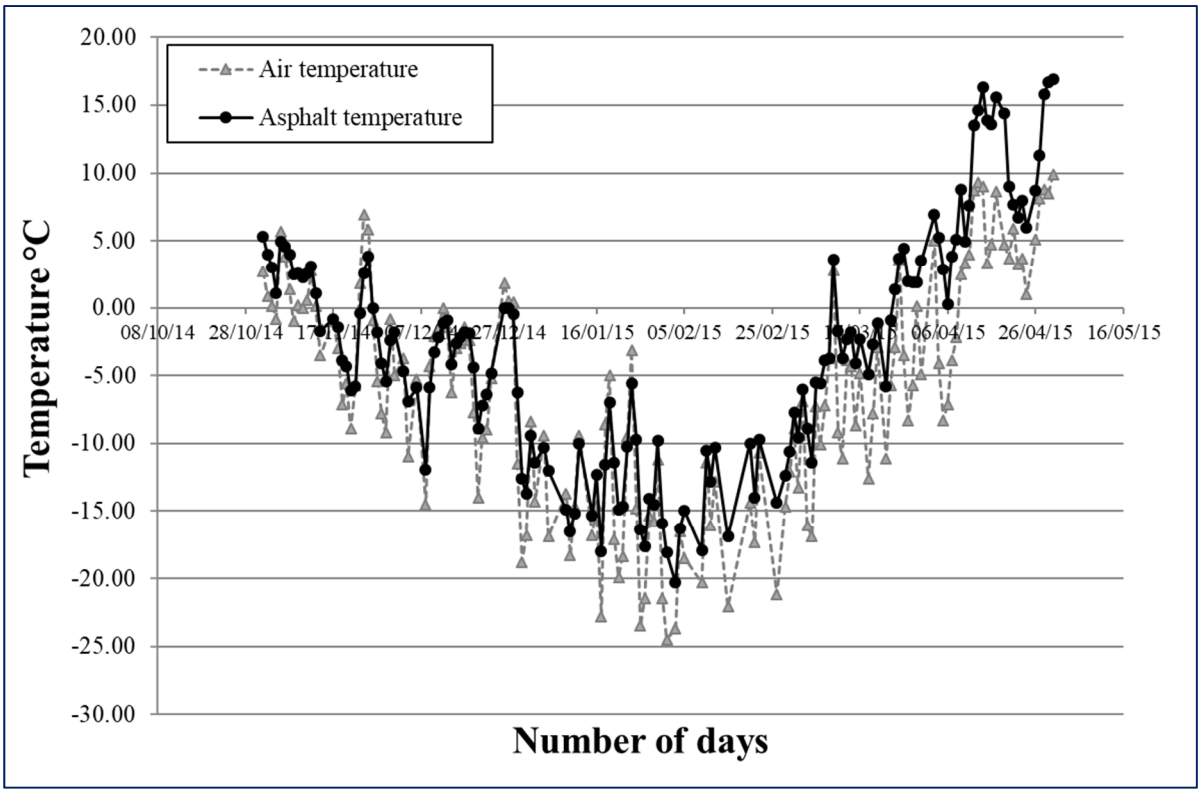

Figure 4.1 Daily temperature history of the Trois Rivere:
Route 155 in Quebec from 1 October 2014 to 1 May 2015

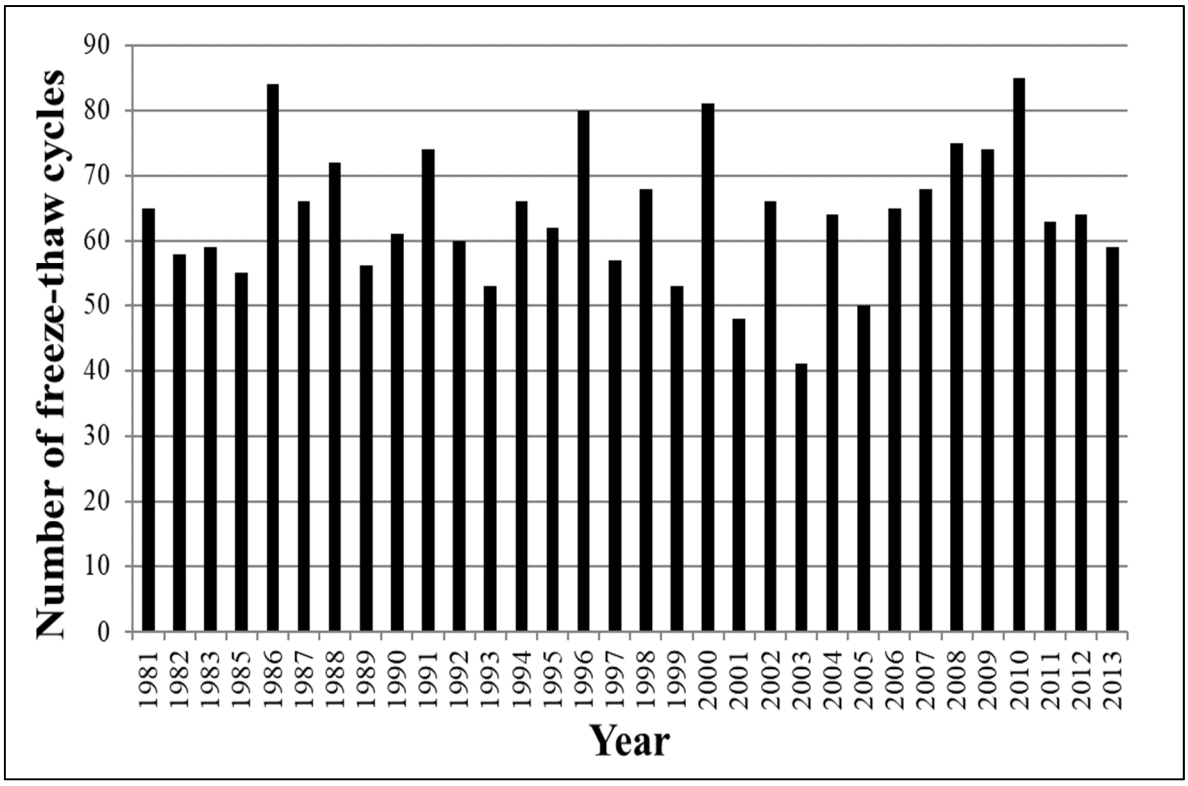

Figure 4.2 Daily number of freeze-thaw cycles in each year from 1981 to 2013, location: Autoroute Félix-Leclerc, section 89-A310

At present, the impact of regional freeze-thaw cycles on bottom-up fatigue cracking has not been considered in Mechanistic-Empirical Pavement Design Method (like PavementME) or other design methods in cold regions. On the other hand, there is a lack of studies on the fatigue characteristics of asphalt mixture after repeated freeze-thaw cycles in the literature. This results in differences between pavement life design and actual pavement's life. The current model of pavement design in cold regions is based on the cumulative fatigue damage for each season without considering the effect of daily freeze-thaw cycles during the late fall and early spring periods (Guy Doré & Zubeck, 2009). Since asphalt fatigue cracking is considered a common phenomenon in Quebec and other regions in Canada (Lamothe et al., 2015), and based on climate data from the LTPP and MTQ, it was decided to analyze the impact of large numbers of freeze-thaw cycles on fatigue characteristics of an asphalt mix. Hence, in this study, thermo-mechanical analyses (complex modulus and fatigue tests) have been conducted to compare the stiffness variation and fatigue life of an asphalt mixture before and after rapid freeze-thaw cycles. The results provide some guidelines to improve the design of asphalt mixtures in cold regions.

4.3 Experimental Consideration

This section describes sample preparation, and the procedures of the freeze-thaw conditioning in detail, including the moisture conditioning, sample preparation before putting the specimens in the chamber and temperature programming for rapid freeze-thaw cycles. Mix design tests were conducted according to the LC method of mix design. LC Method of Mix Design presents the mix design method that was developed by the pavement laboratory (Laboratoire des Chaussées) at the ministry of transportation of Quebec (MTQ). This method is based on the Superpave model and the Laboratoire central des ponts et chaussées de France (LCPC) model.

4.3.1 Test Materials

One type of binder was used in this study with a Superpave™ Performance Grade of PG 64-28 asphalt binder. Asphalt layer systems in pavement structures are usually composed of 2 or

3 different layers with different thicknesses: wearing course, binder course and base course. Asphalt mixture with a nominal maximum aggregate size of 20 mm, called ‘‘Grave Bitume’’ (GB20) which is normally used as a base course in Quebec, was used in this study. Asphalt base layer is the layer that has to resist to fatigue. The base layer does play a major role in bottom-up fatigue cracking resistance. The mix was designed at 6 percent target of air voids to be close to the actual field compaction (Terrel & Al-Swailmi, 1992). The various proportions of each aggregate and characteristics of the reference mix are presented in Table 4.1.

Table 4.1 Asphalt mixture composition and volumetric characteristics

Aggregate gradation		
Sieve No.	GB20, Passing (%)	
	Requirements	Used
28 mm	100	100
20 mm	95-100	98
14 mm	67-90	85
10 mm	52-75	70
5 mm	35-50	41
2.5 mm	-	24
1.2 mm	-	16
0.63 mm	-	12
0.315 mm	-	8.0
0.160 mm	-	7.0
0.08 mm	4.0-8.0	5.5
Filler	-	0.4
Volumetric Characteristics of the mix		
G_{mm}[1]	2.552	
G_{sb}[2]	2.714	
V_{ba}[3] (%)	0.952	
V_{be}[4] (%)	10.202	
b[5] (%)	4.504	

[1] maximum theoretical gravity
[2] bulk specific gravity
[3] volume of binder absorbed
[4] volume of effective binder
[5] binder content

4.3.2 Specimen Preparation

After mix design tests and analysis, four slabs of 500×1800×100 mm^3 (two for reference mix and two for conditioned mix) were compacted with the French laboratory slab compactor (Fig. 3) according to Quebec Standard LC 26-400 (Ministry of Transportation of Quebec, MTQ standard). The percentage of air void in the mix used on the site is usually fixed After mix design tests and analysis, four slabs of 500×1800×100 mm3 (two for reference mix and two for conditioned mix) were compacted with the French laboratory slab compactor (Figure 4.3) according to Quebec Standard LC 26-400 (Ministry of Transportation of Quebec, MTQ standard). The percentage of air void in the mix used on the site is usually fixed between 4 to 8 percent. In this research, the slabs were designed to a targeted air void level of 7%. Cylindrical specimens were cored in the direction of the compaction of the slabs after a 2 week rest period at room temperature and then trimmed to a height of 150 mm and the diameter of 74 mm.

Figure 4.3 French laboratory slab compactor LPC

Before putting instrumentation in place, each sample was weighed to determine its bulk specific gravity (Gmb). After, with Gmb and maximum theoretical specific gravity (Gmm) values, the level of air voids (Pa) was calculated. The actual level of air voids (Va) is calculated according to LC 26-320 (Ministry of Transportation of Quebec, MTQ standard). The saturated surface dry (SSD) technique is the one most commonly used. The bulk specific gravity can be measured by calculating the mass of the specimen in its dry condition, when it is submerged in a water tank, and when it is in its SSD condition.

Measured percentage of air voids are calculated with Equation (4.1):

$$\boldsymbol{P_a = (1 - \left(\frac{G_{mb}}{G_{mm}}\right)) \times 100} \quad (4.1)$$

Subsequently, the slow setting epoxy adhesive was applied to glue the aluminum caps in top and bottom ends of the specimen.

4.3.3 Freeze-Thaw Conditioning

This section describes samples saturation and preparation and the procedure used in freeze-thaw conditioning.

4.3.3.1 Moisture Conditioning Procedure

There is no practical and reliable moisture test to predict the field moisture performance for asphalt mixture in the laboratory. The reason is that the current saturation processes and specimen conditioning methods cannot represent the field conditions, resulting in an underestimation of the effect of moisture for some mixes. Air voids distribution and percentage, as well as the vacuum pressure for achieving moisture saturations, are two main parameters which have significant impacts on moisture testing results (Yi, Shen, Wang, Feng, & Huang, 2016). Saturation process was conducted to introduce liquid the voids from the test

standard specified by LC method for moisture resistance measurements (Ministry of Transportation of Quebec, MTQ standard). Mixtures with more connected voids could easily reach 70 % to 80 % saturation level without severe vacuum pressure conditioning. However, mixtures which have a low percentage of connected air voids are not easy to reach the desired saturation level without being pre-damaged (Kringos, Azari, & Scarpas, 2009). To solve this problem, a constant low pressure of vacuum is required to reach a certain percentage of saturation in the specimen, without creating micro-damage (Yi et al., 2016).

In this research, specimens were divided into 2 different groups. The first group of specimens was kept the air dry (D) as controlled reference specimens (Figure 4.4 (a)). The second group was conditioned through vacuum saturation (Figure 4.4 (b)). For the saturation process, two steps were considered. First, the specimens were placed in a container with a water level at a minimum of 25 mm above the container bottom. Then, the desiccator was filled with deaerated water for 30 min, always under vacuum (Pressure (P) was kept below or equal to 4 KPa or 30 mm- Hg). This conditioning represents field performance for up to four years (Bagampadde, Isacsson, & Kiggundu, 2004). The sample was kept under submersion which is believed to be exactly 30 minutes. Then the degree of saturation was determined. Specimens with more than 80 percent degree of saturation were not used in this study because it was believed that they were damaged during the saturation process. Figure 4.5 indicates the equipment that has been used for this step.

(a) **(b)**

Figure 4.4 Specimens prepared for freeze-thaw cycle and thermo-mechanical test: (a) Reference sample; (b) Specimen covered by Latex membrane to avoid water evaporation during handling and freeze-thaw cycles

Figure 4.5 Saturation process equipment in the laboratory of LCMB

The degree of saturation is defined by using Eq. (2):

$$DS = \frac{100 \times J'}{V_a} \tag{4.2}$$

J' can be determined from Eq. (3);

$$J' = B' - A \tag{4.3}$$

V_a can be determined from Eq. (4).

$$V_a = \frac{P_a E}{100} \tag{4.4}$$

4.3.3.2 Preparation of the Specimens for the Freezing and Thawing

Table 4.2 gives the degree of saturation and the air void's percentage for each specimen. At the end of the saturation process, the specimens were wrapped in a latex membrane, and the waterproofed tape was placed around the sample to prevent water loss during the freeze-thaw cycles (Figure 4.4 (b)). Specimens were conditioned to near 80% degree of saturation as described previously.

Table 4.2 The degree of saturation and the percentage of voids before and after the saturation process for the test specimens

Group	specimen	Percentage of voids	Percentage of saturation	Percentage of voids after saturation
Reference	S1R1	6.8%	0%	0%
	S1R2	6.7%	0%	0%
	S1R3	6.9%	0%	0%
	S1R4	6.6%	0%	0%
Freeze-thaw conditioned (complex modulus)	S2CM150	6.8%	79%	7.0%
	S2CM300	6.9%	79%	6.9%
Freeze-thaw conditioned (fatigue)	S2FT1	6.8%	79%	7.0%
	S2FT2	6.9%	80%	7.2%
	S2FT3	6.6%	79%	6.9%
	S2FT4	6.8%	79%	7.2%

4.3.3.3 Temperature Cycles used for Freeze-Thaw Cycles

There is no standard method to assess the daily rapid freeze-thaw cycles of the asphalt mixture. After the saturation process, each conditioned samples were submitted to 150 and 300 freeze-thaw cycles as set forth in ASTM C-666.92, "Standard Test Method for Resistance of Concrete to Rapid Freezing and Thawing". The cooling and heating rate used was 4.5 °C/min. For each freeze-thaw cycle, two different temperature levels were targeted, which is -18 and 6 °C. The

temperature remained constant for a period of 1.5 hours at each level of temperature. No specimen was oven dried before or after the rapid freeze-thaw testing since it might affect the viscoelastic characteristics of asphalt mix.

Figure 4.6 indicates that there is a difference between the temperature sensor placed in the center of the sample and the temperature sensor placed on the surface of the sample. This behavior was quite expected and is due to the rapid rate of the heating and cooling cycles. This non-homogeneity of the temperature during rapid heating-cooling cycles may increase the potential for thermal cyclic damage since there is a different level of contraction and expansion in the mix.

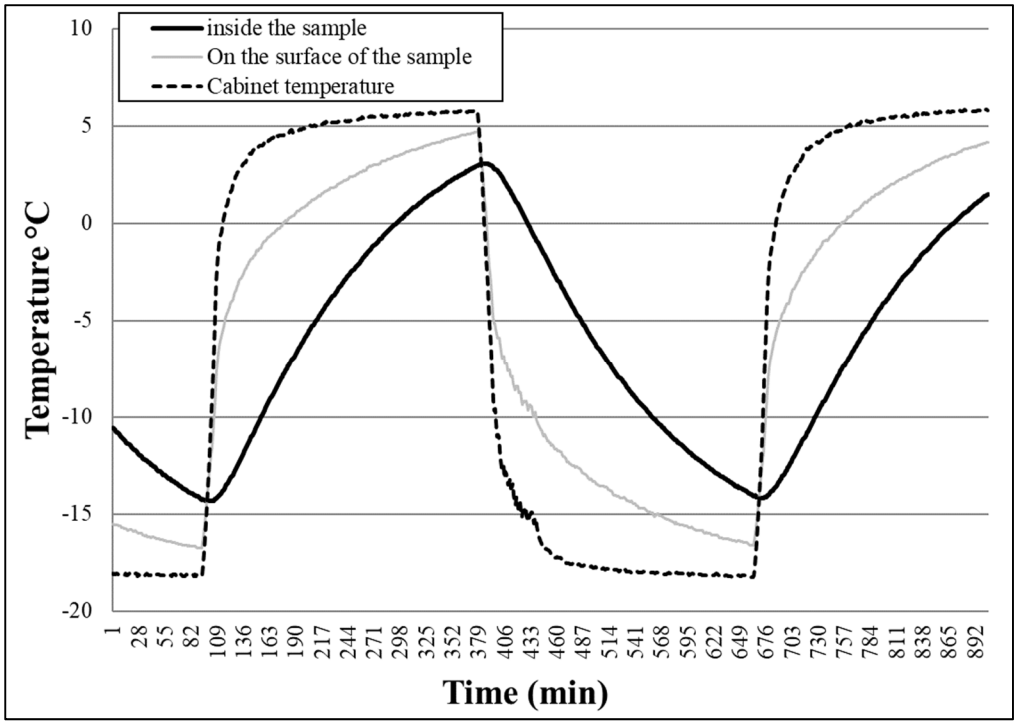

Figure 4.6 Temperature history detected by sensors during a temperature cycling: on the surface of the specimen, inside the specimen, and the cabinet temperature

4.4 Thermo-Mechanical Tests

The equipment, procedure, and the result and discussion of each test are explained in this section.

4.4.1 Test Equipment

The thermo-mechanical tests were performed by using a servo-hydraulic press (MTS 810, TestStar II), with an electronic monitoring system. An environmental cabinet was used for thermal conditioning (heating and cooling) of the specimens (Figure 4.7).

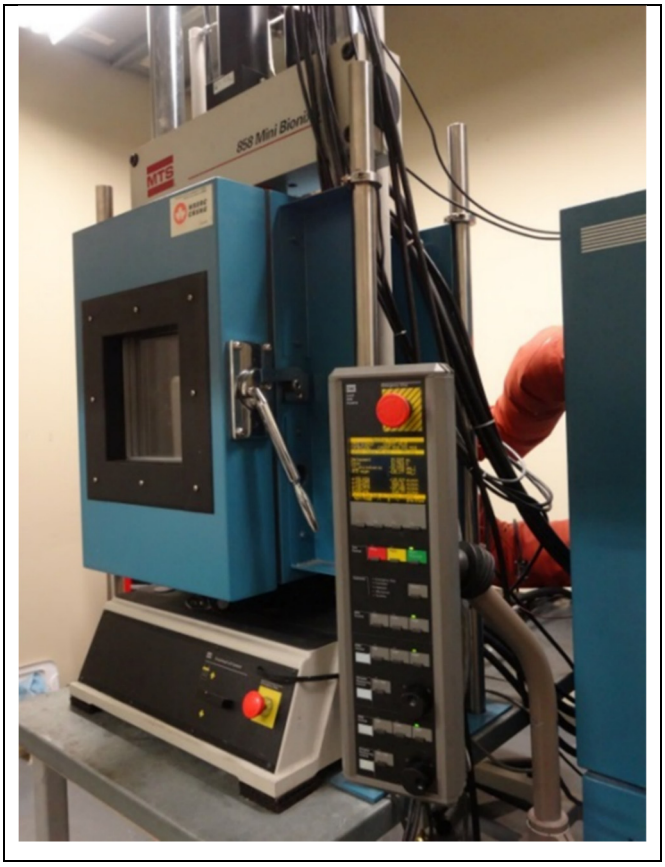

Figure 4.7 MTS Measurement System and environmental chamber

The direct tension-compression test on cylindrical specimens of 150 mm in height and 75 mm in diameter was adopted which is based on MTQ standard. One of the advantages of the tension-compression test is that the stresses and strains are measured directly from the measurements of the force and displacement of the boundary (Perraton et al., 2015). The amplitude of strain was measured with three sensitive extensometers installed around the specimen at an angle of 120° from one another (Figure 4.8). The temperature was monitored during the test by using three surface temperature probes (PT100) to control the temperature and detect any variations in temperature during testing. A stabilization time period (6 hours) was considered when the temperature was changed. This rest period ensures a homogeneous temperature inside and outside the specimen (Tapsoba et al., 2014).

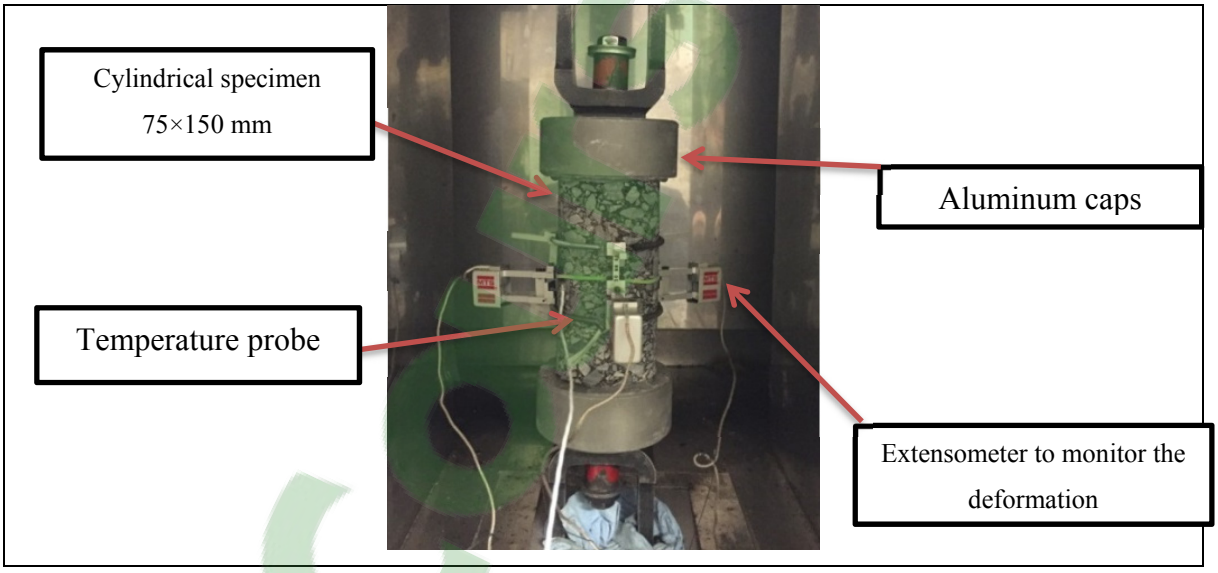

Figure 4.8 Specimen preparations for the thermo-mechanical tests

4.4.2 Test Procedures

4.4.2.1 Complex Modulus Test

In this project, complex modulus tests were performed before and after conducting the rapid freeze-thaw cycles. The MTQ determines the complex modulus of asphalt mixes in accordance

with test method LC 26-700 "Determining the complex modulus of asphalt mixes". The complex modulus (E*) in this test defines the relationship between stress and strain under a continuous sinusoidal loading. Complex modulus is identified by the norm of the modulus that explains the material's stiffness, and is characterized by the dynamic modulus |E*| (Equation (4.5)):

$$|\boldsymbol{E}^*| = \frac{\boldsymbol{\sigma_0}}{\boldsymbol{\varepsilon_0}} \tag{4.5}$$

The Phase angle (φ) is described as a phase lag of the strain behind the stress under the sinusoidal cyclic solicitation. The phase angle is 0° for purely elastic material, and 90° for a purely viscous material. The ratio of the amplitude of the sinusoidal stress of pulsation (ω) applied to the material $\sigma = \sigma_0 \, sin(\omega t)$ and the amplitude of the sinusoidal strain $\varepsilon_t = \varepsilon_0 \, sin(\omega t - \varphi)$ that result in a steady state (Equation (4.6)) (Di Benedetto et al. 2004b).

$$\boldsymbol{E}^* = \frac{\boldsymbol{\sigma}}{\boldsymbol{\varepsilon}} = \frac{\boldsymbol{\sigma_0 e^{i\omega t}}}{\boldsymbol{\varepsilon_0 e^{i(\omega t - \varphi)}}} \tag{4.6}$$

An MTS press was used over a range of various temperatures (−35°C, −25°C, −15°C, −5°C, +5°C, +15°C, +25°C and +35°C) and frequencies (10, 3, 1, 0.3, 0.1, and 0.03 Hz). The target applied strain was fixed at 50 μ-strain to ensure that the measurement was maintained within the linear viscoelastic domain (Herve Di Benedetto, Olard, Sauzéat, & Delaporte, 2004).

4.4.2.2 Fatigue Test

Fatigue phenomenon is occurring under the repetition of loading due to the traffic, especially heavy vehicles. The accumulated damage due to a large number of the repetitions results in stiffness reduction of the materials and leads to failure. The asphalt pavement life is directly affected by this phenomenon, which needs to be correctly considered in order to calculate precise asphalt pavement structural design.

Fatigue test procedure has been developed in DGCB (***D**épartement de **G**énie **C**ivil et **B**âtiment*) at the ENTPE (***É**cole **N**ationale de **T**ravaux **P**ublics de l'**É**tat*, (Lyon, France)). The test was

conducted in laboratory based on the variation of the complex modulus (stiffness) under cyclic solicitation of strain homogeneous test. Mid-value of strain was monitored during the fatigue test to make sure that it remains null. Fatigue tests were performed under the frequency of 10 Hz and the temperature of 10°C conditions. Evolution of the stiffness modulus was controlled by monitoring the axial strain during the test. Wöhler's curve was plotted at the end of the fatigue test analysis. It is based on the evolution of fatigue life at different levels of strain amplitude.

4.5 Results and Discussions

4.5.1 Complex Modulus Test Results

Equation (4.7) was used in order to analyze the results of complex modulus with the 2S2P1D rheological model which was expressed by (Olard et al., 2003).

$$E^*(i\omega\tau) = E_0 + \frac{E_{00} - E_0}{1 + \delta(i\omega\tau)^{-k} + (i\omega\tau)^{-h} + (i\omega\beta\tau)^{-1}} \quad (4.7)$$

The changing of τ by temperature can be explained by means of a shift factor if the time–temperature superposition principle holds:

$$\tau(T) = a_T(T) \times \tau_0 \quad (4.8)$$

Seven criterion (E_{00}, E_0, δ, k, h, β and τ_{0E}) are needed to fully analyze the linear viscoelastic characteristics of the tested specimens at a given temperature and frequency. The progressions of τ_E were determined by the William-Landel-Ferry (WLF) model (Ferry 1980). τ_{0E} was quantified at the selected reference temperature T_{ref}. When the temperature effect is determined, the number of criterion becomes nine, including the two WLF criteria (C_1 and C_2 determined at the reference temperature).

$$\boldsymbol{log(a_T)} = \frac{-C_1 (T - T_s)}{C_2 + (T - T_s)} \quad (4.9)$$

The 2S2P1D modeling parameters in this study are presented in Table 4.3. The k, h, δ parameters are related to the binder rheology (Olard et al. 2003, Di Benedetto et al. 2004b) which are almost same for the three groups. Regarding the other parameters, E00 is the glassy modulus (E when ω→∞), and E0 is the static modulus (E when ω →0), which is related to the void content and aggregate skeleton. The results will fit on a single curve for each test in the Black space, and in the Cole–Cole plane.

Table 4.3 Parameters of the introduced 2S2P1D model for the corresponding mixes

Specimen	V_a (%)	E_0 (MPa)	E_{00}(MPa)	k	h	δ	τ_E (s)
S1R1 (Reference)	6.8	30	40000	0.18	0.55	2.60	0.007
S2CM150 (150 F-T)	6.8	16	40000	0.16	0.55	2.60	0.007
S2CM300 (300 F-T)	6.8	10	33000	0.19	0.60	2.65	0.007

Figure 4.9 shows the experimental test results in the Cole-Cole plane with the 2S2P1D model. A Cole-Cole plane is achieved by plotting the loss modulus versus the storage modulus. The storage modulus is plotted on the real axis (x-axis), and the loss modulus is plotted on the imaginary axis (y-axis). Therefore, the plotted modulus should form a single curve without considering the frequency or temperature (Pellinen, 2002). First of all, the results in Cole-Cole diagram express significant differences before and after the effect of 300 freeze-thaw cycles, while the diagram does not show significant differences between the reference and after 150 freeze-thaw cycles.

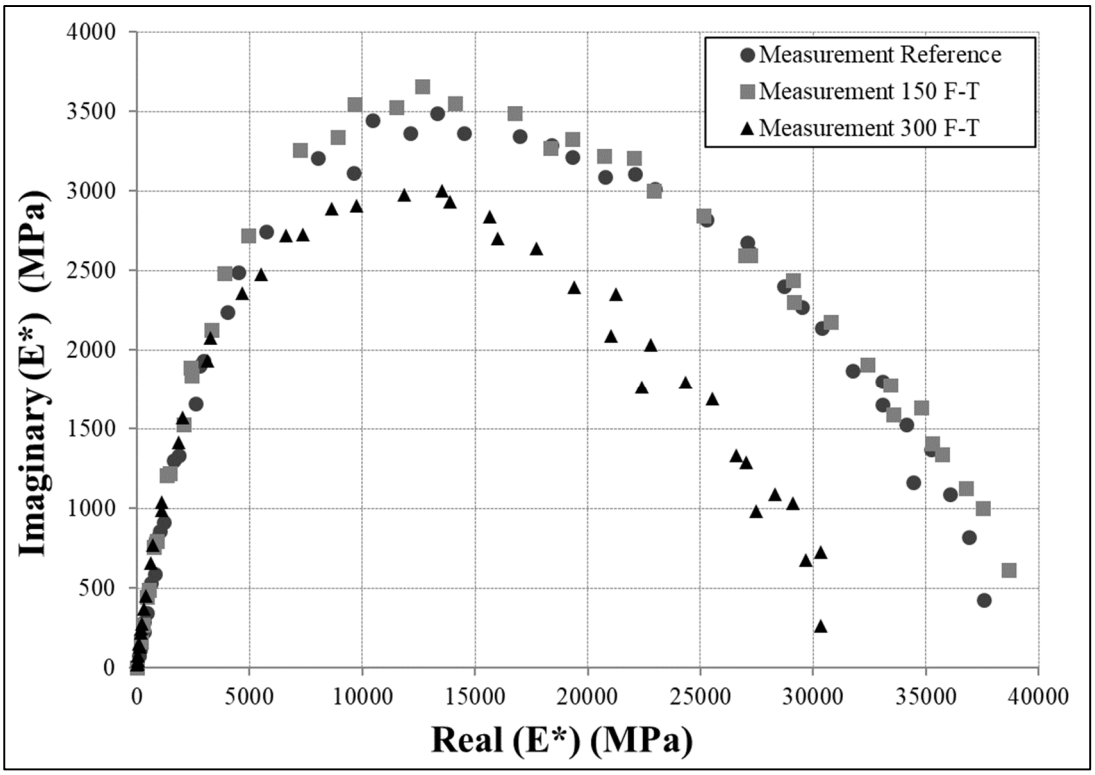

Figure 4.9 Complex modulus results in Cole-Cole diagram

Figure 4.10 shows the complex modulus results in Black Curve diagram. It can be seen that the phase angle reduces in Black curve diagram after reaching a maximum value. The maximum value of the phase angle represents the viscosity of the bitumen at high temperature and depends mostly on the type of the bitumen. In this study, this difference of the maximum value before and after freeze-thaw cycles can be explained as the stripping failure due to the loss of the cohesion within the binder as already mentioned in the literature (Williams and Miknis, 1998; Copeland et al., 2006; Caro et al., 2008).

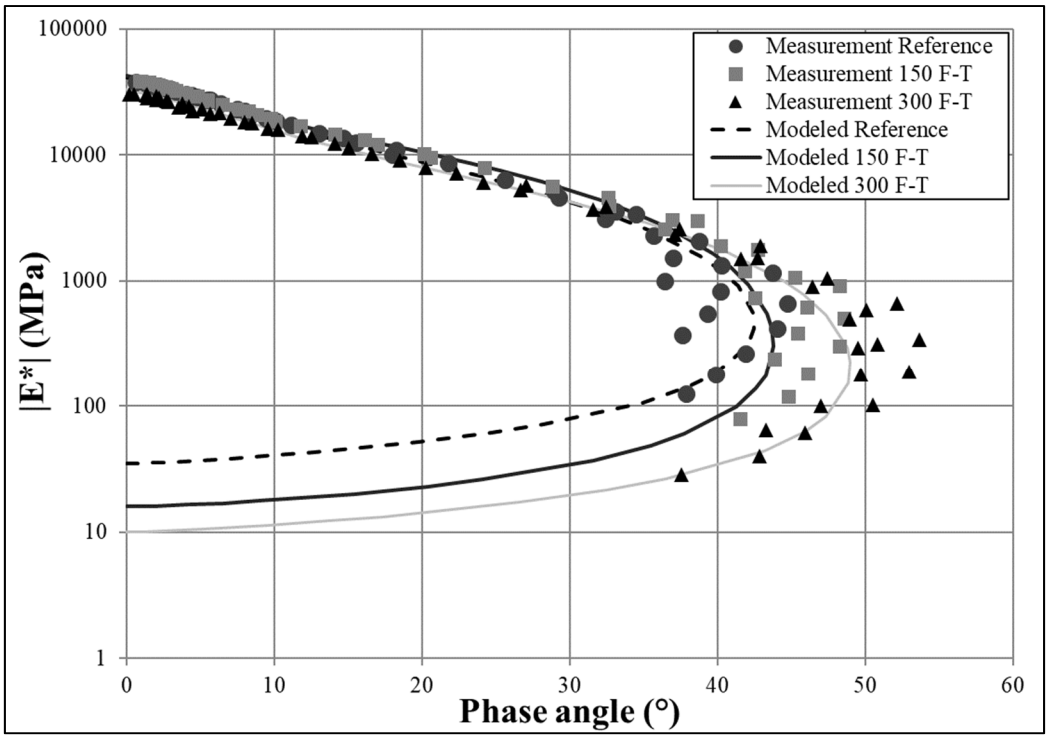

Figure 4.10 Complex modulus results in Black Curve diagram

The results can also be shown on a master curve. To that end, each isothermal curve can be shifted in frequency in order to obtain a single master curve at a reference temperature. Figure 4.11 shows the master curves (complex modulus norm) for the third tested group. As it is indicated in the graph, the top part of the master curve (at high frequencies, low temperature) is equal for all of the reference and conditioned mix after 150 freeze-thaw cycles. This means that the maximum stiffness value of the mix was not changed after the 150 freeze-thaw cycles, while the bottom part of the master curves (at low frequencies, high temperatures) which is associated with the minimum asphalt mixture stiffness value has been changed after the 150 freeze-thaw cycles. The reductions of complex modulus at high and low temperatures are more tangible after the 300 F-T cycle and indicate that the mixture behavior is more sensitive to a high number of rapid freeze-thaw cycles.

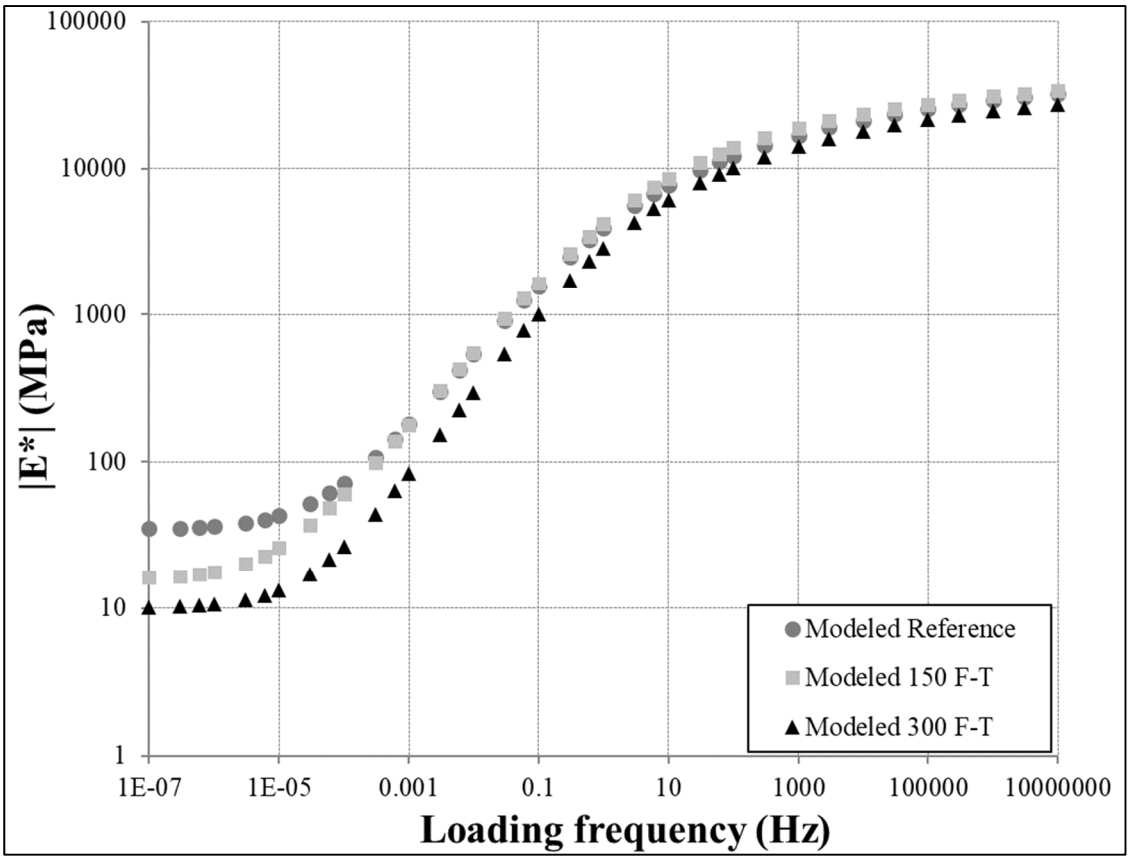

Figure 4.11 Complex modulus results in Master Curve

In order to objectively compare the results for low and high level of freeze-thaw cycles, the condition effect coefficient (C*CEC) was calculated (Di Benedetto et al., 2004). It is defined as a ratio between the complex modulus of the conditioned mix after a number of freeze-thaw cycles E* FT, and the complex modulus of a reference mix E* Ref, at the same frequency. Figure 4.12 compares the C*CEC of 150 and 300 freeze-thaw cycles.

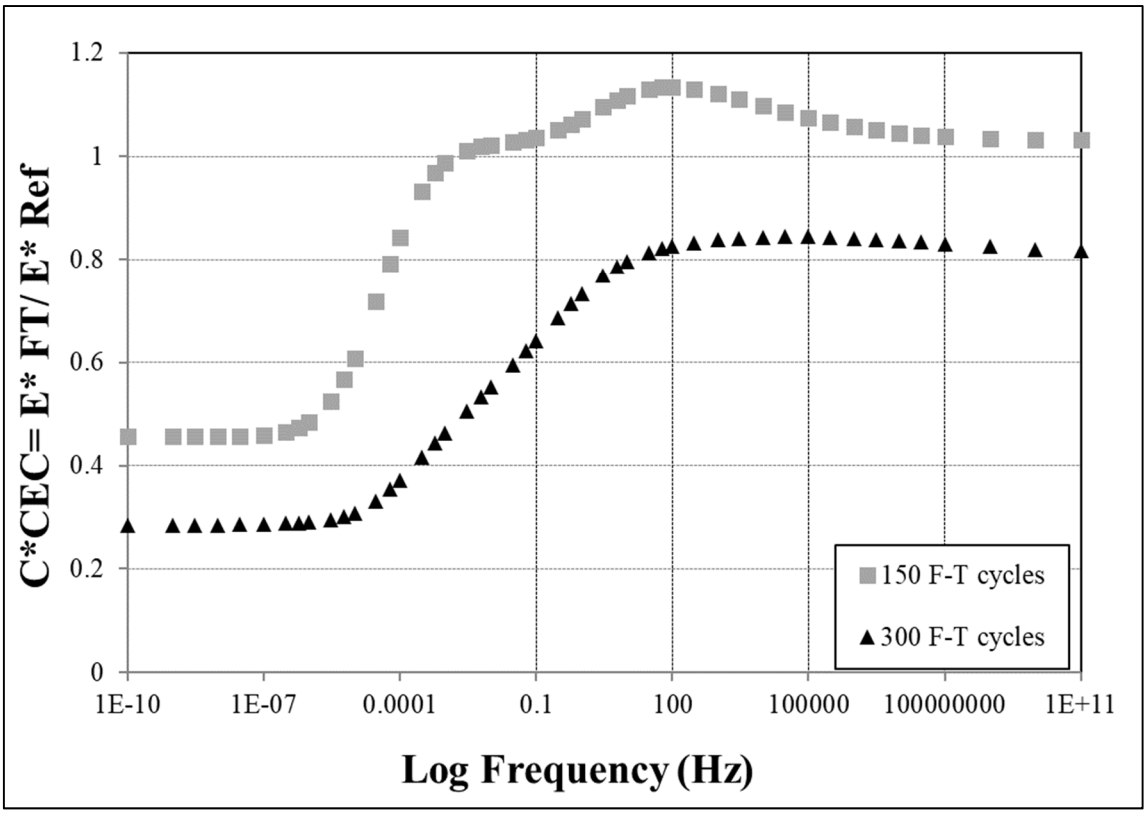

Figure 4.12 Comparison of the effect of 150 rapid F-T cycles and 300 rapid F-T cycles on the stiffness behavior of the mix

It can be observed that the effect of freeze-thaw conditions on the stiffness behavior of the mix is higher with increasing the number of cycles from 150 to 300 for low and high frequencies. The 150 freeze-thaw cycles change the norm of complex modulus at high temperature (low frequency), while the difference of stiffness is negligible at low temperature (high frequency) after 150 F-T cycles. However, stiffness behavior changes with the high value of C*CEC at high temperatures and low value of C*CEC at low temperatures after 300 freeze-thaw cycles.

In general, the results from the Cole-Cole, Black curve, and master curve diagrams do not follow the unique curve before and after the conditioning. Based on the mechanism of the freeze-thaw cycles explained in the literature, the ice expansion load could change the composition of voids and the interior micro-damage might be accumulated during rapid freeze-thaw cycles. The damage from the accumulation of ice expansion load will deteriorate the

asphalt-aggregate bond and allows water to be displaced with the mastic and increase the stripping of aggregates (Si et al., 2014). The stripping is due to the loss of adhesion at the cement-aggregate interfaces and in part by the failure of the cohesion within the binder (Williams and Miknis 1998, Copeland et al. 2006, Caro et al. 2008).

4.5.2 Fatigue Test Results

In this research, fatigue tests were carried out having four different levels of strain amplitude for the reference and conditioned mixes (see Table 4.4). The value of the modulus at the beginning of the test was denoted $|E_0^*|$ which represents the extrapolated value at cycle 1 by assuming the linear characteristics of complex modulus from cycles 2 to 50. Table 4.4 demonstrates the information about the samples, the applied axial strain amplitudes, and the $|E_0^*|$ values for different specimens. The difference of the initial modulus between the reference and conditioned samples specifies the reduction in $|E_0^*|$ value after rapid freeze-thaw cycles which confirm the complex modulus test results.

Table 4.4 Fatigue testing samples characteristics and information

Group	Specimen	Percentage of voids	Percentage of saturation	Average axial strain amplitude (μm/m)	Initial modulus, $\lvert E_0^* \rvert$ (Mpa)		
					Value	Average	Standard deviation
Reference	S1R1	6.8%	0%	71	12563	1073.5	1453.2
	S1R2	6.7%	0%	99	10854		
	S1R3	6.9%	0%	66	10500		
	S1R4	6.6%	0%	84	9025		
Conditioned (After 300 rapid freeze-thaw cycles)	S2FT1	6.8%	79%	97	7041	7524	389.9
	S2FT2	6.9%	80%	74	7400		
	S2FT3	6.6%	79%	62	7720		
	S2FT4	6.8%	79%	113	7935		

4.5.2.1 Fatigue Results Example

The evolution of the stiffness in terms of the number of cycles is mainly used to verify the validity of the test and to determine the apparition of cracks in the specimen (Baaj, Di Benedetto, & Chaverot, 2005). The evaluation of the stiffness is usually divided into three phases during a fatigue test (Baaj et al., 2005). In the first step, stiffness decrease rapidly which cannot be explained only by fatigue. Heating, as well as thixotropy, has an important role in this step. Phase II is characterized by a quasi-linear decrease of stiffness which is characterized by the initiation of microcracks inside the mix. During the phase III, from the coalescence of microcracks, a macro-crack appears and propagate within the materials (Tapsoba et al. 2013).

Figure 4.13 shows the complex modulus evolution for the reference S1R1 sample and the conditioned S2FT3 specimen. The complex modulus decreases quickly for both specimens at the beginning of the test which can be considered as phase I. During phase II, the complex modulus uniformly decreased for the reference specimen, while the conditioned specimen has a non-uniform gradient. The phase III or end of the test is characterized by a rapid decrease of measured values for the reference and slight decrease for the conditioned sample. The difference in behavior of the stiffness evolution curve for the reference and conditioned specimens could result from the presence of water inside the pore structures of the conditioned specimen.

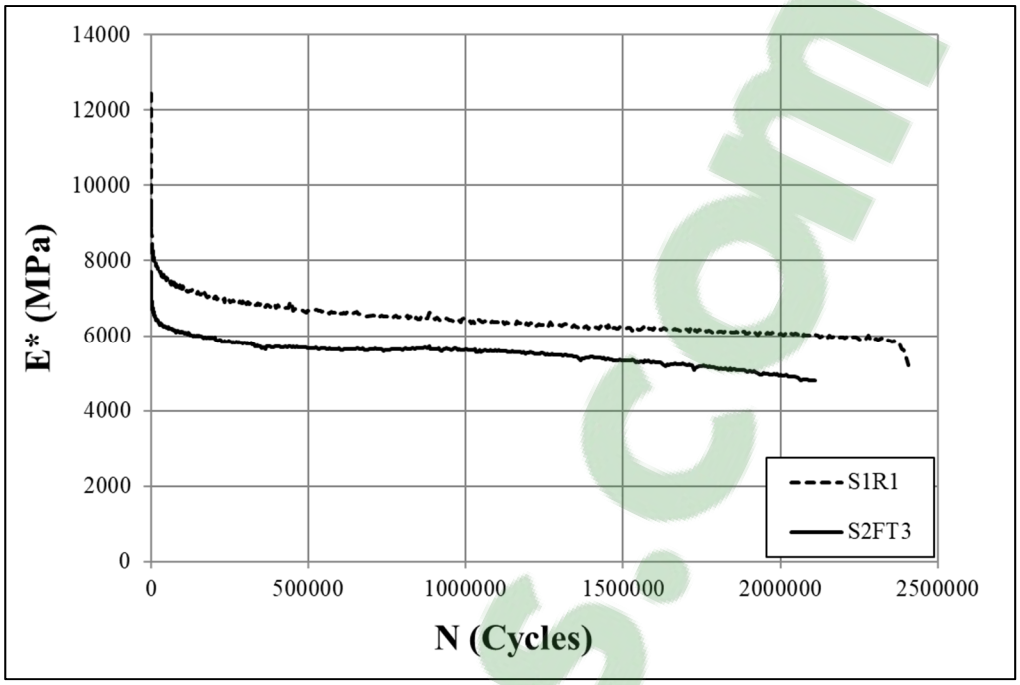

Figure 4.13 Example of the evolution of the complex modulus with time for the S1R1 reference sample and S2FT3 conditioned sample at 70 µdef

4.5.2.2 Fatigue failure criteria

A fatigue failure criterion is considered acceptable if it can precisely recognize the transition location of the phase change from II to III in the evolution of the stiffness during fatigue testing (Perraton et al. 2015). In our experimental program, four criteria were used: Nf50%, NfΔεax, NfΔφ and Nfφmax. Nf50% is a classical fatigue criterion based on modulus decrease which corresponds to a decrease of 50% reduction of the initial stiffness of the specimen (Di Benedetto et al., 2004; Perraton et al., 2015). NfΔεax is based on the reading of the amplitude of strain for each extensometer. A difference of more than 25% of the extensometers reading can be considered as increasing heterogeneity within the specimen. NfΔφ is a difference of more than 5° of the extensometer phase angle reading with the mean value. The corresponding number of cycles is associated with failure. Finally, Nfφmax is based on the evolution of the phase angle; maximum value of the phase angle is associated with the transition of phase II/III. Tapsoba et al. (2013) have compared these criteria together, and they concluded that all criteria

used to give almost the same results. Furthermore, they revealed that Nfφmax and NfΔεax are closer and can strongly show the phase change of II to III threshold.

Table 4.5 summarizes the fatigue life for all specimens tested. With those test results, it was decided to define NfII/III criterion along with Nf50% criterion for further analysis. NfII/III is associated with the transition between phases II as well as phases III and it is based on the average value of the NfΔεax, NfΔφ and Nfφmax.

Table 4.5 Experimental test results: summary of the N_f for tested samples

Group	Specimen	Deformation (μdef)	$N_{f50\%}$	$N_{f\Delta\varepsilon ax}$	$N_{f\Delta\varphi}$	$N_{f\varphi max}$	$N_{fII/III}$
Reference	S1R1	71	1,304,196	2,320,762	2,401,068	2,300,816	2,340,882
	S1R2	99	1,129,038	934,396	1,213,946	1,043,658	1,064,000
	S1R3	66	5,381,624	4,855,565	4,527,469	4,763,199	4,715,411
	S1R4	84	4,558,950	2,511,005	2,425,127	2,563,868	2,500,000
Conditioned (After 300 rapid freeze-thaw cycles)	S2FT1	97	179,460	99720	129323	-	114,521
	S2FT2	74	845,929	813316	833388	845929	830,878
	S2FT3	62	2,110,893	1564927	2090861	1559919	1,738,569
	S2FT4	113	160,000	126997	144553	159601	143,717

4.5.2.3 Analysis of fatigue life

Fatigue test results are usually expressed as the graphical presentation which is usually given by the fatigue curve or so-called Wöhler curve (Baaj et al., 2005; Perraton et al., 2015). Wöhler curve represents the log number of cycles at failure (fatigue life) versus the amplitude of the applied strain in logarithmic axes. In these axes, Wöhler curves for asphalt mixes are classically straight lines. They are represented by Equation (4.10).

$$N_f = K_1 \varepsilon^{-K_2} \tag{4.10}$$

Considering the failure at 1 million cycles, then the Equation (4.9) becomes Equation (4.11):

$$\frac{Nf}{10^6} = \frac{\varepsilon^{-C2}}{\varepsilon_6} \tag{4.11}$$

Figure 4.14 and Figure 4.15 indicate the $N_{f50\%}$'s Wöhler curve and $N_{fII/II}$'s Wöhler curve respectively for the reference and conditioned samples. They represent the number of cycles of failure versus the amplitude of the applied strain in logarithmic axes. Table 4.6 summarizes the fatigue parameters for $N_{f50\%}$ and $N_{fII/II}$. Based on the fatigue test results analyzed by using $N_{f50\%}$ and $N_{fII/II}$ Criteria, the following outcome is considered:

E_0 decreased substantially after freeze-thaw cycles which confirm the results of the complex modus test.

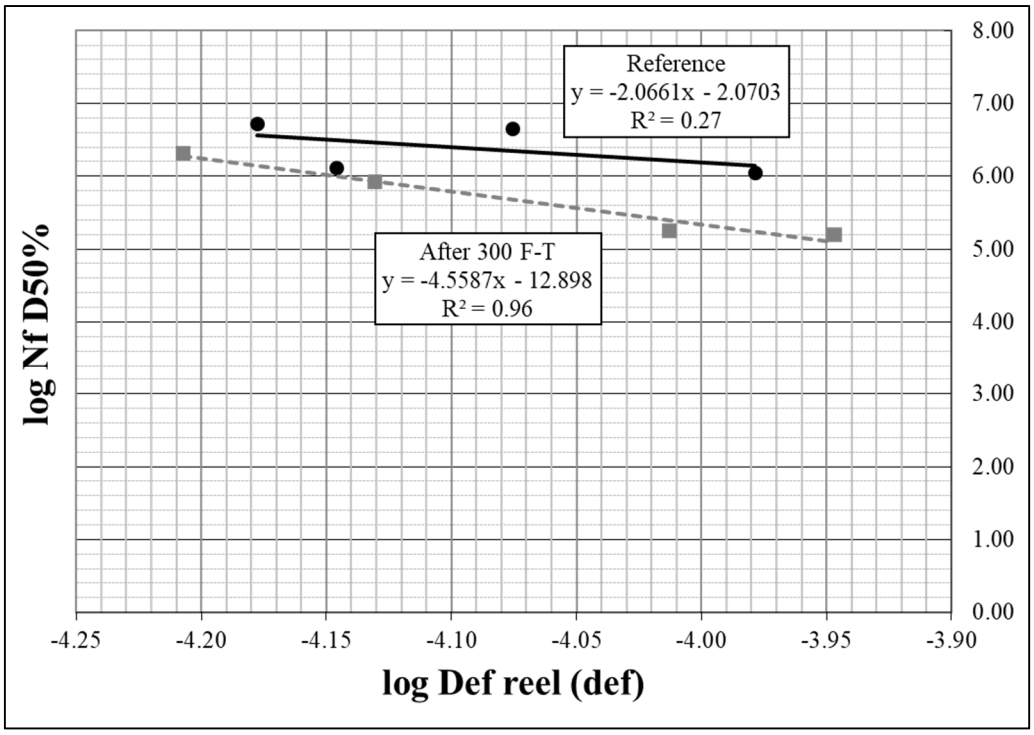

Figure 4.14 Wöhler curve Nf50% for the reference and conditioned specimens

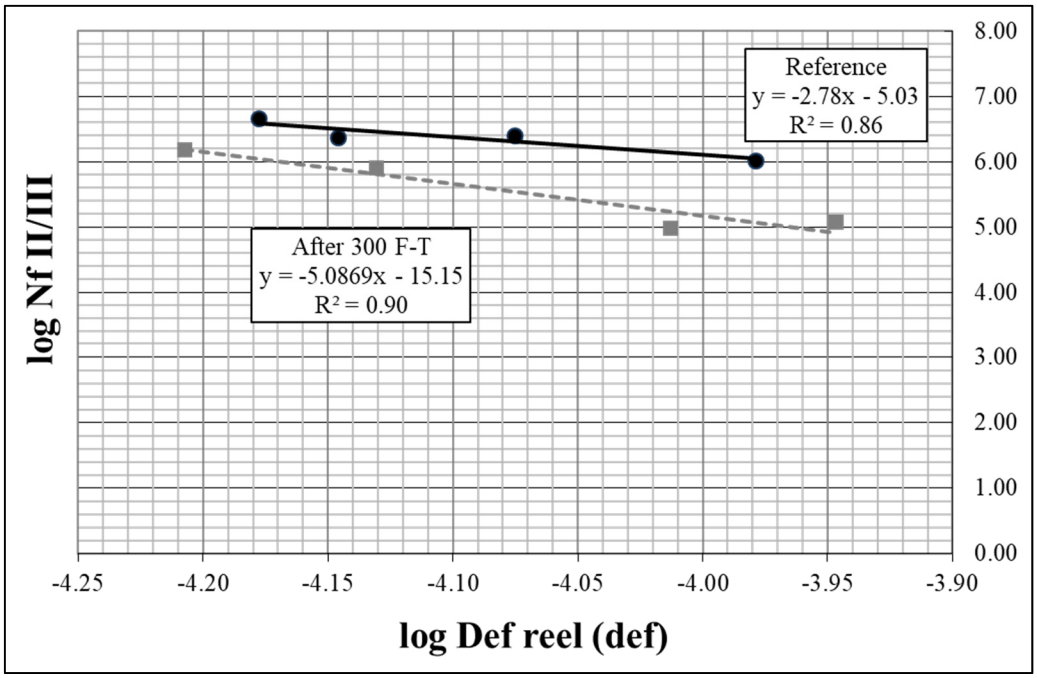

Figure 4.15 Wöhler curve NfII/III for the reference and conditioned specimens

Table 4.6 Fatigue parameters for different criteria

Criteria	Parameters for the reference mix				Parameters for the conditioned mix			
	K_1	K_2	R_2	ε_6	K_1	K_2	R_2	ε_6
$N_{f50\%}$	8.51E-03	2.07	0.27	91.65	1.27E-13	4.56	0.96	73.38
$N_{fII/III}$	1.19E-05	2.76	0.86	103.63	3.81E-15	4.90	0.90	70.17

Regarding fatigue test results, the $N_{fII/III}$ failure criterion seems to be more accurate than $N_{f50\%}$ criterion because it can precisely recognize the transition location of the phase change from II to III by calculating the average of the value of N_f from three different criteria.
R^2 values are closer to one for $N_{f\,II/III}$ criterion. This explains that the regression line perfectly fits the data and it proves that the regression model based on $N_{f\,II/III}$ criterion is more accurate than the model based on $N_{f50\%}$.

The slope of the curve is steeper for conditioned mix and is more tangible for $N_{f50\%}$ criteria. This means that the conditioned mix has lower fatigue life at high strain amplitude (heavy truck loads). At low strain amplitude, the number of cycles obtained with the criteria for both reference and conditioned samples is closer.

ε_6 value is much greater for the reference mix. This value corresponds to the strain amplitude for a failure at 1,000,000 cycles. The $N_{f50\%}$ criterion gives a lower value of ε6 than the $N_{fII/III}$ criterion for the reference mix.

Figure 4.16 shows the comparison of a parameter of ε_6 for the reference samples and after the environmental freeze-thaw cycles. The percentage of reduction of the ε_6 after 300 rapid freeze-thaw cycles is 19.93% for $N_{f50\%}$ and 32.29% for $N_{f\,II/III}$ criteria respectively.

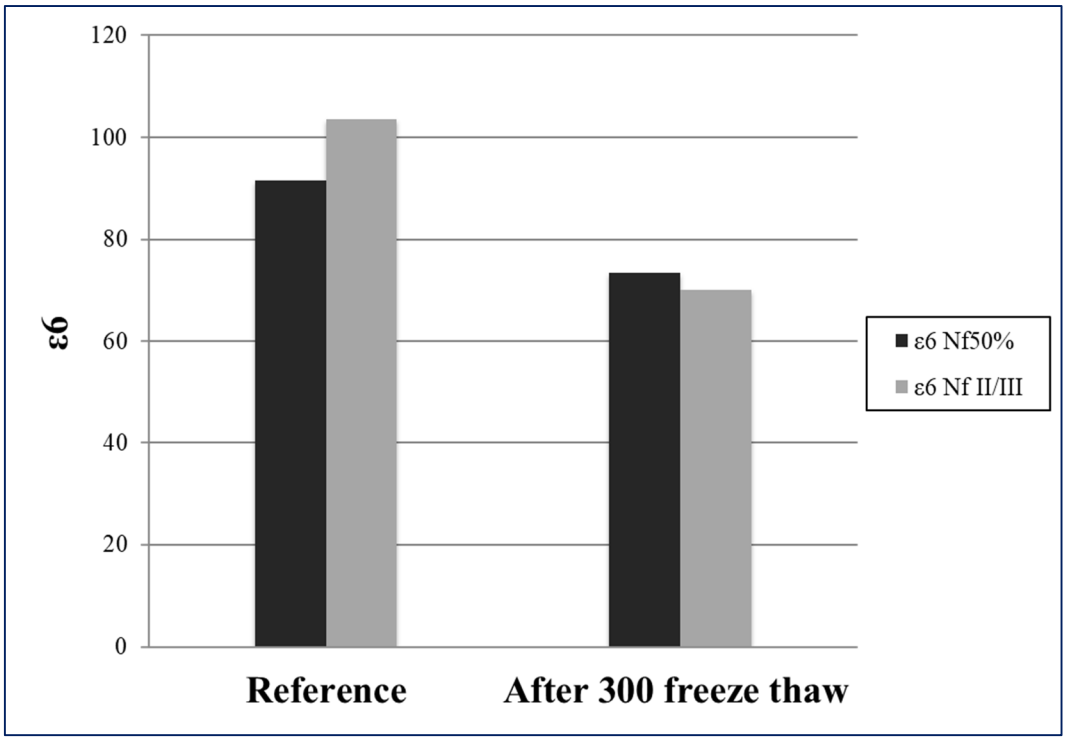

Figure 4.16 Comparison of parameter of ε6 for the reference samples and after the environmental freeze-thaw cycles

4.5.2.3 Damage at failure

In asphalt mixture fatigue testing, it is possible to calculate the damage of the sample during testing. The method to calculate damage at failure developed in the DGCB laboratory of ENTPE (Baaj et al., 2005; Di Benedetto et al., 2004; Soltani, 1998). It is done by comparing the stiffness modulus at a given number of cycles with the initial stiffness modulus. The damage at failure is calculated with the Equation (4.12).

$$D_{III} = (E_0 - E_{III})/E_0 \quad (4.12)$$

Researchers have shown that the damage value D_{III} associated with the transition of phase II/III is a function of the strain amplitude. Figure 4.17 illustrates the damage values at failure for the reference and conditioned mixes are different by having the different R^2 values. The damage

at failure decreased substantially after the freeze-thaw cycles. It means that the failure for the conditioned samples is not only caused by fatigue test effects.

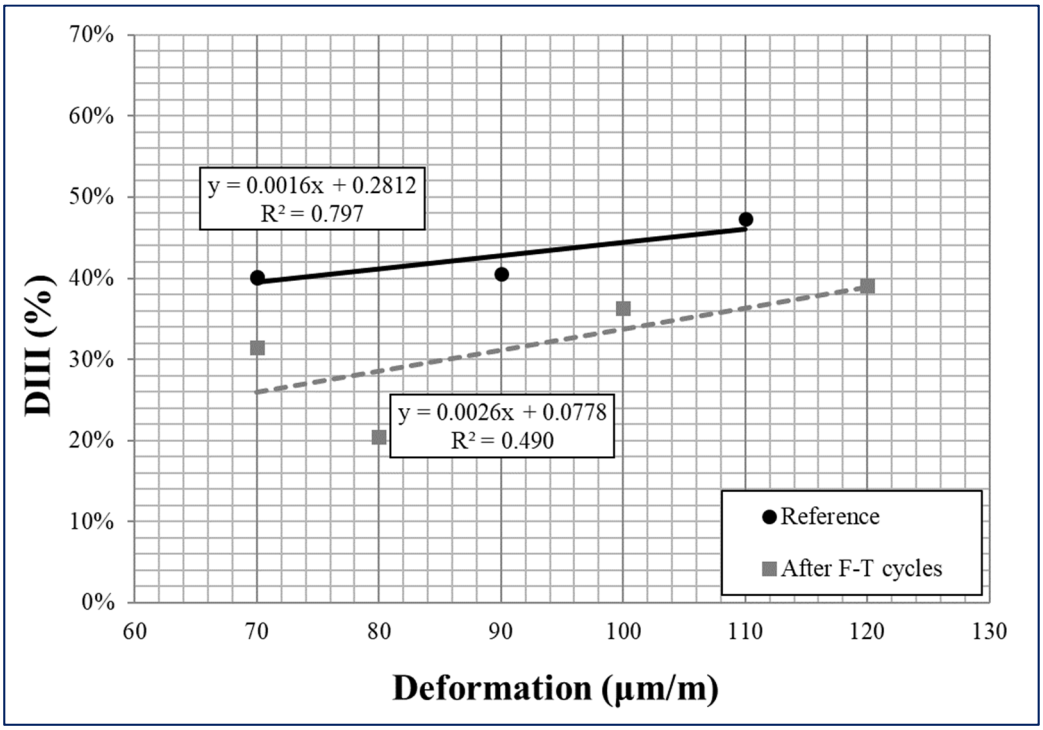

Figure 4.17 Damage at failure analysis for the reference and conditioned specimens

4.5.2.4 Modified damage at the end of phase II

The modified DGCB procedure is used to evaluate the damage at the end of phase II taking into account the biasing effect occurring mainly during the phase I. The evolution of complex modulus was assumed as linear with a number of applied cycles within three intervals including, I) i=0, from 40’000 to 80’000 cycles; II) i=1, from 50’000 to 150’000 cycles; and III) i=2 from 150’000 to 300’000 cycles.

The modified damage at failure is calculated by Equation 4.13 (Tapsoba et al., 2013):

$$D_{IIIc} = D_{III} - C_i \times (E_0 - E_{00i})/E_0 \quad (4.13)$$

Figure 4.18 gives raw damage (D_III) and corrected damage (D_IIIc) according to the level of deformation amplitude before and after freeze-thaw cycles. Biasing effects develop to the level of deformation, which is rational since the source of biasing effect depends on the value of dissipated viscous energy (Tapsoba et al., 2013).

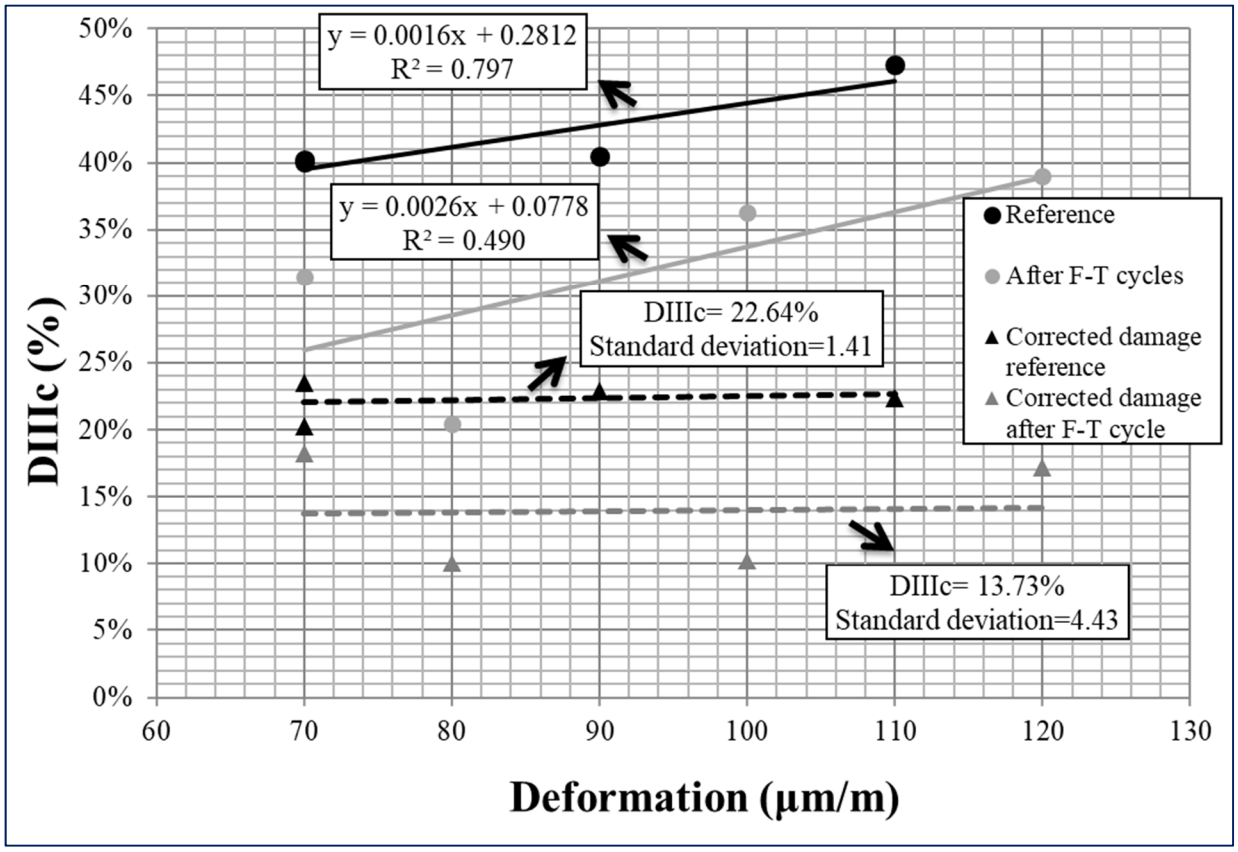

Figure 4.18 Damage values of the transition between phases II and III: DIIIc is the correction from artifact effect

D_{IIIc} is equal to 22.64% with a standard deviation of 1.41 for the reference mix, and D_{IIIc} is equal to 13.73% with a standard deviation of 4.43 for the conditioned mix. The damage reduction for the conditioned mix can be considered as deterioration of samples during freeze-thaw cycles. The reduction in fatigue damage for the conditioned mix is due to the stiffness

reduction after freeze-thaw cycles. This can be considered as the initiation of microcracks during freeze-thaw cycles.

4.6 Test repetitions

Different replicates were used for fatigue analysis, and non-destructive complex modulus tests were repeated on given specimens.

4.6.1 Complex modulus test

Three specimens have been considered for each group (reference, 150 freeze-thaws (F-T), and 300 F-T). Since the complex modulus test is the nondestructive test, it is possible to check the same specimen again. The amplitude of the modulus and the phase angles are compared for each frequency and temperature, if the results have less than 10% differences, the tests are considered good. Otherwise, we take the second specimen and repeat the test. The average results of the repetitions are calculated from the measurement data for every frequency and temperature.

4.6.2 Fatigue test

Three specimens have been prepared for every level of strain amplitude (24 specimens in total). The first two specimens were tested. Check the ratio, if the ratio is one or close to one, the tests are considered good. Otherwise, we take the third specimen and repeat the test. Table 4.7 shows the ratios of $N_{f50\%}$ and $N_{fII/III}$ values obtained from the first specimens to the $N_{f50\%}$ and $N_{fII/III}$ values obtained from the replicate specimens.

Table 4.7 Ratios of $N_{f50\%}$ and $N_{fII/III}$ values obtained from the first specimens to the $N_{f50\%}$ and $N_{fII/III}$ values obtained from the replicate specimens

Group	Specimen	Percentage of voids	Percentage of saturation	Average axial strain (μm/m)	$N_{f50\%}$	$N_{fII/III}$	Repetition or original	Ratio ($N_{f50\%}$ Repetition/Original)	Ratio ($N_{fII/III}$ Repetition/Original)
Reference	S1R1	6.8%	0%	71	1,304,196	2,340,882	Original	1.02	1.00
Reference	S1R1 R*	6.8%	0%	70	1,334,126	2,344,450	Repetition		
Reference	S1R2	6.7%	0%	99	1,129,038	1,064,000	Original	1.09	0.88
Reference	S1R2 R*	6.7%	0%	103	1,118,140	940,980	Repetition		
Reference	S1R3	6.9%	0%	66	5,381,624	4,715,411	Original	1.00	1.00
Reference	S1R3R*	6.9 %	0%	64	5,382,412	4,721,475	Repetition		
Reference	S1R4	6.6 %	0%	84	4,558,950	2,500,000	Original	1.00	1.00
Reference	S1R4R*	6.6 %	0%	84	4,560,852	2,522,104	Repetition		
Conditioned (after 300 freeze-thaw cycles)	S2FT1	6.8 %	79%	97	179,460	114,521	Original	1.06	1.14
Conditioned	S2FT1 R*	6.8%	77%	95	190,002	130,257	Repetition		
Conditioned	S2FT2	6.9%	80%	74	845,929	830,878	Original	0.97	1.00
Conditioned	S2FT2 R*	6.9%	80%	72	834,920	829,145	Repetition		
Conditioned	S2FT3	6.6%	79%	62	2,110,893	1,738,569	Original	1.13	1.11
Conditioned	S2FT3 R*	6.6%	75%	60	2,375,100	1,921,690	Repetition		
Conditioned	S2FT4	6.8%	79%	113	160,000	143,717	Original	0.88	0.90
Conditioned	S2FT4 R*	6.8%	80%	115	141,023	129,346	Repetition		

R* : repeated specimen

4.7 Summary and Conclusions

This paper studied the effect of freeze-thaw cycles on the performance of asphalt mixture. The overall results can be listed as below.

Results have shown that the effect of freeze-thaw cycles is important to consider during the design life of asphalt pavements. As expected, rapid freeze-thaw cycles affect the stiffness behavior of the mix. The effect of freeze-thaw conditions on the stiffness behavior of the mix is higher with increasing the number of cycles from 150 to 300 for low and high frequencies.

- The 150 freeze-thaw cycles change the norm of complex modulus at high temperatures (low frequencies), while the stiffness does not change at low temperatures after 150 F-T cycles. However, stiffness behavior changes with a higher rate at high temperatures and the lower rate at low temperatures after 300 freeze-thaw cycles.
- Regarding fatigue test results, the $N_{fII/III}$ failure criterion seems to be more accurate than $N_{f50\%}$ criterion. In this case, the reference mixture has much better performance with respect to the resistance to fatigue cracking than after the condition of the environmental freeze-thaw cycles.
- Regarding the fatigue damage results, since E_0 of the conditioned mix was much lower than the reference and because of the results from the complex modulus test which displayed the stiffness reduction and changed in viscoelastic behavior after the 300 freeze-thaw cycles, it is concluded that the degradation of the conditioned mix started before the fatigue test and during freeze-thaw cycles.

It should be noted that further studies are necessary to develop a modified fatigue equation (for Quebec region) by considering the relationships between rapid freeze-thaw cycles in laboratory and the real ones in field by collecting cores, without considering other factors, such as loading, aging, etc.

4.8 Notation

The following symbols are used in this paper:
A = mass of the dry specimen, gr;
$a_T(T)$ = shift factor at temperature T;
B' = mass of the saturated, surface dry specimen can be calculated after partial saturation, gr;
C_1 = constant;
C_2 = constant;
D_{III} = damage at failure is calculated;
D_{IIIc} = modified damage at failure;
E = volume of the specimen, cm^3;
E_0 = norm of the initial modulus (stiffness at cycle 1);
E_0 = static modulus when ($\omega \rightarrow 0$);
E_{00} = glassy modulus when ($\omega \rightarrow \infty$);
E_{00i} = stiffness at cycle 1 measured by linear extrapolation for interval I;
E_{III} = norm of the modulus at the transition between phases II and III;
$|E^*|$ = norm of the complex modulus;
f_r = frequency;
G_{mb} = bulk specific gravity;
G_{mm} = maximum theoretical specific gravity of the mixture;
h, k = constant parameters parabolic elements of the model ($0 < k < h < 1$);
J' = volume of water absorption, cm^3;
K_1 = constant that depend on both material and chosen criterion;
K_2 = constant that depend on both material and chosen criterion;
$N_{f50\%}$ = classical fatigue criterion;
$N_{fII/III}$ = average value of the $N_{f\Delta\varepsilon ax}$, $N_{f\Delta\varphi}$ and $N_{f\varphi max}$;
$N_{f\Delta\varepsilon ax}$ = reading of the amplitude of strain for each extensometer;
$N_{f\Delta\varphi}$ = difference of more than 5° of the extensometer phase angle reading with the mean value;
$N_{f\varphi max}$ = maximum value of the phase angle is associated with the transition of phase II/III;
T_s = reference temperature (constant);
V_a = actual level of air voids, %;
σ_0 = maximum stress amplitude;
δ (delta) = constant;
ε_0 = peak recoverable strain amplitude;
φ = Phase angle;
ω = stress of pulsation (equal to $2\pi f_r$);
DS = percentage of the degree of saturation of the specimen;
i = complex number defined by $i^2 = -1$;
η = newtonian viscosity ($\eta = (E_{00} - E_0)\,\beta\,\tau$ when $\omega \rightarrow 0$);

τ = characteristic time which depends only on temperature;
β = dimension constant;
ε = axial strain amplitude;
ε_6 = axial strain amplitude at 1 million cycles;
$\tau_0 = \tau(T_{ref})$ at reference temperature $T_{re.}$

4.9 Acknowledgements

The research work presented in this paper is part of the NSERC industrial research Chair on the interaction between heavy loads, climate, and pavements (i3c). The authors are grateful to the Quebec Ministry of Transportation (MTQ) for their technical support in this project.

4.10 References

Arambula, E., Masad, E., & Martin, A. E. (2007). Influence of air void distribution on the moisture susceptibility of asphalt mixes. Journal of Materials in Civil Engineering, 19(8), 655–664.

ASTM. (2008). Standard Test Method for Resistance of Concrete to Rapid Freezing and Thawing. ASTM International.

Baaj, H., Di Benedetto, H., & Chaverot, P. (2005). Effect of binder characteristics on fatigue of asphalt pavement using an intrinsic damage approach. Road Materials and Pavement Design, 6(2), 147–174. https://doi.org/10.1080/14680629.2005.9690003

Badeli, S., Carter, A., & Doré, G. (2016). The importance of asphalt mixture air voids on the damage evolution during freeze-thaw cycles. Canadian Technical Asphalt Association.

Bagampadde, U., Isacsson, U., & Kiggundu, B. M. (2004). Classical and Contemporary Aspects of Stripping in Bituminous Mixes. Road Materials and Pavement Design, 5(1), 7–43. https://doi.org/10.1080/14680629.2004.9689961

Bausano, J., & Williams, R. C. (2009). Transitioning from AASHTO T283 to the simple performance test using moisture conditioning. Journal of Materials in Civil Engineering, 21(2), 73–82.

Caro, S., Masad, E., Bhasin, A., & Little, D. N. (2008). Moisture susceptibility of asphalt mixtures, Part 1: mechanisms. International Journal of Pavement Engineering, 9(2), 81–98. https://doi.org/10.1080/10298430701792128

Carter, A., & Paradis, M. (2010). Laboratory Characterization of the Evolution of the Thermal Cracking Resistance with the Freeze-thaw Cycles.

Copeland, A., & Kringos, N. (2006). Determination of bond strength as a function of moisture content at the aggregate-mastic interface. In 10th International Conference on Asphalt Pavements. Quebec, Canada, 709-718.

Di Benedetto, H., Olard, F., Sauzéat, C., & Delaporte, B. (2004). Linear viscoelastic behaviour of bituminous materials: From binders to mixes. Road Materials and Pavement Design, 5(sup1), 163–202.

Doré, G., & Imbs, C. (2002). Development of a new mechanistic index to predict pavement performance during spring thaw. Cold Regions Engineering.

Doré, G., & Zubeck, H. (2009). Cold regions pavement engineering. Retrieved from http://trid.trb.org/view.aspx?id=903094

Feng, D., Yi, J., Wang, D., & Chen, L. (2010). Impact of salt and freeze–thaw cycles on performance of asphalt mixtures in coastal frozen region of China. Cold Regions Science and Technology, 62(1), 34–41.

Feng, D., Yi, J., Wang, L., & Wang, D. (2009). Impact of Gradation Types on Freeze-Thaw Performance of Asphalt Mixtures in Seasonal Frozen Region Decheng. In ICCTP 2009: Critical Issues in Transportation Systems, Planning, Development, and Management: Proceedings of the Ninth International Conference on Chinese Transportation Professionals. (pp. 2562–2568).

Ferry, J. D. (1980). Viscoelastic properties polymers. John Wiley & Sons.

Goh, S. W., & You, Z. (2012). Evaluation of hot-mix asphalt distress under rapid freeze-thaw cycles using image processing technique. In CICTP 2012: Multimodal Transportation Systems—Convenient, Safe, Cost-Effective, Efficient (pp. 3305–3315).

Islam, M. R., & Tarefder, R. a. (2014). Quantifying Traffic- and Temperature-Induced Fatigue Damages of Asphalt Pavement. Transportation Infrastructure Geotechnology, 2(1), 18–33. https://doi.org/10.1007/s40515-014-0014-3.

Jackson, N., & Vinson, T. (1996). Analysis of Thermal Fatigue Distress of Asphalt Concrete Pavements. Transportation Research Record: Journal of the Transportation Research Board, 1545, 43–49. https://doi.org/10.3141/1545-06

Janoo, V., & Berg, R. (1990). Thaw weakening of pavement structures in seasonal frost areas. Transportation Research Record.

Kringos, N., Azari, H., & Scarpas, A. (2009). Identification of parameters related to moisture conditioning that cause variability in Modified Lottman Test. Transportation Research

Record : Journal of the Transportation Research Board, 6931(2127), 1–11. https://doi.org/10.3141/2127-01

Lamothe, S., Perraton, D., & Di Benedetto, H. (2015). Contraction and expansion of partially saturated hot mix asphalt samples exposed to freeze–thaw cycles. Road Materials and Pavement Design, 16(2), 277–299.

MA, B., WEI, Y., WANG, L., & ZHAO, C. (2010). Analysis on Flexural Tensile Characteristics of Asphalt Mixture in Cold Plateau Region [J]. Journal of Highway and Transportation Research and Development, 3, 10.

Masad, E., & Somadevan, N. (2002). Microstructural Finite-Element Analysis of Influence of Localized Strain Distribution on Asphalt Mix Properties. Journal of Engineering Mechanics, 128(10), 1105–1114.

Olard, F., Di Benedetto, H., Eckmann, B., & Triquigneaux, J. P. (2003). Linear Viscoelastic Properties of Bituminous Binders and Mixtures at Low and Intermediate Temperatures. Road Materials and Pavement Design, 4(1), 77–107.

Özgan, E., & Serin, S. (2013). Investigation of certain engineering characteristics of asphalt concrete exposed to freeze–thaw cycles. Cold Regions Science and Technology, 85, 131–136.

Paradis, M., & Langlois, P. (2006). Using TSRST to Determine the Influence of Thermal Fatigue on Hot Mix Properties. In 10th international conference on asphalt pavements-august 12 to 17, 2006, quebec city, canada.

Pellinen, T. K. (2002). Investigation of the use of dynamic modulus as an indicator of hot-mix asphalt peformance.

Perraton, D., Touhara, R., Di Benedetto, H., & Carter, A. (2015). Ability of the classical fatigue criterion to be associated with macro-crack growth. Materials and Structures, 48(8), 2383–2395.

Si, W., Ma, B., Li, N., Ren, J. P., & Wang, H. N. (2014). Reliability-based assessment of deteriorating performance to asphalt pavement under freeze-thaw cycles in cold regions. Construction and Building Materials, 68, 572–579.

Simonsen, E., & Isacsson, U. (1999). Thaw weakening of pavement structures in cold regions. Cold Regions Science and Technology, 29(2), 135–151.

Soltani, M. A. (1998). Comportement en fatigue des enrobés bitumineux.

Tang, N., Sun, C. J., Huang, S. X., & Wu, S. P. (2013). Damage and corrosion of conductive asphalt concrete subjected to freeze–thaw cycles and salt. Materials Research Innovations, 17(sup1), 240–245.

Tapsoba, N., Sauzéat, C., & Di Benedetto, H. (2013). Analysis of Fatigue Test for Bituminous Mixtures. Journal of Materials in Civil Engineering, 25(6), 701–710.

Tapsoba, N., Sauzéat, C., Di Benedetto, H., Baaj, H., & Ech, M. (2014). Behaviour of asphalt mixtures containing reclaimed asphalt pavement and asphalt shingle. Road Materials and Pavement Design, 15(2), 330–347.

Tarefder, R. A., & Islam, M. R. (2014). Measuring Fatigue Damages from an Instrumented Pavement Section due to Day-Night and Yearly Temperature Rise and Fall in Desert Land of the West. In International Symposium of Climatic Effects on Pavement and Geotechnical Infrastructure 2013 (pp. 78–88).

Tashman, L., Masad, E., D'Angelo, J., Bukowski, J., & Harman, T. (2002). X-ray tomography to characterize air void distribution in superpave gyratory compacted specimens. International Journal of Pavement Engineering, 3(1), 19–28.

Terrel, R. L., & Al-Swailmi, S. (1992). Final Report on Water Sensitivity of Asphalt-Aggregate Mixtures Test Development. Strategic Highway Research Program.

Williams, T., & Miknis, F. (1998). Use of environmental SEM to study asphalt-water interactions. Journal of Materials in Civil Engineering.

Yi, J., Shen, S., Wang, D., Feng, D., & Huang, Y. (2016). Effect of Testing Conditions on Laboratory Moisture Test for Asphalt Mixtures. Journal of Testing and Evaluation, 44(2), 20150128. https://doi.org/10.1520/JTE20150128

Zeng, M., & Shields, D. H. (1999). Nonlinear thermal expansion and contraction of asphalt concrete. Canadian Journal of Civil Engineering, 26(1), 26–34.

CHAPTER 5

EVALUATION OF THE DURABILITY AND THE PERFORMANCE OF AN ASPHALT MIX INVOLVING ARAMID PULP FIBER (APF): COMPLEX MODULUS BEFORE AND AFTER FREEZE-THAW CYCLES, FATIGUE, AND TSRST TESTS

Saeed Badeli [a], Alan Carter [b], Guy Doré [c], Saeed Saliani [d]

[a,b,d] Department of Construction Engineering, École de Technologie Supérieure, 1100 Notre-Dame Ouest, Montréal, Québec, Canada H3C 1K3

[c] Department of Construction Engineering, Université Laval, Quebec, Canada, G1V 0A6

Article published in Construction and Building Materials,
Volume 174, 20 June 2018, PP. 60-71
DOI: https://doi.org/10.1016/j.conbuildmat.2018.04.103

5.1 Abstract

The main deteriorations of asphalt pavements in cold regions are due to the effect of heavy traffics, water action, low-temperature fluctuations, freeze-thaw cycles and the combination of all these factors together. Fiber additives are mainly used as reinforcement materials in asphalt pavements to improve the tensile properties and increase the strength against low-temperature cracking and potholes. Aromatic polyamide fiber (aramid fiber) is used in advanced composite materials since it has a very high tensile strength, modulus, and high cohesiveness. Whether the addition of Aramid Pulp Fiber (APF) can effectively improve the fatigue life, thermal performance, and durability of asphalt mixture under repeated freeze-thaw cycles are also major problems needed to be investigated properly. In this regard, thermo-mechanical analyses (complex modulus, fatigue, and thermal restrain specimen test (TSRST)) have been conducted on the asphalt mix with a nominal maximum aggregate size of 20 mm, known as Grave Bitume (GB20) in Quebec, Canada. The improvement effect of APF incorporation is assessed to compare the stiffness variation before and after 300 rapid freeze-thaw cycles, fatigue behavior, and thermal strength. The results indicate the ability of APF to increase the durability of the GB 20 mix against freeze-thaw cycles. The TSRST and fatigue results also show that the APF

additives can increase the performance of the GB 20 mix against low temperature cracking and heavy truckloads.

Keywords: HMA; Fiber Additives; Kevlar; Aramid Pulp Fiber; Fatigue; TSRST; Complex modulus; Freeze-thaw cycles; moisture damage; Durability of an asphalt mixture.

5.2 Introduction

Hot Mix Asphalt (HMA) is a complex material that consists of asphalt binder, aggregate, and air voids, which is used as the first layer in flexible pavements. HMA is a typical viscoelastic material that has different behavior during different seasons of a year (Doré & Zubeck, 2009). The main deterioration of HMA in cold regions is due to the effect of heavy traffics, water action, low-temperature fluctuations, and freeze-thaw cycles. Researchers and engineers are trying to improve the performance and durability of HMA and consequently increase the service life of flexible pavements considering those deterioration factors.

Premature cracking and potholes are very common problems in Quebec and other regions in Canada (Doré, Konrad, & Roy, 1997, 1999; Pascale, Doré, & Prophète, 2004). Canada ranks seventh in the world in terms of road network length. More than 90 percent of the paved roads in Canada are flexible pavements. More than 50 percent of municipal roads are in fair, poor, or very poor conditions (DuPont, 2014). Pavement structures in Canada experience severe temperature variations in a year (Doré & Zubeck, 2009). These significant temperature variations in combination with the moisture inside the pores result in the development of premature deterioration of asphalt pavements (Badeli, Carter, & Doré, 2016, 2018a, 2018b).

Fiber additives are mainly used as reinforcement materials in Portland cement concrete and asphalt mixes (Huang & White, 1996; Abtahi, Sheikhzadeh, & Hejazi, 2010). Fibers are added to HMA to improve the tensile properties and performance (Abtahi et al., 2010). Fibers are added to open-graded-friction-course (OGFC) mixes and stone matrix asphalt (SMA) mixes during transportation and laying to prevent draindown and leakage (Chen, Xu, Chen, & Zhang,

2009). The dynamic modulus, viscoelasticity, moisture susceptibility, and reflective cracking would improve with the addition of fibers (Chen et al., 2009; Huang & White, 1996; McDaniel, 2015; Wu, Ye, Li, & Yue, 2007). It can also enable multifunctional applications, increased durability, increase fatigue and rutting performance of asphalt mixes (McDaniel, 2015; Park, El-Tawil, Park, & Naaman, 2015; Tanzadeh, Vafaeian, & Yusefzadeh-Fard, 2017; Tapkin, 2008).

Previous research demonstrated the importance of using Aramid Pulp Fiber (APF) in road construction (Badeli, Saliani, & Carter, 2017a, 2017b; McDaniel, 2015; Mirabdolazimi & Shafabakhsh, 2017; Mitchell et al., 2010; Park et al., 2015; Saliani et al., 2017). Kevlar® is the trademark of a para-aramid synthetic polymer fiber, which can be used in advanced composite materials since it has a very high tensile strength, modulus, and high cohesiveness. It was introduced in the early 70s by DuPont production. According to NCHRP synthesis 475, aramid fiber brings many advantages to asphalt mixes including increase the performance (rutting and fatigue), improve the strength and stability (McDaniel, 2015). Kaloush (2010) investigated the performance of an asphalt mix with and without using polypropylene and aramid fibers. The final results concluded that the reinforced mix had better performance in terms of permanent deformation and thermal cracking (Kaloush et al., 2010). Bennert (2012) investigated the polyolefin and aramid fibers in the plant produced mixes. Mixes were produced in the same batch plant using the same mix design. The control mix was slightly stiffer than the reinforced mix at low temperature. On the other hand, phase angle analysis showed that the fiber mix is more viscous than the control mix. Beam fatigue test also indicated that both mix had the same fatigue resistance (McDaniel, 2015).

A recent study in the laboratory of LCMB at the Ecole de Technologie Superieure conducted the indirect tensile strength test (ITS) on APF mixes (Badeli et al., 2017a). It was found that the addition of the APF could increase the ductility and tensile strength even at minus temperatures (Saliani et al., 2017). Previous studies demonstrated some advantages of using APF in asphalt mixtures such as better rutting resistant and delay in cracking propagation (Tanzadeh et al., 2017). The research of the performance of an APF mix under cold region

environment conditions such as the freeze-thaw cycles and thermal stress restrained specimens (TSRST) are crucial to carrying out. Whether the addition of APF can effectively improve the fatigue life; thermal performance, and the durability of asphalt mix under repeated freeze-thaw cycles are also major problems needed to be investigated properly.

HMA in pavements is usually divided into three sublayers with different thicknesses into cold regions. Base asphaltic layer plays a crucial role in bottom-up fatigue cracking (Badeli et al., 2018a). This is while, at the bottom of the base layer, the percentage of air voids is higher, which is usually due to a poor compaction during road construction, and also the tensile strain is higher because of the behavior of flexible pavements in terms of traffic, especially heavy vehicles. This can be getting worse during thaw periods when there is a high potential for the capillary rise. Water can penetrate through the saturated granular base layer. On the other hand, the bearing capacity of underlying granular layers reduces considerably during the thaw periods due to insufficient pavement drainage and melting of ice (Badeli et al., 2018a; Doré & Zubeck, 2009). Therefore, reinforcing the asphaltic base-layer can be one of the effective solutions to improve the quality of pavement structures.

In view of this, the primary objective of this paper is to study the thermo-mechanical analyses (complex modulus, fatigue, and TSRST tests) on the asphalt-base mix (which is known as GB20 mix in Quebec, Canada) and improvement effect of APF incorporation are studied to compare the stiffness variation before and after 300 rapid freeze-thaw cycles, fatigue life, and thermal strength.

5.3 Experimental Program

5.3.1 Materials

5.3.1.1 Fiber

The fiber used in this work is Aramid Pulp Fiber (APF) provided by DuPont production (Badeli et al., 2017a). It is known as Kevlar® brand pulp, with the product code of 1F361 (Figure 5.1) (Badeli et al., 2017a, 2017b). Figure 5.1 (a) indicates that the existence of micro-roots in aramid pulp fibers under a microscope. These micro-roots can anchor themselves in HMA and lead to increase the tensile characteristics of the reinforced mix. Table 5.1 shows the specifications of 1F361. The static energy of APF makes it difficult to achieve a homogeneous mix when used in HMA (Badeli et al., 2017b).

Aramid pulp is a highly fibrillated material with fibers of less than 1mm in length that is used in high abrasion materials like brake pads (Dupont, 2015) or as viscosity controller for adhesive or sealants (Dupont, 1999). It has several times more tensile strength than ordinary HMA (it is around 3000 MPa) (Tanzadeh et al., 2017). If this additive properly homogenized with HMA, it can carry increase the tensile characteristics of the asphalt mix. The use of pulp (shorter fibers) should prove to be cost-effective and achieve more surface contact area. Also, because of the very short length, the pulp should be easier to mix in HMA than longer fiber. It is our hypothesis that the mechanical properties and the durability of HMA would be enhanced by the presence of the pulp or short fiber in cold regions.

Table 5.1 APF specifications provided by DuPont production

Property	Specifications
Specific gravity	1-44-1.45 @ 20 ℃
Useful temperature range	-200 to 350 ℃
Specific gravity	1.45
Water solubility	Insoluble
Color	Yellow
Specific surface area	7-11 m^2/g

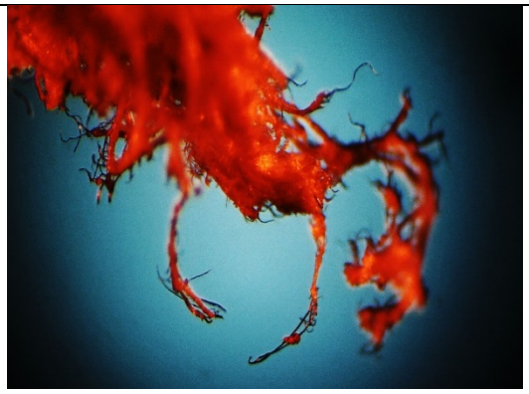

(a)

(b)

Figure 5.1 Aramid Pulp Fiber: (a) microscopic view (100 µm), (b) texture of APF

5.3.1.2 Bitumen

One type of asphalt binder was used in this study with a Superpave™ Performance Grade of PG 64-28 asphalt binder. Properties of the bitumen used in this study are presented in Table 5.2.

Table 5.2 characteristics of bitumen PG 64-28

	Properties						
	Density (g/cm3) at 25°C	Density (g/cm3) at 15°C	Storage stability (°C)	Viscosity Brookfield (Pa.s), at 135 °C	Viscosity Brookfield (Pa.s), at 165 °C,	High temperature for characterization T_H (°C)	Low temperature for characterization T_L (°C)
Value	1.026	1.033	0.4	0.455	0.132	65.1	-28.8
Standard	AASHTO T228	AASHTO T228	LC 25-003	AASHTO T 316	AASHTO T 316	Reported by supplier (Bitumar Inc.)	Reported by supplier (Bitumar Inc.)

5.3.1.3 Aggregate

To prepare the reference and the APF mix, the same source of materials are used for both mixes. The aggregate gradation which is used in this work is presented in Figure 5.2. The

specification for GB20 mix is according to the LC Method of Mix Design. It states the mix design method that is established by the pavement laboratory at the ministry of transportation of Quebec (MTQ) (Québec, 2016a).

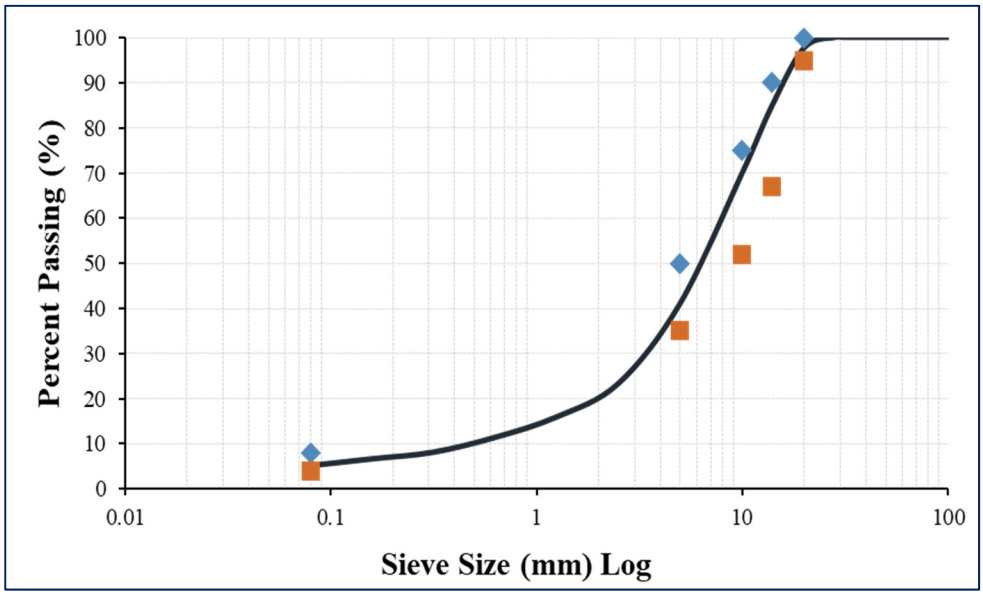

Figure 5.2 Specification for GB20 mix type according to the MTQ and aggregate gradation

5.3.2 Mix Design

Asphalt concrete with a nominal maximum aggregate size of 20 mm, known as Grave Bitume (GB20) which is normally used as an asphalt base layer in Quebec, is selected as the reference mix in this research. Asphalt base layer is the layer that has to resist fatigue and tensile stress. The void content has a clear influence on the stiffness of the material which can greatly influence the fatigue resistance. Lowering the number and size of voids reduces the probability of initiation of cracks and the speed of propagation. The mix was designed at the target of 6.50 percent air voids to represent the actual field compaction (Terrel & Al-Swailmi, 1993).

week rest period (curing time) at ambient temperature based on the Quebec Standard (Québec, 2016b). The first Slab for each mix is sawed into three sections. Three specimens are cored

from each section (Section A for TSRST, 6 specimens used from the section B and C for the fatigue and complex modulus tests). The second slab for each mix (Slab B) is sawed and the specimens are prepared for the freeze-thaw condition. The graphical preparation of specimens from the slab A is indicated in Figure 5.3.

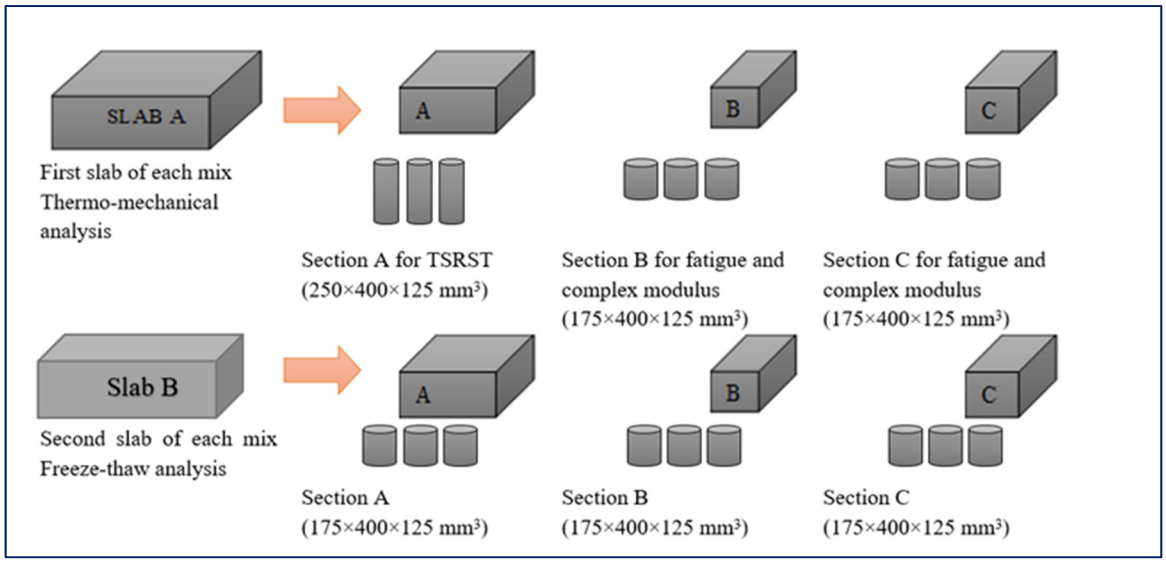

Figure 5.3 Graphical specimen's preparation

Before putting instrumentation in place, each specimen is weighed to determine its bulk specific gravity (G_{mb}). After measuring the G_{mb}, the percentage of air voids (P_a) is calculated according to the G_{mm}, and G_{mb} values. The percentage of air voids (Pa) is calculated according to the LC 26-320 (Québec, 2016b). Subsequently, the slow setting epoxy adhesive was applied to glue the aluminum caps in top and bottom ends of the specimens. Characteristics of the specimens are described in Table 5.3.

Table 5.3 Characteristics of the tested specimens

Mix type	Type of test	Number of specimens	Average Specimens height (mm)	Average Specimens diameter (mm)	Average air void content (%)	Standard deviation of the air void content (%)
Reference	Fatigue	6	150	74	6.5	0.21
Reference	TSRST	3	233	60	6.2	0.17
Reference	Freeze-thaw	4	149	74	6.6	0.19
Fiber	Fatigue	6	153	74	6.1	0.18
Fiber	TSRST	3	235	60	6.2	0.12
Fiber	Freeze-thaw	3	150	74	6.5	0.17

5.4 Thermomechanical Test Equipment

The thermomechanical tests (performance tests, and complex modulus test) are conducted by using a servo-hydraulic press (MTS 810, TestStar II), along with an electronic monitoring system devices. The MTS environmental simulator chamber is utilized for thermal conditioning of the specimens during the tests (Figure 5.4 (b)). The strain amplitude is measured with three sensitive extensometers installed around the specimens at an angle of 120° from one another (Figure 5.4 (a)). The temperature is controlled during the tests by installing three surface temperature probes to monitor the temperature and report any variations in temperature during testing. A rest period of 6 hours is applied when the temperature is turned to another temperature. This stabilization time period provides a homogeneous temperature inside and outside the tested specimens (Tapsoba et al., 2014).

5.4.1 Performance Tests

5.4.1.1 Fatigue Test

Fatigue phenomenon is occurring under the repetition of loading due to the traffic, especially heavy vehicles. The accumulated damage due to a large number of the repetitions results in

stiffness reduction of the materials and leads to failure. The asphalt pavement life is directly affected by this phenomenon, which needs to be correctly considered in order to calculate precise asphalt pavement structural design.

Fatigue test procedure has been developed in DGCB (Département de Génie Civil et Bâtiment) at the ENTPE (École Nationale de Travaux Publics de l'État, (Lyon, France)) (Di Benedetto, Nguyen, & Sauzéat, 2011). The test was conducted in laboratory based on the variation of the complex modulus (evolution of stiffness) under cyclic solicitation of strain homogeneous test. The direct tension-compression test on cylindrical specimens of 150 mm in height and 75 mm in diameter was adopted which is based on MTQ standard. Figure 5.4 indicates an example of fatigue tested specimen inside the MTS chamber before and after the test. Mid-value of strain was monitored during the fatigue test to make sure that it remains null. Fatigue tests were performed under the frequency of 10 Hz and the temperature of 10°C conditions. Temperature and frequency influence the rigidity of the asphalt mix. This influence will be favorable or harmful depending on the mode of solicitation used. At high temperature (≥ 15 ° C), material fatigue is explained by a modification of the molecular structure of the bitumen (self-healing experience) and at low temperatures, there is rather formation and development of cracks in bitumen and aggregates. Evolution of the stiffness modulus was controlled by monitoring the axial strain during the test. Wöhler's curve was plotted at the end of the fatigue test analysis. It is based on the evolution of fatigue life at different levels of strain amplitude.

(a)

(b)

(c)

Figure 5.4 (a) Example of fatigue tested specimen inside the environmental chamber, (b) MTS environmental chamber, (c) Broken specimen after fatigue test

5.4.1.2 Thermal Stress Restrained Specimen Tests (TSRST)

The thermal stress restrained specimen test (TSRST) was identified as a performance test under the Strategic Highway Research Program (SHRP) to simulate the low-temperature distress. Previous research showed that the TSRST test gives better field prediction than other test methods (Vinson, Kanerva, & Zeng, 1994). The procedure of the TSRST test is based on the theory that the contraction of asphalt mixes in the pavement structures are longitudinally restrained when temperature drops (Alan Carter, 2002). As the temperature decreases at a rate of 10°C/hour, the thermal stress inside the specimen increases, when the induced stress exceeds the strength of the material, specimen breaks and test stops automatically. Before cooling begins, a conditioning period of 6 hours at 5°C is performed. Figure 5.5 indicates an example of TSRST tested specimen inside the MTS chamber before and after the test.

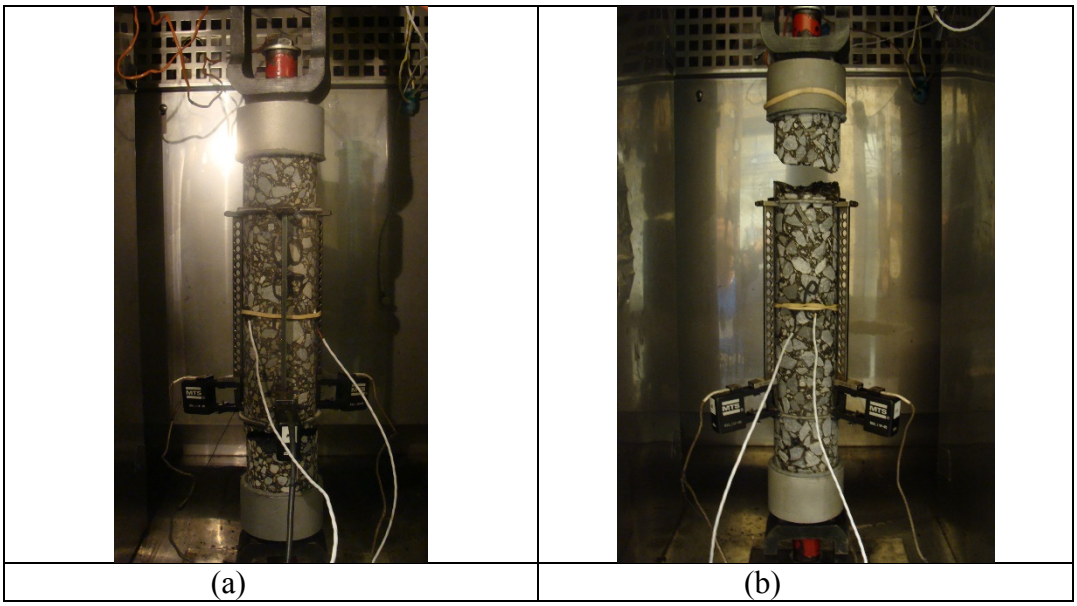

(a) (b)

Figure 5.5 TSRST test installation: (a) before the test, (b) broken specimen after the test

5.4.2 Complex Modulus Test

In this project, complex modulus tests are implemented on the specimens before and after conducting the freeze-thaw cycles in the MTS environmental chamber. The MTQ determines the complex modulus of asphalt mixes in accordance with test method LC 26-700 (Québec, 2016b). The complex modulus (E*) for asphalt mixtures defines the relationship between stress and strain under a continuous sinusoidal loading. It depends on the duration of load, delayed through time, and temperature. Complex modulus is identified by the norm of the modulus that explains the material's stiffness, and is characterized by the dynamic modulus |E*| (Equation (5.1)):

$$|E^*| = \frac{\sigma_0}{\varepsilon_0} \tag{5.1}$$

Where σ0 is the maximum stress amplitude and ε0 is the peak recoverable strain amplitude. The Phase angle (φ) is described as a phase lag of the strain behind the stress under the sinusoidal cyclic solicitation (Lachance-Tremblay, Vaillancourt, & Perraton, 2016). The phase angle is 0° for purely elastic material, and 90° for a purely viscous material. The ratio of the

amplitude of the sinusoidal stress of pulsation (ω) applied to the material $\sigma = \sigma_0 \, sin(\omega t)$ and the amplitude of the sinusoidal strain $\varepsilon_t = \varepsilon_0 \, sin(\omega t - \varphi)$ that result in a steady state (Equation (5.2)) (Di Benedetto et al., 2004).

$$E^* = \frac{\sigma}{\varepsilon} = \frac{\sigma_0 e^{i\omega t}}{\varepsilon_0 e^{i(\omega t - \varphi)}} \tag{5.2}$$

Summary of the experimental test parameters is shown in Table 5.4.

Table 5.4 Experimental parameters for the complex modulus tests

Test parameters	**Test conditions**
Test temperatures :	35°C, −25°C, −15°C, −5°C, +5°C, +15°C, +25°C and +35°C
Test frequencies :	10, 3, 1, 0.3, 0.1, and 0.03 Hz
Type of test:	Tension-compression
Time stabilization at target temperature :	6 h
Mechanical loadings:	Maximum of 30 cycles per frequency
Loading amplitude:	50 µm/m
Loading condition:	Sinusoidal cyclic loading, control strain $\varepsilon_{average}$= 0 µm/m

5.4.3 Freeze-thaw Cycles

This section describes specimen's saturation, preparation, and the procedure used in freeze-thaw conditioning.

5.4.3.1 Moisture Conditioning Procedure

Saturation process was conducted to introduce liquid in the voids from the test standard specified by LC method for moisture resistance measurements (Québec, 2016b). Saturation process followed the same procedure conducted by previous research (Badeli et al., 2016, 2018a, 2018b). The equipment consists of a vacuum pump, a pressure gauge pycnometer, and a desiccator. The equipment is illustrated in Figure 5.6 (a). Several steps are performed to saturate the specimens. First, at atmospheric pressure, a specimen is placed on sand courses inside a desiccator. Subsequently, the pycnometer is filled with water. The pressure in the pycnometer is lowered and maintained at a pressure bellow than 4 kPa. After 5 minutes, the V1 is open allowing filling the desiccator from the deaerated water and covering completely the specimen. The specimen is kept immersed for at least 5 minutes and always at the pressure bellow than 4 kPa. Then, the pump is stopped and the pressure in the desiccator is controlled so that it comes back gradually to the atmosphere pressure. Afterwards, the test specimen is removed from the desiccator, dried with a damp cloth to remove the excess water while ensuring that it remains saturated, weighing in the air, and covered with a latex membrane to prevent loss of liquid during handling and freeze-thaw cycles (Figure 5.7 (a)).

Specimens with more than 80 percent degree of saturation were not used in this study because it was believed that they were damaged during the saturation process. Figure 5.6 (b) indicates the equipment that has been used for this step. At the end of the saturation process, the specimens were protected with latex membrane, and the waterproofed tape was placed around the specimens to prevent water loss during the freeze-thaw cycles (Figure 5.7 (a)).

5.4.3.2 Steel jig for restraining the specimens during freeze-thaw cycles

The selected specimens for the freeze-thaw cycles that are already glued with aluminum caps are equipped with steel jigs in order to be held in place during the freeze-thaw cycles. This condition can simulate the behavior of asphalt pavement in the field (Carter & Paradis, 2010).

Figure 5.7 (b) indicates the specimens were equipped with aluminum and steel jigs. The principle behind the theory of using the steel jig along with the aluminum jig is based on the prevention of the contraction/expansion movements during freeze-thaw cycles. The thermal contraction coefficients for the steel is around 12.1×10-6/ °C and for the Aluminum is 22.5×10-6/ °C. For temperature cycles from 5 to -20 °C, it was calculated that a tested specimen would contract 16.5 μm and the thermal expansion coefficient of asphalt mixtures in this temperature range is approximately 21×10-6/ °C (Carter & Paradis, 2010).

5.4.3.3 Temperature cycles used for freeze-thaw cycles

There is no standard method to assess the daily rapid freeze-thaw cycles of the asphalt mixture. After the saturation process, specimens were subjected to 150 and 300 freeze-thaw cycles as set forth in ASTM C-666.92, "Standard Test Method for Resistance of Concrete to Rapid Freezing and Thawing" (ASTM, 2008). The cooling and heating rate used was 4.5 °C/min. For each freeze-thaw cycle, two different temperature levels were targeted, which is -18 and 6 °C. The temperature remained constant for a period of 1.5 hours at each level of temperature. No specimen was oven dried before or after the rapid freeze-thaw testing since it might affect the viscoelastic characteristics of asphalt mix (Badeli et al., 2016; Badeli et al., 2018b). Figure 5.6 (c) indicates the equipment that has been used for this step. Figure 5.8 indicates that there is a difference between the temperature sensor placed in the center of a dummy specimen and the temperature sensor placed on the surface of a dummy specimen. This behavior was quite expected and is due to the rapid rate of the heating and cooling cycles. This non-homogeneity of the temperature during freeze-thaw cycles may increase the potential for thermal cyclic damage since there is a different level of contraction/expansion in the mix (Badeli et al., 2018a).

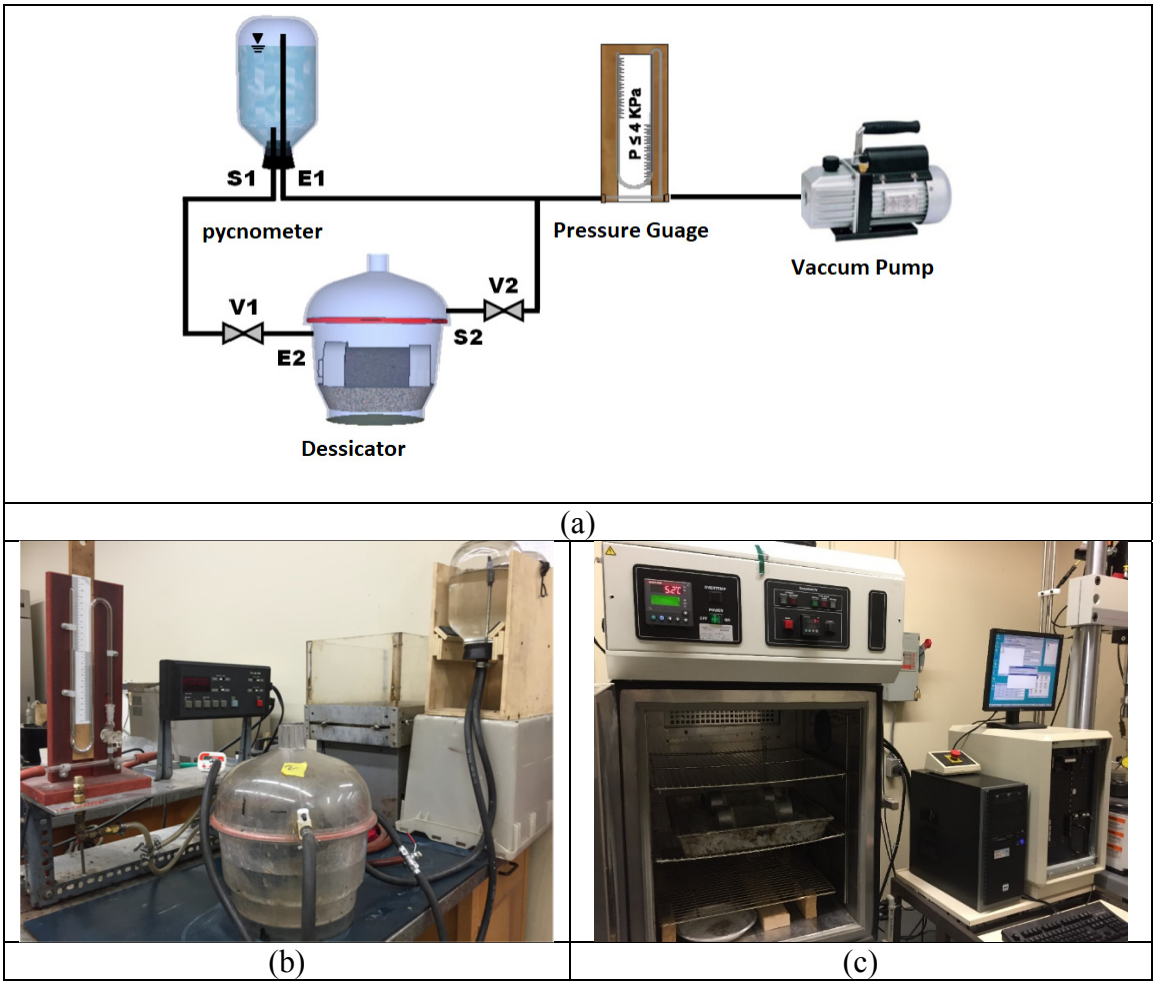

(a)

(b) (c)

Figure 5.6 Freeze-thaw preparations: (a) and (b) specimen's saturation equipment, (c) environment chamber and computer device to program heating/cooling cycles

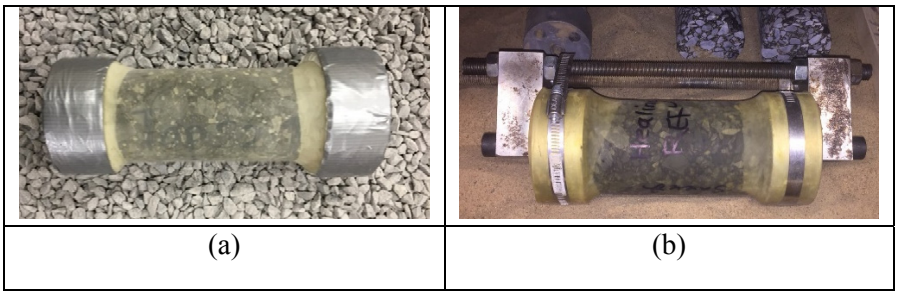

(a) (b)

Figure 5.7 Saturated specimens: (a) covering the specimen with Latex membrane to protect against water loss, (b) steel jig to restrain the specimen during freeze-thaw cycles

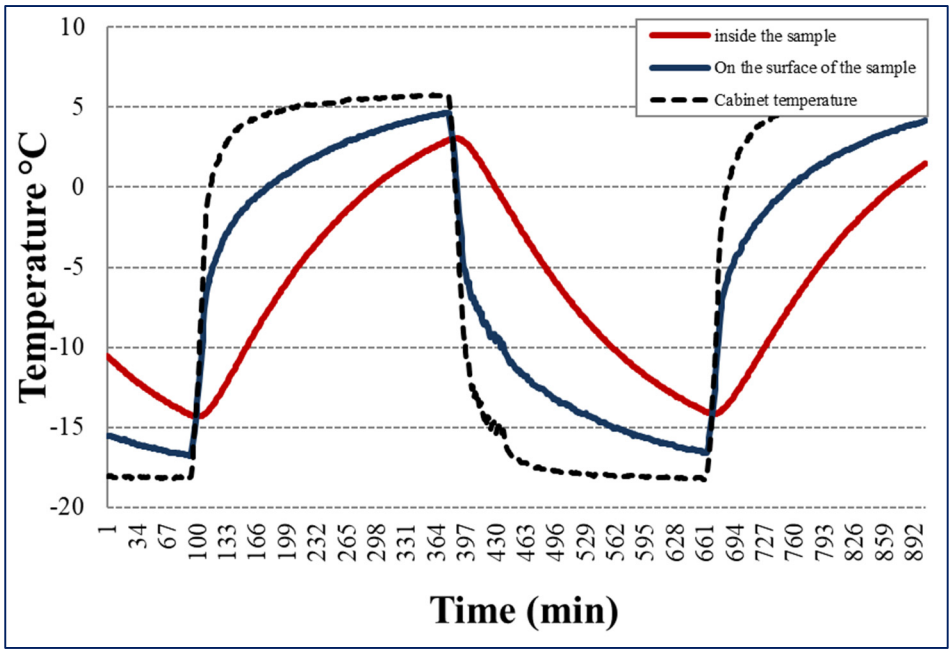

Figure 5.8 Temperature history detected by sensors during 58th temperature cycling: on the surface of a dummy specimen, inside the specimen, and the cabinet temperature

5.5 Results and Discussions

5.5.1 Fatigue Test

From the deformation amplitudes and the stress, the value of the norm complex module is calculated (| E*|). In this research, fatigue tests were carried out having four different levels of strain amplitude for each mix. The value of the modulus at the beginning of the test was denoted $|E_0^*|$ which represents the extrapolated value at cycle 1 by assuming the linear characteristics of complex modulus from cycles 2 to 50 (Perraton et al., 2015). It is necessary to know the value of the initial module of the material in order to calculate the apparent damage of the asphalt mixture during the fatigue test. Evaluation of the linear characteristics of stiffness modulus for both mixes is also conducted during complex modulus test. Table 5.5 demonstrates the information about the specimens, the applied axial strain amplitudes, and the $|E_0^*|$ values for different specimens. The difference of the average of the initial modulus

between the reference and APF specimens specifies the lower in the average of the |E0*| value for the APF mix with the lower standard deviation. This high stiffness modulus at the begging of the fatigue test for the fiber reinforced mix can be due to the effect of the addition of Aramid fiber in the mix. As already mentioned, Aramid fiber has several times more tensile strength than ordinary hot mix asphalt (Tanzadeh et al., 2017).

These results could be explained in this way that in fiber reinforced mixtures, we could take advantage of reinforcement in the case that the tensile strength of the fiber reinforced fibers is higher than that of the reinforced mixture (asphalt concrete). The tensile strength of Aramid fibers is equal to 3000 MPa which is several times more than that of the ordinary asphalt concrete. Therefore reinforcement of the asphalt concrete, using the composite aramid fibers results into the increased tensile strength of the mixture and higher resistance against the fatigue cracking.

Table 5.5 Fatigue specimen's characteristics and information

Group	Specimen	Air voids (%)	Average axial strain amplitude (μm/m)	Initial modulus, $\|E^*_0\|$ (MPa)		
				Value	Average	Standard deviation
Reference mix	S1RM1	6.8%	71	12563	10735.50	1453.20
	S1RM2	6.7%	99	10854		
	S1RM3	6.9%	66	10500		
	S1RM4	6.6%	84	9025		
Fiber mix	S2FM5	6.3%	74	7817	7361.50	568.87
	S2FM8	6.6%	85	7452		
	S2FM9	6.4%	94	7639		
	S2FM10	6.8%	73	6538		

5.5.1.1 Fatigue failure criteria

The evolution of the stiffness (|E*|) in terms of the number of cycles is mainly used to verify the validity of the test and to determine the apparition of cracks in the specimen (Badeli et al.,

2018a). The evolution of |E*| is usually divided into three phases during a fatigue test (Figure 4). In the first step, |E*| decreases rapidly which cannot be explained only by fatigue. Heating, as well as thixotropy, has an important role in this step (Perraton et al., 2015). Phase II is characterized by a quasi-linear decrease of stiffness which is characterized by the initiation of microcracks inside an asphalt mix. During the phase III, from the coalescence of microcracks, a macro-crack appears and propagates within the materials (Tapsoba et al., 2014).

A fatigue failure criterion is considered acceptable if it can precisely recognize the transition location of the phase change from II to III in the evolution of the stiffness during fatigue testing (Basueny, Perraton, & Carter, 2014). In this experimental program, it is decided to define $N_{fII/3}$ criterion for further analysis. $N_{fII/3}$ is associated with the transition between phases II as well as phases III and it is based on the average value of the $N_{f50\%}$, $N_{f\Delta\varepsilon ax}$, $N_{f\Delta\varphi}$, and $N_{f\varphi max}$. $N_{f50\%}$ is a classical fatigue criterion based on modulus decrease which corresponds to a decrease of 50% reduction of the initial stiffness ($|E^*_0|$) of the specimen as shown in Fig. 9 (Basueny et al., 2014). $N_{f\Delta\varepsilon ax}$ is based on the reading of the amplitude of strain for each extensometer. A difference of more than 25% of the extensometers reading can be considered as increasing heterogeneity within the specimen. $N_{f\Delta\varphi}$ is a difference of more than 5° of the extensometer phase angle reading with the mean value. The corresponding number of cycles is associated with failure. Finally, $N_{f\varphi max}$ is based on the evolution of the phase angle; maximum value of the phase angle is associated with the transition of phase II/III. Tapsoba et al. (2013) have compared these criteria together, and they concluded that all criteria used to give almost the same results. Furthermore, they revealed that $N_{f\varphi max}$ and $N_{f\Delta\varepsilon ax}$ are closer and can strongly show the phase change of II to III threshold (Tapsoba et al., 2014). The information of the values of N_f for all the specimens in both groups are shown in Table 5.6. This table shows that the value of $N_{fII/3}$ is related to the amplitude of the strain. Results of $N_{fII/3}$ for both mixes are used to analyze the fatigue life by the Wöhler curve.

Table 5.6 Experimental test results: summary of the N_f for the tested specimens

Group	Specimen	Air voids (%)	Average axial strain amplitude (µm/m)	$N_{f50\%}$	$N_{f\Delta\varepsilon ax}$	$N_{f\Delta\varphi}$	$N_{f\varphi max}$	$N_{fII/III}$
Reference mix	S1RM1	6.8%	71	1,304,196	2,320,762	2,401,068	2,300,816	2,405,986
	S1RM2	6.7%	99	106,390	105,300	89,132	99,178	100,000
	S1RM3	6.9%	66	5,381,624	4,855,565	4,527,469	4,763,199	4,715,411
	S1RM4	6.6%	84	4,558,950	2,511,005	2,425,127	2,563,868	2,500,000
Fiber mix	S2FM5	6.3%	74	5,339,648	5,267,021	5,200,987	5,012,344	5,205,000
	S2FM8	6.6%	85	651,166	650,193	640,001	610,500	637,965
	S2FM9	6.4%	94	109,102	100,000	99,201	91,697	100,000
	S2FM10	6.8%	73	3,351,213	3,201,901	3,110,290	3,180,596	3,211,000

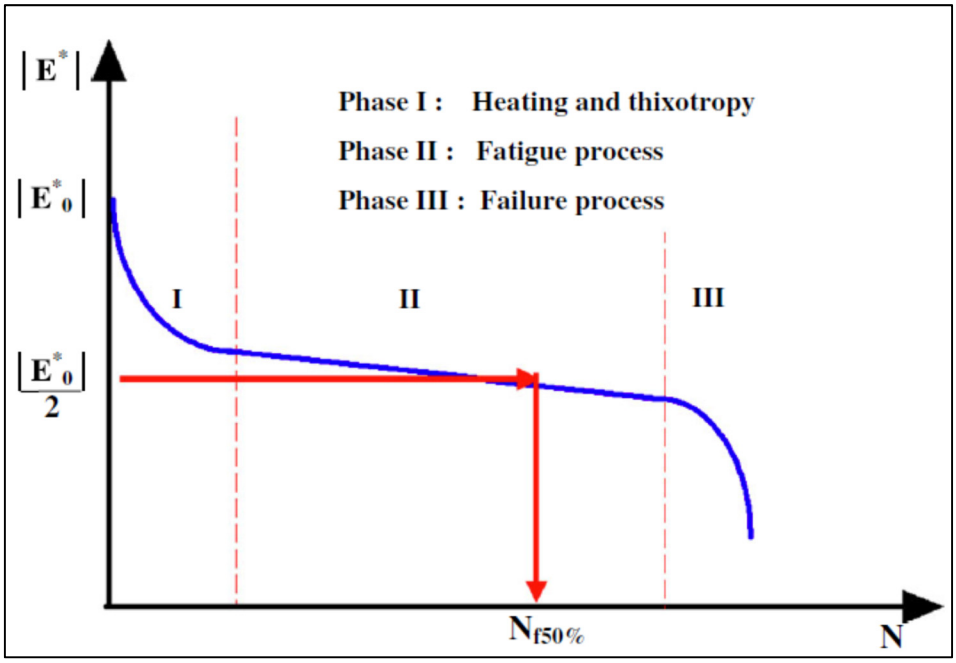

Figure 5.9 Evolution of the norm of the complex modulus according to number of cycles (Perraton et al., 2015)

5.5.1.2 Analysis of fatigue life

Fatigue test results are usually expressed as the graphical presentation which is usually given by the fatigue curve or so-called Wöhler curve (Perraton et al., 2015). Wöhler curve demonstrates the log number of cycles at failure (fatigue life) versus the amplitude of the applied strain in logarithmic axes. In these axes, Wöhler curves for asphalt mixes are classically straight lines. They are expressed by Equation (5.3).

$$N_f = C_1 \varepsilon^{-C_2} \tag{5.3}$$

where, ε = axial strain amplitude; and C1 and C2 = two constants that depend on both material and chosen criterion.

Considering the failure at 1 million cycles, then the Equation (5.3) becomes Equation (5.4):

$$\frac{N_f}{10^6} = \frac{\varepsilon^{-C2}}{\varepsilon_6} \tag{5.4}$$

where ε6 represents strain amplitude for which failure occurs after 1 million cycles.

Figure 5.10 indicates the $N_{fII/3}$'s Wöhler curve for the reference and APF mixes. It represents the number of cycles of failure versus the amplitude of the applied strain in logarithmic axes. Table 5.7 summarizes the fatigue parameters for both mixes. Based on the fatigue test results analyzed by using $N_{fII/3}$ Criterion, it is observed that the average value of the $|E_0^*|$ is higher for the reference mix than the APF mix as it is noted earlier. R^2 value is closer to one for the APF mix than the reference mix. This explains that the regression line perfectly fits the data and it proves that the regression model based on $N_{fII/3}$ criterion is more accurate for the reference mix than the APF mix. The slope of the curve is steeper for the APF mix than the reference mix. This means that the reference mix has lower fatigue life at high strain amplitude (heavy truckloads). The behavior of the mix at high strain amplitude is more depends on the mastic and its cohesion. Adhesion and cohesion are two important parameters of bitumen that affects the performance and durability of asphalt mix (Mirabdolazimi & Shafabakhsh, 2017). In this

regard, the results can explain that the cohesion of the mastic increases for the mix using the APF.

At low strain amplitude, the reference mix has higher fatigue life than the APF mix. The value of ε_6 is almost same for both mixes. The value corresponds to the strain amplitude for a failure at 10^6 cycles.

Table 5.7 Fatigue test result's parameters based on the $N_{fII/3}$

Group	C_1	C_2	R^2	ε_6
Reference mix	2.32E-30	8.72	0.77	82.09
Fiber mix	1.65E-54	14.61	0.97	81.59

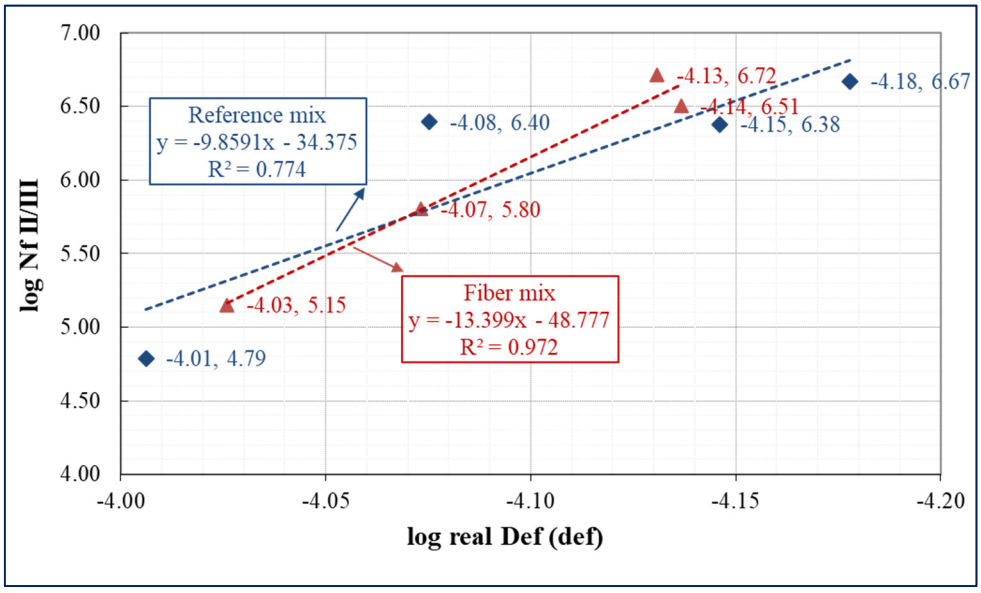

Figure 5.10 Wöhler curve ($N_{fII/III}$) for the reference and APF mixes

5.5.2 TSRST Test

The results of the TSRST test for the reference and the APF mix is indicated in Figure 5.11. The important parameters in the TSRST graph include but not limited to fracture strength, fracture temperature, transition stress, transition temperature, and slope of the elastic part of

the stress temperature plot. In Table 5.8, average results (three repetitions on three different specimens for each asphalt mixture) are summarized. In general, the TSRST shows good repeatability for both mixes. In the first place of the test, there is a slow rise in thermal stress which is mostly due to a relaxation of the asphalt mix (Basueny et al., 2014). However, beyond the transition temperature (around -13.5 °C in reference mix and -22 °C in APF mix), the relationship between the temperature as well as the thermally induced stresses is almost linear. The transition temperature defines where the material changes its behavior from viscoelastic to elastic, or vice versa.

The TSRST results indicate that the APF affects the cracking temperature of GB20 asphalt mix. The average fracture strength and fracture temperature for the APF specimens were 2.6 MPa and -36 °C and for the reference specimens were 3.6 MPa and -28 °C, respectively. Both of the failure and transition temperatures are influenced by the addition of APF. The difference in fracture temperature between the reference mix and fiber mix is about 8 °C. Fig. 11 indicates that the addition of aramid fiber in the GB20 mix decreased the fracture strength, fracture temperature. It is very interesting to notice that the same trend is clear on the value of the transition temperatures.

Based on the fatigue, TSRST, and IDT from the previous study, it is clear to say that the tensile strength of the reinforced mix is improved. The tensile strength of the Aramid fiber is around 3000 MPa which is significantly more than the ordinary hot mix asphalt (Tanzadeh et al., 2017). Therefore, the addition of the Aramid pulp fibers into the asphalt mix can result into the improvement of the tensile strength and performance of HMA in cold regions.

Table 5.8 TSRST Test Results

Mix type	Average fracture temperature		Average Fracture strength		Average Transition temperature		Average Transition strength	
	Value (^{0}C)	CV (%)	Value (MPa)	CV (%)	Value (^{0}C)	CV (%)	Value (MPa)	CV (%)
Reference	-28	6	3.601	5	-13.5	6	2.260	7
APF	-36	7	2.651	6	-22	7	1.755	7
CV: Coefficient of variation which is calculated by dividing the standard deviation from the mean value.								

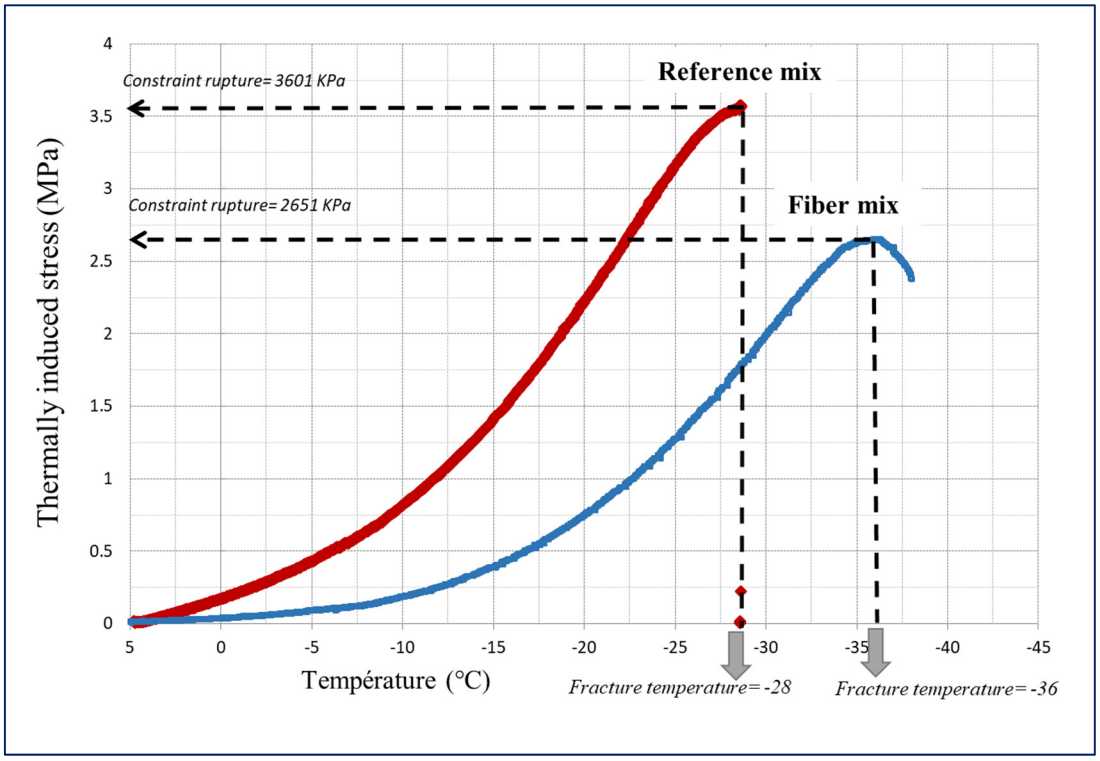

Figure 5.11 TSRST curve for the reference and APF mix

5.5.3 Freeze-thaw Durability

Complex modulus test is a kind of indirect analysis to assess the durability of asphalt mixtures. In this study, the GB20 asphalt mix is evaluated before and after 300 freeze-thaw cycles. Experimental test results of the APF mix and the reference mix are shown in Figure 5.12, and Figure 5.13 in the Cole-Cole and black space diagrams before and after freeze-thaw conditioning respectively.

A Cole-Cole plane is achieved by plotting the loss modulus versus the storage modulus. The storage modulus is plotted on the real axis (x-axis), and the loss modulus is plotted on the imaginary axis (y-axis). First of all, the results in Cole-Cole diagram express significant differences before and after the effect of freeze-thaw cycles for the reference mix, while the diagram does not show significant differences before and after freeze-thaw cycles for the APF mix. The previous study showed that the presence of ice increases the stiffness at minus temperatures for the saturated mix, but it decreases substantially after a large number of freeze-thaw cycles (Badeli et al., 2016, 2018a, 2018b). This reduction in stiffness is probably due to the striping of the mix. In fig. 12, the stiffness decreases substantially after freeze-thaw cycles for the reference mix. The graph shrinks and moves along the left side. This can show that both of the loss and storage modulus decrease after a large number of rapid freeze-thaw cycles. Complex modulus results for the APF mix indicate that the APF mix is less sensitive to the freeze-thaw cycles than the reference mix. This is due to the high tensile characteristics of Aramid pulp fiber which make the mix more durable during the repetition of rapid freeze-thaw cycles.

Figure 5.13 shows the complex modulus results in Black Curve diagram. It can be seen that the phase angle reduces in Black curve diagram after reaching a maximum value. The maximum value of the phase angle represents the viscosity of the bitumen at high temperature and depends mostly on the type of the bitumen (Basueny et al., 2014). The graph shows that the phase angle increases as the value of |E*| decreases after the freeze-thaw cycles for both mixes at high temperatures. This difference of the maximum value of phase angle before and

after freeze-thaw cycles can be explained as the loss of cohesion in the binder itself (Badeli et al., 2018b).

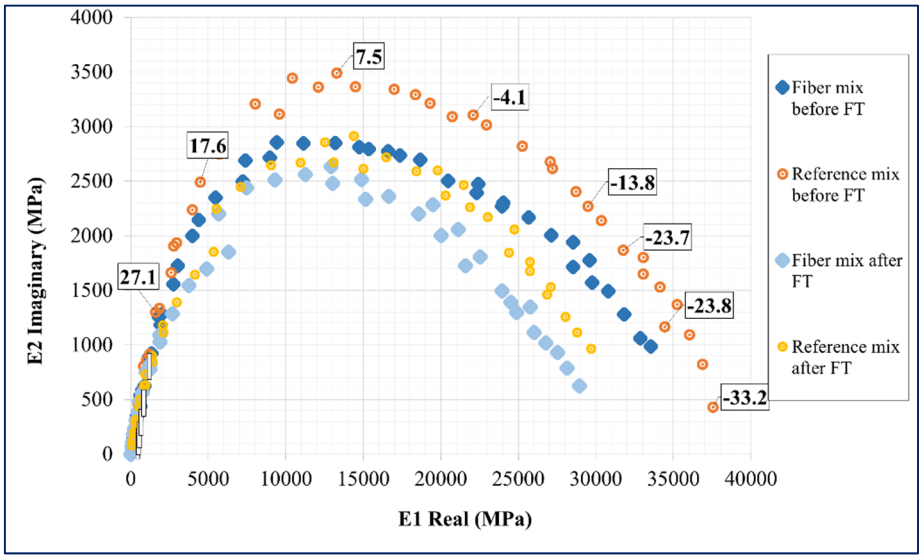

Figure 5.12 Evolution of the complex modulus in the Cole-Cole plot

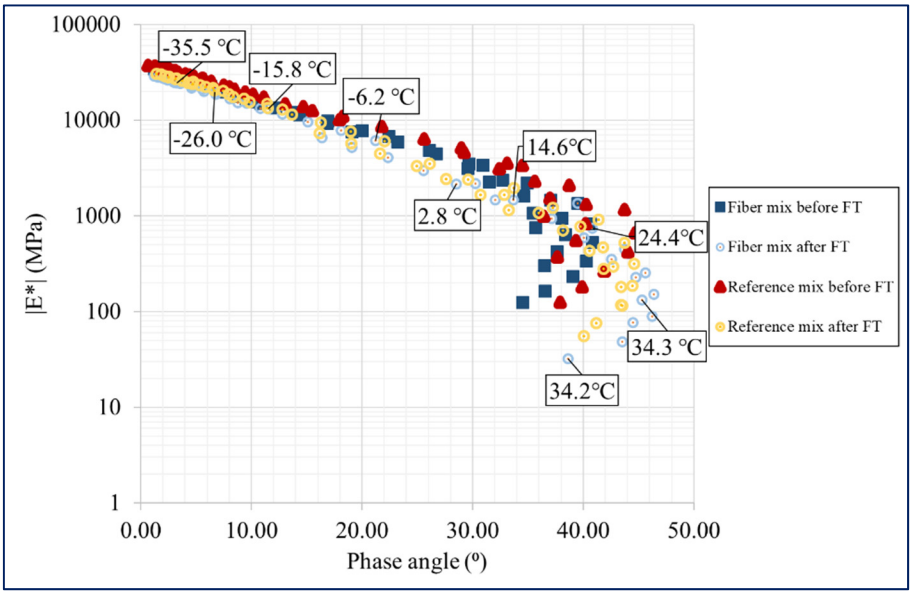

Figure 5.13 Evolution of the complex modulus in the black diagram

5.5.3.1 Analysis of the Master Curve

The 2S2P1D (two Springs, two Parabolic elements, and one Dashpot) modeling are used to analyze the experimental test results in the master curve (Equation (5.5)) (Herve Di Benedetto et al., 2004).

$$E^*(2S2P1D) = E_0 + \frac{E_{00} - E_0}{1 + \delta(i\omega\tau)^{-k} + (i\omega\tau)^{-h} + (i\omega\beta\tau)^{-1}} \quad (5.5)$$

The 2S2P1D parameters are described in Table 5.9.

Table 5.9 Description of the parameters of the 2S2P1D equation

Parameter	Description
i	Complex number can be defined by $i^2 = -1$
E_0	Static modulus when $\omega \rightarrow 0$
E_{00}	Glassy modulus when $\omega \rightarrow \infty$
ω	Pulsation and equal to $2\pi f_r$
f_r	Frequency
τ	Time characteristic and it depends only on temperature
δ	Constant parameter which is related to binder rheology
β	Dimension constant
η	Newtonian viscosity and can be calculated as $\eta = (E_{00} - E_0)\beta\ \tau$ when $\omega \rightarrow 0$
h	Constant parameter which is related to binder rheology
k	Constant parameter which is related to binder rheology ($0 < k < h < 1$)

The changing of τ temperature can be explained by means of a shift factor if the time-temperature superposition principle holds:

$$\tau(T) = a_T(T) \times \tau_0 \quad (5.6)$$

where $\tau_0 = \tau(T_{ref})$ at reference temperature Tref, and $a_T(T)$ is shift factor at temperature T.

Seven criterion (E_0, E_{00}, β, δ, h, k, and τ0) is needed to fully analyze the linear viscoelastic characteristics of the specimens at a specified temperature and frequency. The progressions of τ were determined by the William-Landel-Ferry (WLF) model. τ_0 was quantified at the selected reference temperature Tref. When the temperature effect is determined, the number of criteria becomes nine, including the two WLF criteria (C1 and C2 determined at the reference temperature).

$$log(a_T) = \frac{-C_1 (T - T_s)}{C_2 + (T - T_s)} \quad (5.7)$$

Where, aT (T) is the shift factor at temperature T, T0 = T (Ts) is determined at the reference temperature Ts. Ts is reference temperature (constant), C1 and C2 are constants.

The 2S2P1D modeling parameters in this study are presented in Table 5.10. The k, h, and δ parameters are related to the binder rheology and are almost same for the three groups (Di Benedetto et al., 2004). Regarding the other parameters, E_{00} is the glassy modulus (E* when ω→∞) which represents the highest stiffness at high temperature (low frequency), and E_0 is the static modulus (E* when ω →0) which is related to the void content and aggregate skeleton and represents the highest stiffness at low temperature (high frequency). The results will fit on a single curve for each test in the Black space, and in the Cole-Cole plane.

The results show that the stiffness value at low temperature is almost same for both mixes after the freeze-thaw cycles. E0 reduces 16% after freeze-thaw cycles for the APF mix, while it reduces more than 17% after freeze-thaw cycles for the reference mix. Regarding the E_{00} parameter, the Table 5.10 shows that the static modulus reduces for both mixes with almost a same rate. There is 66% reduction of the value of E_{00} for the reference mix and 60% reduction of the value of E_{00} for APF mix. This explains that the APF mix has higher stiffness value at high temperature (low frequency).

The results can also be shown on a master curve. To that end, each isothermal curve can be shifted in frequency in order to obtain a single master curve at a reference temperature. Figure 5.14 shows the master curves for the third tested group. The top part of the curve corresponds to a maximum value of |E*|. Highest stiffness value associated with the lowest temperature and highest frequency. The bottom part of the master curve represents a minimum value of |E*|. Lowest stiffness value is associated with the highest temperature and lowest frequency of the test.

As it is indicated in Figure 5.14, the stiffness values decrease after the freeze-thaw cycles for the reference mix. The reduction is greater at high temperatures/low frequencies. This can be explained as the degradation of the reference mixture after freeze-thaw cycles. In contrast, the stiffness increases for the APF, especially at the medium and high temperatures. This was found in the saturated mix before the freeze-thaw conditioning in the past studies and is probably due to the water pore pressure (Badeli et al., 2018b). This explains that the durability increases after using APF to the mix. No degradation occurs to the APF mix after 300 freeze-thaw cycles. This can be due to the increased in adhesion of the APF mix and cohesion of its mastic.

Table 5.10 2S2P1D parameters

Mixture	Freeze-thaw conditioning	Number of specimens	Air Voids		2S2P1D parameters					
			Average air voids (%)	Standard deviation (%)	E_{00} (MPa)	E_0 (MPa)	k	h	δ	β
Reference	Before	2	6.85	0.14	35	40,000	0.18	0.52	2.20	600
Reference	After	2	6.90	0.19	12	33,000	0.17	0.55	2.20	600
APF	Before	2	6.45	1.12	50	37,000	0.17	0.55	2.60	600
APF	After	2	6.76	0.17	20	31,000	0.19	0.55	2.70	600

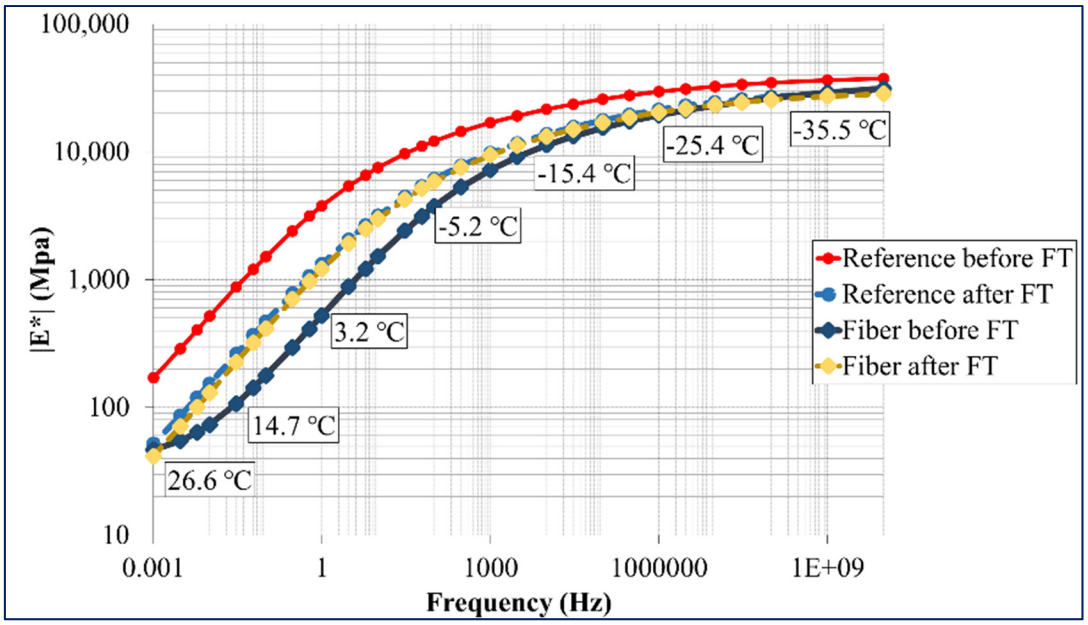

Figure 5.14 Master curves for both groups before and after freeze-thaw cycles

5.6 Conclusion

The primary objective of this paper is to study the thermo-mechanical analyses (complex modulus, fatigue, and TSRST tests) on the GB20 asphalt mix and improvement effect of APF incorporation are studied to compare the stiffness variation before and after 300 rapid freeze-thaw cycles, fatigue life, and thermal strength. The important findings are presented below:

- It is observed that the average value of the $|E_0^*|$ in the fatigue test is higher for the reference mix than the APF mix.
- The slope of the Wöhler's curve is steeper for the APF mix than the reference mix which results in lower fatigue life at high strain amplitude (heavy truckloads) for the reference mix.
- The value of ε6 is almost same for both mixes. The value corresponds to the strain amplitude for a failure at 106 cycles.
- TSRST test results show that the addition of aramid fiber in the GB20 mix decreased the fracture strength, fracture temperature.

- The Cole-Cole shows that the both of the loss and storage modulus decrease after a large number of rapid freeze-thaw cycles, while the graph indicates that the APF mix is less sensitive to the freeze-thaw cycles than the reference mix.
- The results from the black diagram show that the phase angle increases as the value of |E*| decreases after the freeze-thaw cycles for both mixes at high temperatures.
- The master curve shows that the stiffness values decrease after the freeze-thaw cycles for the reference mix. The reduction is greater at high temperatures/low frequencies. In contrast, the stiffness increases for the APF, especially at the medium and high temperatures.

5.7 Acknowledgements

NSERC and DuPont Company have financially supported a part of the research work. The Authors also would like to thank DuPont Protection Solutions and Ms. France Rochette for their help and support in the development of this study.

The National Sciences and Engineering Research Council of Canada (NSERC) Industrial Research Chair on the Interaction of Heavy Loads–Climate–Pavement of Laval University (i3C) funds a part of this research work.

5.8 References

Abtahi, S. M., Sheikhzadeh, M., & Hejazi, S. M. (2010). Fiber-reinforced asphalt-concrete - A review. Construction and Building Materials, 24(6), 871–877. https://doi.org/10.1016/j.conbuildmat.2009.11.009

ASTM. (2008). Standard Test Method for Resistance of Concrete to Rapid Freezing and Thawing. ASTM International.

Badeli, S., Carter, A., & Doré, G. (2016). The importance of asphalt mixture air voids on the damage evolution during freeze-thaw cycles. Canadian Technical Asphalt Association.

Badeli, S., Carter, A., & Doré, G. (2018a). Complex Modulus and Fatigue Analysis of Asphalt Mix after Daily Rapid Freeze-Thaw Cycles. Journal of Materials in Civil Engineering, 30(4), 4018056.

Badeli, S., Carter, A., & Doré, G. (2018b). Effect of laboratory compaction on the viscoelastic characteristics of an asphalt mix before and after rapid freeze-thaw cycles. Cold Regions Science and Technology, 146, 98–109.

Badeli, S., Saliani, S., & Carter, A. (2017a). Effect of Short Aramid Fibers on Asphalt Performance. Substance ÉTS.

Badeli, S., Saliani, S., & Carter, A. (2017b). Effet des fibres courtes d'aramide sur la performance de l'asphalte. Substance ÉTS.

Basueny, A., Perraton, D., & Carter, A. (2014). Laboratory study of the effect of RAP conditioning on the mechanical properties of hot mix asphalt containing RAP. Materials and Structures, 47(9), 1425–1450.

Carter, A. (2002). Rhéologie en petite déformation des enrobés bitumineux et mesure de leur résistance à basse température à partir de l'essai TSRSTS. École de technologie supérieure.

Carter, A., & Paradis, M. (2010). Laboratory Characterization of the Evolution of the Thermal Cracking Resistance with the Freeze-thaw Cycles.

Chen, H., Xu, Q., Chen, S., & Zhang, Z. (2009). Evaluation and design of fiber-reinforced asphalt mixtures. Materials and Design, 30(7), 2595–2603. https://doi.org/10.1016/j.matdes.2008.09.030

Di Benedetto, H., Nguyen, Q. T., & Sauzéat, C. (2011). Nonlinearity, heating, fatigue and thixotropy during cyclic loading of asphalt mixtures. Road Materials and Pavement Design, 12(1), 129–158.

Di Benedetto, H., Olard, F., Sauzéat, C., & Delaporte, B. (2004). Linear viscoelastic behaviour of bituminous materials: From binders to mixes. Road Materials and Pavement Design, 5(sup1), 163–202.

Doré, G., Konrad, J.-M., & Roy, M. (1997). Role of deicing salt in pavement deterioration by frost action. Transportation Research Record: Journal of the Transportation Research Board, (1596), 70–75.

Doré, G., Konrad, J.-M., & Roy, M. (1999). Deterioration model for pavements in frost conditions. Transportation Research Record: Journal of the Transportation Research Board, (1655), 110–117.

Doré, G., & Zubeck, H. K. (2009). Cold regions pavement engineering.

DuPont. (2014). The world's biggest road networks. Retrieved from http://www.roadtraffic-technology.com/features/featurethe-worlds-biggest-road-networks-4159235/.

Huang, H., & White, T. D. (1996). Dynamic Properties of Fiber-Modified. Transportation Research Record: Journal of the Transportation Research Board, 98–104. Retrieved from https://doi.org/10.3141/1545-13

Kaloush, K. E., Biligiri, K. P., Zeiada, W. A., Rodezno, M. C., & Reed, J. X. (2010). Evaluation of fiber-reinforced asphalt mixtures using advanced material characterization tests. Journal of Testing and Evaluation, 38(4), 400–411.

Lachance-Tremblay, Éric, Vaillancourt, M., & Perraton, D. (2016). Evaluation of the impact of recycled glass on asphalt mixture performances. Road Materials and Pavement Design, 17(3), 600–618.

McDaniel, R. S. (2015). Fiber Additives in Asphalt Mixtures. https://doi.org/10.17226/22191

Mirabdolazimi, S. M., & Shafabakhsh, G. (2017). Rutting depth prediction of hot mix asphalts modified with forta fiber using artificial neural networks and genetic programming technique. Construction and Building Materials, 148, 666–674. https://doi.org/10.1016/j.conbuildmat.2017.05.088

Mitchell, M. R., Link, R. E., Kaloush, K. E., Biligiri, K. P., Zeiada, W. A., Rodezno, M. C., & Reed, J. X. (2010). Evaluation of Fiber-Reinforced Asphalt Mixtures Using Advanced Material Characterization Tests. Journal of Testing and Evaluation, 38(4), 102442. https://doi.org/10.1520/JTE102442

Park, P., El-Tawil, S., Park, S. Y., & Naaman, A. E. (2015). Cracking resistance of fiber reinforced asphalt concrete at -20 °c. Construction and Building Materials, 81, 47–57. https://doi.org/10.1016/j.conbuildmat.2015.02.005

Pascale, P., Doré, G., & Prophète, F. (2004). Characterization of tire impact on the pavement behaviour. Canadian Journal of Civil Engineering, 31(5), 860–869.

Perraton, D., Touhara, R., Di Benedetto, H., & Carter, A. (2015). Ability of the classical fatigue criterion to be associated with macro-crack growth. Materials and Structures, 48(8), 2383–2395.

Québec, M. M. des T. du. (2016a). Enrobés: Formulation selon la méthode LC. Retrieved from http://www3.publicationsduquebec.gouv.qc.ca/produits/ouvrage_routier.fr.html

Québec, M. M. des T. du. (2016b). Recueil des méthodes d'essai LC. Retrieved from http://www3.publicationsduquebec.gouv.qc.ca/produits/ouvrage_routier/guides/guide2.fr.html

Saliani, S. S., Eng, M., Carter, A., Baaj, H., Eng, P., & Badeli, S. (2017). Investigation of the Tensile Strength of Hot Mix Asphalt Incorporating Pulp Aramid Fiber.

Tanzadeh, J., Vafaeian, M., & Yusefzadeh-Fard, M. (2017). Laboratory study on the performance of hybrid macro soil fiber reinforced mixture. Construction and Building Materials, 134, 50–55. https://doi.org/10.1016/j.conbuildmat.2016.12.053

Tapkin, S. (2008). The effect of polypropylene fibers on asphalt performance. Building and Environment, 43(6), 1065–1071. https://doi.org/10.1016/j.buildenv.2007.02.011

Tapsoba, N., Sauzéat, C., Di Benedetto, H., Baaj, H., & Ech, M. (2014). Behaviour of asphalt mixtures containing reclaimed asphalt pavement and asphalt shingle. Road Materials and Pavement Design, 15(2), 330–347.

Terrel, R. L., & Al-Swailmi, S. (1993). The role of pessimum voids concept in understanding moisture damage to asphalt concrete mixtures. Transportation Research Record, (1386).

Vinson, T. S., Kanerva, H. K., & Zeng, H. (1994). Low temperature cracking: field validation of the Thermal Stress Restrained Specimen Test (TSRST). Strategic Highway Research Program SHRP-A, 401.

Wu, S., Ye, Q., Li, N., & Yue, H. (2007). Effects of fibers on the dynamic properties of asphalt mixtures. Journal of Wuhan University of Technology-Mater. Sci. Ed., 22(4), 733–736. https://doi.org/10.1007/s11595-006-4733-3.

CONCLUSION AND RECOMENDATIONS

In mechanical empirical pavement design guide (MEPDG), the designer chooses a pavement structure and then analyses the design in details to make sure that it meets design criteria, such as rutting and fatigue cracking. As yet there have not been any fatigue criterions to take into account freeze-thaw cycles. This issue is fundamental to the fatigue durability of a road pavement. The fatigue durability problem asphalt mixture subjected to freeze-thaw cycles has not been sufficiently studied yet. The main objective of this study is to conduct the thermomechanical tests on the base-course asphalt mixture (which is known as GB20 in Quebec standard) before and after rapid freeze-thaw cycles. Results have shown that the effect of freeze-thaw cycles is important to consider during the design life of asphalt pavements. The overall findings can be listed as below.

- The stiffness behavior changes with a higher rate at high temperatures and the lower rate at low temperatures after large number of rapid freeze-thaw cycles.
- Specimen with high percentage of voids has a much higher latent heat of fusion than the specimen with low percentage of voids. These can show the importance of the compaction effort which results to have different density.
- The results indicate that the compaction level significantly affects the behavior of the mix after a large number of rapid freeze-thaw cycles.
- The maximum value of the phase angle after 300 freeze-thaw cycles increase for the mix with high percentage of air voids (low level of compaction). The increase in viscosity (at very high temperatures) and a decrease in stiffness (at very low temperatures) after 300 freeze-thaw cycles the mix with high percentage of voids is probably due to the stripping problem.
- Comparison between the laboratory determined and predicted data indicated that the relative bias in the modulus prediction after 300 freeze-thaw cycles, especially due to the high percentage of voids.
- Regarding the fatigue damage results, since initial stiffness modulus of the conditioned mix was much lower than the reference and because of the results from the complex modulus

test that displayed the stiffness reduction and changed in viscoelastic behavior after 300 freeze-thaw cycles, it is concluded that the degradation of the conditioned mix started before the fatigue test and during freeze-thaw cycles.

- Regarding fatigue test results, the reference mixture has a much better performance with respect to the resistance to fatigue cracking than after the condition of the environmental freeze-thaw cycles.
- Results also show that using Aramid pulp fiber results decreased in fracture strength and fracture temperature in TSRST test.
- The slope of the Wöhler's curve is steeper for the APF mix than the reference mix which results in lower fatigue life at high strain amplitude (heavy truckloads) for the reference mix.
- Comparison of the Aramid fiber mix and the reference mix show that the stiffness values decrease after the freeze-thaw cycles for the reference mix. The reduction is greater at high temperatures/low frequencies. In contrast, the stiffness increases for the Aramid fiber mix, especially at the medium and high temperatures.

Further studies are suggested to develop the fatigue and dynamic modulus prediction formula for Quebec region. This can be developed by considering the relationships between laboratory specimens and the real ones in field (by collecting cores or field section assessments), without considering other factors, such as loading, aging, etc. In the meantime, the field data with different compaction levels can be obtained from the site condition to find an actual predicted formula. Based on the initial results, next steps of the research have been developed in different aspects.

1. Pavement design modification: modification on the prediction model for stiffness modulus. Statistical comparison between the determined results from the laboratory and predicted data calculated from the current Witczak formula indicated that there is relative bias in the modulus prediction after 300 FT cycles, especially due to the high percentage of voids. This was considered by applying the improved equation to the predicted values.

2. Mix design modification with using appropriate additives.

The improvement effect of Aramid Pulp Fiber was assessed to compare the stiffness variation before and after 300 rapid freeze-thaw cycles, fatigue behavior, and thermal strength. The results demonstrated the ability of Aramid Pulp Fiber to increase the durability of the GB 20 mix against freeze-thaw cycles. The TSRST and fatigue results also show that the APF additives can increase the performance of the GB 20 mix against low temperature cracking and heavy truckloads.

3. Construction practice in the field (proper compaction and compaction modification).

The laboratory results indicated that the compaction level significantly affects the behavior of the mix after a large number of rapid FT cycles.

BIBLIOGRAPHY

Abojaradeh, M. (2003). Predictive fatigue models for Arizona asphalt concrete mixtures, (December).

Advanced Asphalt Technologies, LLC. (2011). A Manual for Design of Hot Mix Asphalt with Commentary (Vol. 673). Transportation Research Board.

Al-Qadi, I., Hassan, M., & Elseifi, M. (2005). Field and theoretical evaluation of thermal fatigue cracking in flexible pavements. Transportation Research Record: Journal of the Transportation Research Board, (1919), 87–95.

Arabani, M., & Kamboozia, N. (2014). New achievements in visco-elastoplastic constitutive model and temperature sensitivity of glasphalt. International Journal of Pavement Engineering, 15(9), 810–830. https://doi.org/10.1080/10298436.2014.893317

Baaj, H., Di Benedetto, H., & Chaverot, P. (2005). Effect of binder characteristics on fatigue of asphalt pavement using an intrinsic damage approach. Road Materials and Pavement Design, 6(2), 147–174. https://doi.org/10.1080/14680629.2005.9690003

Bagampadde, U., Isacsson, U., & Kiggundu, B. M. (2004). Classical and Contemporary Aspects of Stripping in Bituminous Mixes. Road Materials and Pavement Design, 5(1), 7–43. https://doi.org/10.1080/14680629.2004.9689961

Barrie, P. J. (2000). Characterization of porous media using NMR methods. Annual Reports on NMR Spectroscopy, 41, 265–316.

Bausano, J., Kvasnak, A., & Williams, R. (2006). Development of Simple Performance Tests Using Laboratory Test Procedures to Illustrate the Effects of Moisture Damage on Hot Mix Asphalt.

Bausano, J., & Williams, R. C. (2009). Transitioning from AASHTO T283 to the simple performance test using moisture conditioning. Journal of Materials in Civil Engineering, 21(2), 73–82.

Bayat, A., Knight, M. A., & Soleymani, H. R. (2012). Field monitoring and comparison of thermal-and load-induced strains in asphalt pavement. International Journal of Pavement Engineering, 13(6), 508–514.

Behiry, A. E. A. E.-M. (2013). Laboratory evaluation of resistance to moisture damage in asphalt mixtures. Ain Shams Engineering Journal, 4(3), 351–363. https://doi.org/10.1016/j.asej.2012.10.009

Benedetto, H., Roche, C., Baaj, H., Pronk, A., & Lundström, R. (2004). Fatigue of bituminous mixtures. Materials and Structures, 37(3), 202–216.

Bilodeau, J. P., & Doré, G. (2017). Flexible pavement damage during spring thaw: A field study using the falling weight deflectometer. Canadian Journal of Civil Engineering, 45(3), 227-234.

Caro, S., Masad, E., Bhasin, A., & Little, D. N. (2008). Moisture susceptibility of asphalt mixtures, Part 1: mechanisms. International Journal of Pavement Engineering, 9(2), 81–98. https://doi.org/10.1080/10298430701792128

Carter, A., & Paradis, M. (2010). Laboratory Characterization of the Evolution of the Thermal Cracking Resistance with the Freeze-thaw Cycles. Retrieved from data.abacus.hr

Carvalho, R., & Schwartz, C. (2006). Comparisons of flexible pavement designs: AASHTO empirical versus NCHRP Project 1-37A mechanistic-empirical. Transportation Research Record: Journal of the Transportation Research Board, (1947), 167–174.

Chen, J.-S., Lin, K.-Y., & Young, S.-Y. (2004). Effects of Crack Width and Permeability on Moisture-Induced Damage of Pavements. Journal of Materials in Civil Engineering, 16(3), 276–282. https://doi.org/10.1061/(ASCE)0899-1561(2004)16:3(276)

Chen, X., & Huang, B. (2008). Evaluation of moisture damage in hot mix asphalt using simple performance and superpave indirect tensile tests. Construction and Building Materials, 22(9), 1950–1962. https://doi.org/10.1016/j.conbuildmat.2007.07.014

Cheng, D., Little, D. N., Lytton, R. L., & Holste, J. C. (2003). Moisture damage evaluation of asphalt mixtures by considering both moisture diffusion and repeated-load conditions. Transportation Research Record: Journal of the Transportation Research Board, 1832(1), 42–49.

Copeland, A. (2007). Influence of moisture on bond strength of asphalt-aggregate systems. Zhurnal Eksperimental'noi I Teoreticheskoi Fiziki.

Deblois, K., Bilodeau, J.-P., & Dore, G. (2010). Use of falling weight deflectometer time history data for the analysis of seasonal variation in pavement response. Canadian Journal of Civil Engineering, 37(9), 1224–1231.

Copeland, A., Youtcheff, J., Kringos, N., & Scarpas, A. (2006). Determination of bond strength as a function of moisture content at the aggregate-mastic interface. -AUGUST 12 TO 17.

Deblois, K., Bilodeau, J.-P., & Dore, G. (2010). Use of falling weight deflectometer time history data for the analysis of seasonal variation in pavement response. Canadian Journal of Civil Engineering, 37(9), 1224–1231.

Di Benedetto, H., Olard, F., Sauzéat, C., & Delaporte, B. (2004). Linear viscoelastic behaviour of bituminous materials: From binders to mixes. Road Materials and Pavement Design, 5(sup1), 163–202.

Doré, G. (2004). Development and validation of the thaw-weakening index. International Journal of Pavement Engineering, 5(4), 185–192.

Doré, G., Flamand, M., & Pascale, P. (2002). Analysis of the wavelength content of the longitudinal profiles for C-LTPP test sections. Canadian Journal of Civil Engineering, 29(1), 50–57.

Doré, G., Konrad, J.-M., & Roy, M. (1997). Role of deicing salt in pavement deterioration by frost action. Transportation Research Record: Journal of the Transportation Research Board, (1596), 70–75.

Doré, G., & Zubeck, H. (2009). Cold regions pavement engineering. Retrieved from http://trid.trb.org/view.aspx?id=903094

El-Hakim, M., & Tighe, S. (2014). Impact of freeze-thaw cycles on mechanical properties of asphalt mixes. Transportation Research Record: Journal of the Transportation Research Board, (2444), 20–27.

Epps, J. A., & Monismith, C. L. (1972). Fatigue of asphalt concrete mixtures-summary of existing information. Fatigue of Compacted Bituminous Aggregate Mixtures, ASTM STP, 508, 19–45.

Goh, S. W., & You, Z. (2012). Evaluation of hot-mix asphalt distress under rapid freeze-thaw cycles using image processing technique. In CICTP 2012: Multimodal Transportation Systems—Convenient, Safe, Cost-Effective, Efficient (pp. 3305-3315).

Huang, S.-C., & Di Benedetto, H. (2015). Advances in asphalt materials: Road and pavement construction. Woodhead Publishing.

Huang, S., Robertson, R. E., Branthaver, J. F., & Petersen, J. C. (2005). Impact of Lime Modification of Asphalt and Freeze – Thaw Cycling on the Asphalt – Aggregate Interaction and Moisture, (December), 711–718.

Huang, Y. H. (2004). Pavement Analysi s and Desig n. University of Kentucky: Pearson Prentice Hall.

Huang, Y. H. (2004). Pavement analysis and design.

Islam, M. R., & Tarefder, R. A. (2015). Coefficients of thermal contraction and expansion of asphalt concrete in the laboratory. Journal of Materials in Civil Engineering, 27(11), 04015020.

Islam, M. R., Mannan, U. A., Rahman, A., & A., T. R. (2014). Simplified Thermal Stress Model to Predict Low Temperature Cracks in Flexible Pavement. Pavement Materials, Structures, and Performance, 251–261.

Jaffee, A. M., & Kajander, R. E. (2002). U.S. Patent No. 6,432,482. Washington, DC: U.S. Patent and Trademark Office.

Jenks, C. W., Jencks, C. F., Harrigan, E. T., Adcock, M., Delaney, E. P., & Freer, H. (2011). NCHRP Report 673: A manual for design of hot mix asphalt with commentary. Transportation Research Board, Washington, DC.

Kennedy, T. W., Roberts, F. L., & Lee, K. W. (1983). Evaluation of moisture effects on asphalt concrete mixtures.

Kosek, J., Štěpánek, F., & Marek, M. (2005). Modeling of transport and transformation processes in porous and multiphase bodies. Advances in Chemical Engineering, 30, 137–203.

Kringos, N., Azari, H., & Scarpas, A. (2009). Identification of parameters related to moisture conditioning that cause variability in Modified Lottman Test. Transportation Research Record : Journal of the Transportation Research Board, 6931(2127), 1–11.

Lammam, C., & MacIntyre, H. (2017). Myths of Infrastructure Spending in Canada. Fraser Institute.

Lamothe, S., Perraton, D., & Di Benedetto, H. (2015). Contraction and expansion of partially saturated hot mix asphalt samples exposed to freeze–thaw cycles. Road Materials and Pavement Design, 16(2), 277–299.

Little, D. N., & Jones, D. R. (2003). Chemical and mechanical processes of moisture damage in hot-mix asphalt pavements. In Transportation Research Board National Seminar, San Diego, CA, USA (pp. 37–70).

Lytton, R. L. (2004). Adhesive fracture in asphalt concrete mixtures. Asphalt Technology Handbook. Marcel Dekker, Monticello, New York.

Maupin, G. W., & Diefenderfer, B. K. (2006). Design of a high-binder--high-modulus asphalt mixture. Virginia Transportation Research Council.

McCann, M., Anderson-Sprecher, R., & Thomas, K. P. (2005). Statistical Comparison Between SHRP Aggregate Physical and Chemical Properties and the Moisture Sensitivity of Aggregate-Binder Mixtures. Road Materials and Pavement Design, 6(2), 197–215. https://doi.org/10.1080/14680629.2005.9690005

Mills, B. N., Tighe, S. L., Andrey, J., Smith, J. T., & Huen, K. (2009). Climate change implications for flexible pavement design and performance in southern Canada. Journal of Transportation Engineering, 135(10), 773–782.

MTQ : Ministère des Transports du Québec, 2005. Enrobés : Formulation selon la méthode LC. Gouvernement du Québec, 111 p.

Olard, F. (2012). GB5 mix design: high-performance and cost-effective asphalt concretes by use of gap-graded curves and SBS modified bitumens. Road Materials and Pavement Design, 13(sup1), 234–259.

Olard, F., Di Benedetto, H., Eckmann, B., & Triquigneaux, J. P. (2003). Linear Viscoelastic Properties of Bituminous Binders and Mixtures at Low and Intermediate Temperatures. Road Materials and Pavement Design, 4(1), 77–107.

Özgan, E., & Serin, S. (2013). Investigation of certain engineering characteristics of asphalt concrete exposed to freeze–thaw cycles. Cold Regions Science and Technology, 85, 131–136.

Partl, M. N., Bahia, H. U., Canestrari, F., De la Roche, C., Di Benedetto, H., Piber, H., & Sybilski, D. (2012). Advances in interlaboratory testing and evaluation of bituminous materials: state-of-the-art report of the RILEM technical committee 206-ATB (Vol. 9). Springer Science & Business Media.

Pascale, P., Doré, G., & Prophète, F. (2004). Characterization of tire impact on the pavement behaviour. Canadian Journal of Civil Engineering, 31(5), 860–869.

Popik, M., Juhasz, M., Chan, S., Donovan, H., & St-Laurent, D. (2013). TAC Pavement ME User Group–Canadian Climate Trials. In Transportation Association of Canada, 2013 Annual Conference, Winnipeg, Manitoba.

Prowell, B. (2010). Validating the fatigue endurance limit for hot mix asphalt.

Quebec Government (2017). Protecting the road network is a priority. https://www.transports.gouv.qc.ca/en/camionnage/Documents/fiches_degel_ang.pdf

Roberson, R., & Siekmeier, J. (2002). Determining material moisture characteristics for pavement drainage and mechanistic empirical design. Research Bulletin. Minnesota Department of Transportation. Office of Materials and Road Research.

Savard, Y., De Blois, K., Boutonnet, M., Hornych, P., & Mauduit, C. (n.d.). Analysis of Seasonal Bearing Capacity Correlated to Pavement Deterioration in Cold Region.

Shu, X., Huang, B., Shrum, E. D., & Jia, X. (2012). Laboratory evaluation of moisture susceptibility of foamed warm mix asphalt containing high percentages of RAP. Construction and Building Materials, 35, 125–130.

Si, W., Ma, B., Li, N., Ren, J. P., & Wang, H. N. (2014). Reliability-based assessment of deteriorating performance to asphalt pavement under freeze-thaw cycles in cold regions. Construction and Building Materials, 68, 572–579.

Solaimanian, M., Bonaquist, R. F., & Tandon, V. (2006). Improved Conditioning Procedure for Predicting the Moisture Susceptibility of HMA Pavements.

Soltani, M. A. (1998). Comportement en fatigue des enrobés bitumineux.

Stern, N. (2006). Stern review report on the economics of climate change.

Stroup-Gardiner, M., & Epps, J. A. (1987). Four variables that affect the Performance of Lime in Asphalt-Aggregate Mixtures. Transportation Research Record, 1115, 12–22.

Stuart, K. D. (1990). Moisture damage in asphalt mixtures-a state-of-the-art report.

Tang, N., Sun, C. J., Huang, S. X., & Wu, S. P. (2013). Damage and corrosion of conductive asphalt concrete subjected to freeze–thaw cycles and salt. Materials Research Innovations, 17(sup1), 240–245.

Tapsoba, N., Sauzéat, C., & Di Benedetto, H. (2013). Analysis of Fatigue Test for Bituminous Mixtures. Journal of Materials in Civil Engineering, 25(6), 701–710.

Terrel, R. L., & Al-Swailmi, S. (1992). Final Report on Water Sensitivity of Asphalt-Aggregate Mixtures Test Development. Strategic Highway Research Program.

Theyse, H., De Beer, M., & Rust, F. (1996). Overview of South African mechanistic pavement design method. Transportation Research Record: Journal of the Transportation Research Board, (1539), 6–17.

Williams, T., & Miknis, F. (1998). Use of environmental SEM to study asphalt-water interactions. Journal of Materials in Civil Engineering.

Xu, H., Guo, W., & Tan, Y. (2016). Permeability of asphalt mixtures exposed to freeze–thaw cycles. Cold Regions Science and Technology, 123, 99–106.

Yi, J., Shen, S., Wang, D., Feng, D., & Huang, Y. (2016). Effect of Testing Conditions on Laboratory Moisture Test for Asphalt Mixtures. Journal of Testing and Evaluation, 44(2), 20150128. https://doi.org/10.1520/JTE20150128

Zeng, M., & Shields, D. H. (1999). Nonlinear thermal expansion and contraction of asphalt concrete. Canadian Journal of Civil Engineering, 26(1), 26–34.

Zubeck, H., & Vinson, T. (1996). Prediction of low-temperature cracking of asphalt concrete mixtures with thermal stress restrained specimen test results. Transportation Research Record: Journal of the Transportation Research Board, (1545), 50–58.